

Stellar laboratories

X. New Cu IV – VII oscillator strengths and the first detection of copper and indium in hot white dwarfs $\star, \star\star, \star\star\star$

T. Rauch¹, S. Gamrath², P. Quinet^{2,3}, M. Demleitner⁴, M. Knörzer¹, K. Werner¹, and J. W. Kruck⁵

¹ Institute for Astronomy and Astrophysics, Kepler Center for Astro and Particle Physics, Eberhard Karls University, Sand 1, 72076 Tübingen, Germany
e-mail: rauch@astro.uni-tuebingen.de

² Physique Atomique et Astrophysique, Université de Mons – UMONS, 7000 Mons, Belgium

³ IPNAS, Université de Liège, Sart Tilman, 4000 Liège, Belgium

⁴ Astronomisches Rechen-Institut (ARI), Centre for Astronomy of Heidelberg University, Mönchhofstraße 12–14, 69120 Heidelberg, Germany

⁵ NASA Goddard Space Flight Center, Greenbelt, MD 20771, USA

Received 3 September 2019; accepted 23 March 2020

ABSTRACT

Context. Accurate atomic data is an essential ingredient for the calculation of reliable non-local thermodynamic equilibrium (NLTE) model atmospheres that are mandatory for the spectral analysis of hot stars.

Aims. We aim to search for and identify for the first time spectral lines of copper (atomic number $Z = 29$) and indium ($Z = 49$) in hot white dwarf (WD) stars and to subsequently determine their photospheric abundances.

Methods. Oscillator strengths of Cu IV – vi were calculated to include radiative and collisional bound-bound transitions of Cu in our NLTE model-atmosphere calculations. Oscillator strengths of In IV – vi were compiled from the literature.

Results. We newly identified 1 Cu IV , 51 Cu V , 2 Cu VI , and 5 In V lines in the ultraviolet (UV) spectrum of DO-type WD RE 0503–289. We determined the photospheric abundances of 9.3×10^{-5} (mass fraction, 132 times solar) and 3.0×10^{-5} (56 600 times solar), respectively; we also found Cu overabundances in the DA-type WD G191–B2B (6.3×10^{-6} , 9 times solar).

Conclusions. All identified Cu IV –vi lines in the UV spectrum of RE 0503–289 were simultaneously well reproduced with our newly calculated oscillator strengths. With the detection of Cu and In in RE 0503–289, the total number of trans-iron elements ($Z > 28$) in this extraordinary WD reaches an unprecedented number of 18.

Key words. atomic data – line: identification – stars: abundances – stars: individual: G191–B2B – stars: individual: RE 0503–289 – virtual observatory tools

1. Introduction

The hydrogen-deficient (DO-type) white dwarf (WD) RE 0503–289 (WD 0501–289; McCook & Sion 1999a,b) is located in the $\log T_{\text{eff}} - \log g$ plane (Fig. 1, $T_{\text{eff}} = 70\,000 \pm 2000$ K and $\log(g / \text{cm s}^{-2}) = 7.5 \pm 0.1$; Rauch et al. 2016b) in the transition zone between those post-asymptotic giant branch (post-AGB) stars with still high luminosity and a stellar wind still strong enough to provide a chemically homogeneous photosphere and the WD cooling sequence where gravity efficiently pulls metals down and out of the photosphere. In this region the interplay of radiative levitation and gravitational settling is responsible for stratification, i.e., metals float up and, thus strong abundance enhancements are observed. Trans-iron

elements (TIEs), with their many spectral lines due to their only partially filled electron shells, are especially involved in this process. Thus, although unexpected, it was not surprising that Werner et al. (2012b) discovered lines of ten TIEs in the ultraviolet (UV) spectrum of RE 0503–289. Due to the lack of atomic data for TIEs at that time, it was only possible to determine the Kr and Xe abundances that are about 450 and 3800 times solar, respectively.

Since 2012 we have calculated oscillator strengths of several TIEs (Table A.4) and successfully identified their lines in the spectra of RE 0503–289, G191–B2B (WD 0501+527; McCook & Sion 1999a,b, see additional references in Table A.4), WD 0111+002, PG 0109+111, and PG 1707+427 (Hoyer et al. 2017). To search for Cu and In lines in the UV spectrum of RE 0503–289 and G191–B2B, we calculated new oscillator strengths for Cu and compiled In data from the literature. In Sect. 2, we briefly describe the available UV observations. Our model-atmosphere code and the considered atomic data is introduced in Sect. 3. We summarize our results and conclude in Sect. 4.

\star Based on observations with the NASA/ESA Hubble Space Telescope, obtained at the Space Telescope Science Institute, which is operated by the Association of Universities for Research in Astronomy, Inc., under NASA contract NAS5-26666.

$\star\star$ Based on observations made with the NASA-CNES-CSA Far Ultraviolet Spectroscopic Explorer.

$\star\star\star$ Tables A.13 to A.16 are only available via the German Astrophysical Virtual Observatory (GAVO) service TOSS (<http://dc.g-vo.org/TOSS>).

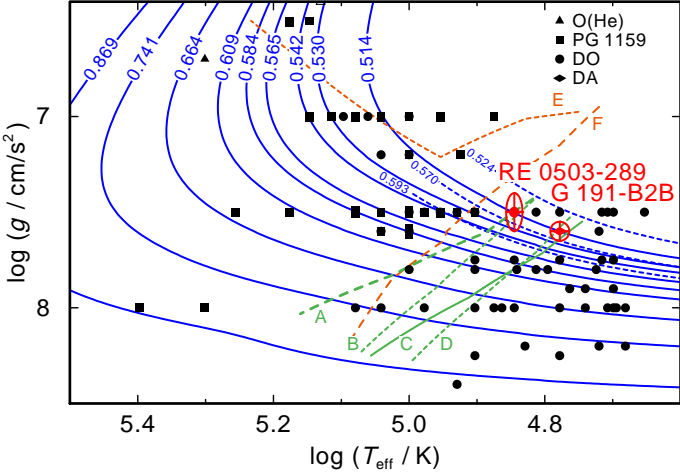


Fig. 1. Location of RE 0503–289 (with its error ellipse) and related objects (Hügelmeyer et al. 2006; Kepler et al. 2016; Reindl et al. 2014b,a; Werner & Herwig 2006) in the $\log T_{\text{eff}} - \log g$ plane¹. Evolutionary tracks for H-deficient (Althaus et al. 2009, full lines) and H-rich WDs (Miller Bertolami 2016, dashed lines) labeled with their respective masses in M_{\odot} are plotted for comparison. “Wind limits” of Unglaub & Bues (their Figs. 6 and 13, 2000, digitized with Dexter²) are shown. The lines indicate for H-deficient stars A: so-called PG 1159 wind limit calculated with $M = 1.29 \times 10^{-15} L^{1.86}$; B and C: photospheric carbon content is reduced by factors of 0.5 and 0.1, respectively; D: no PG 1159 star is known to the right of this line, and for H-rich stars E: wind limit; and F: He/H = 10^{-3} (by number).

2. Observations

For our spectral analysis, we used UV spectra obtained with the Far Ultraviolet Spectroscopic Explorer (FUSE, $910 \text{ \AA} < \lambda < 1190 \text{ \AA}$, resolving power $R \approx 20\,000$) and the Hubble Space Telescope / Space Telescope Imaging Spectrograph (HST/STIS, $1144 \text{ \AA} < \lambda < 1709 \text{ \AA}$ with $R = 2.3 \times 10^5$ for G191–B2B and $R \approx 45\,800$ for RE 0503–289). All spectra are described in detail in Rauch et al. (2013) and Hoyer et al. (2017).

The observed spectra shown here (FUSE for $\lambda \leq 1188 \text{ \AA}$, STIS otherwise) were shifted to rest wavelengths, using $v_{\text{rad}} = 24.56 \text{ km s}^{-1}$ for G191–B2B (Lemoine et al. 2002) and 25.8 km s^{-1} for RE 0503–289 (Hoyer et al. 2017). To compare them with our synthetic spectra, they were convolved with Gaussians to simulate the respective instrument resolving power.

3. Model atmospheres and atomic data

For the precise spectral analysis of hot stars, model atmospheres that consider deviations from the local thermodynamical equilibrium (LTE) are mandatory. The Tübingen non-local thermodynamic equilibrium (NLTE) model-atmosphere package (TMAP, Werner et al. 2012a) can calculate such models that it assumes radiative and hydrostatic equilibrium and plane-parallel geometry. The Tübingen Model Atom Database (TMAD, Rauch & Deetjen 2003) provides the model atoms for elements with atomic number below 20. TMAD has been constructed as part of the Tübingen contribution to the German Astrophysical Virtual Observatory (GAVO).

The ionization stages of Cu iv-vii and In iv-vi were represented in the model atoms using so-called super levels and su-

Table 1. Statistics of the Cu iv - vii, atomic levels and line transitions from Tables A.13 - A.16 and of In iv - vi compiled from the literature (Sect. 4). The super levels and lines are used in our model-atmosphere calculations.

Ion	Atomic levels	Lines	Super levels	Super lines
Cu iv	297	8785	7	15
v	247	5456	7	16
vi	254	3797	7	9
vii	217	2253		
In iv	231	564	7	15
v	396	919	7	16
vi	167	176	8	9

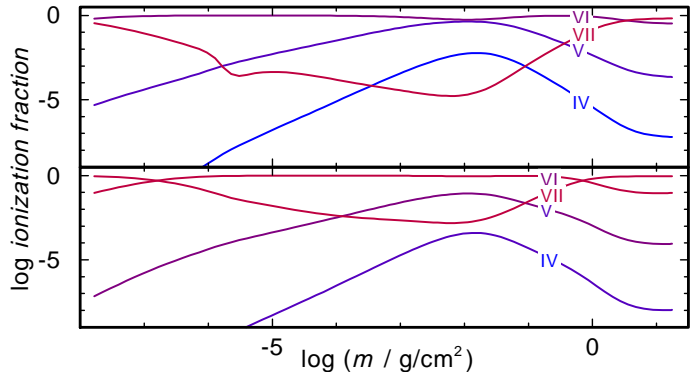


Fig. 2. Ionization fractions of Cu (top panel) and In (bottom) in our RE 0503–289 model. m is the column mass, measured from the outer boundary of our model atmospheres.

per lines. These were calculated via a statistical approach by our Iron Opacity and Interface (IrOnIc, Rauch & Deetjen 2003; Müller-Ringat 2013). To enable IrOnIc to read our new Cu and In data, we transferred it into Kurucz-formatted files (cf. Rauch et al. 2015b). The statistics of our Cu and In model atoms are listed in Table 1.

Our models consider opacities of He, C, N, O, Al, Si, P, S, Ca, Sc, Ti, V, Cr, Mn, Fe, Co, Ni, Cu, Zn, Ga, Ge, As, Se, Kr, Sr, Zr, Mo, Sn, In, Te, I, Xe, and Ba. Details about the models are given in Rauch et al. (2016b). Cu v-vi and In vi are the dominant ionization stages in the line-forming region ($-4 \leq \log m \leq 0.5$) of the photosphere of RE 0503–289 (Fig. 2).

The calculation of the Cu and In absorption cross sections is performed according to Rauch & Deetjen (2003). For the collisional bound-bound transitions we use the van Regemorter formula (van Regemorter 1962) for known f-values and an approximate formula for unknown f-values. The quadratic Stark effect is considered for radiative bound-bound transitions by an approximate formula given by (Cowley 1970, 1971). The Seaton (1962) formula is employed to calculate collisional and radiative bound-free cross sections with a hydrogen-like threshold value.

For Cu and In (and all other elements), level dissolution (pressure ionization) is considered following Hummer & Mihalas (1988) and Hubeny et al. (1994).

Available atomic data of Cu iv-vii ions. The main source of atomic data related to the Cu iv-vii spectra is the paper published by Sugar & Musgrove (1990) in which the available experimental energy levels of the copper atom, in all stages of ionization, have been compiled together with ionization energies, either experimental or theoretical, experimental Landé g-factors, and leading components of calculated eigenvectors. This com-

¹ cf. <http://www.astro.physik.uni-potsdam.de/~nreindl/He.html> for stellar parameters

² <http://dc.zah.uni-heidelberg.de/sdexter>

pilation is still being used as the standard reference database for the copper ions of interest at the National Institute of Standards and Technology (NIST, Kramida et al. 2019). More precisely, in Sugar and Musgrove and NIST compilations for Cu IV, experimental values are reported for 187 levels of the $3d^8$, $3d^74s$, $3d^75s$, $3d^74d$, and $3d^64s^2$ even-parity configurations and 110 levels of the $3d^74p$ odd-parity configuration. These data are based on earlier analyses by Schröder & van Kleef (1970), Meinders (1976), and Meinders & Uijlings (1980) who observed the copper spectrum using a sliding spark light source. In the case of Cu V, the first work was reported by van Kleef et al. (1975) who found a few energy levels in $3d^7$ and $3d^64p$ configurations. This work was completed by van Kleef et al. (1976) who identified many $3d^7 - 3d^64p$ and $3d^64s - 3d^64p$ lines, allowing them to classify all the levels of the $3d^7$ configuration, as well as 53 of the 63 levels of $3d^64s$ and 175 of the 180 levels of $3d^64p$. The initial line identification in the Cu VI spectrum was performed by Poppe et al. (1974) which was considerably extended a few years later by Raassen & Van Kleef (1981), who used new exposures of a sliding spark discharge to analyze the $3d^6 - 3d^54p$ and $3d^54s - 3d^54p$ transition arrays. This analysis led to the identification of all levels in the $3d^6$ configuration, except the highest 1S_0 , as well as 208 of the 214 levels in $3d^54p$ and 13 of the 74 levels in $3d^54s$. Finally, the analysis of the Cu VII spectrum by van het Hof et al. (1990) appeared too late to be included in the compilation of Sugar & Musgrove (1990). They determined all 37 levels of the $3d^5$ ground configuration and 129 of the 180 possible levels of the $3d^44p$ configuration. With regard to the radiative parameters, very few studies have focused on the determination of electric dipole transition rates in Cu IV–VII ions so far. To our knowledge, the only available data were recently obtained by Aggarwal et al. (2016) who used the quasi-relativistic approach (QR) with a very large configuration interaction (CI) expansion to compute oscillator strengths and transition probabilities in Cu VI.

Oscillator strength calculations for the Cu IV–VII ions. The method adopted in our work to model the atomic structures and compute the radiative parameters in the Cu IV–VII ions was the pseudo-relativistic Hartree-Fock (HFR) approach originally introduced by Cowan (1981) and modified to take core-polarization effects into account, giving rise to the so-called HFR+CPOL method (see, e.g., Quinet et al. 1999, 2002; Quinet 2017).

For Cu IV, configuration interaction was considered among the configurations $3d^8$, $3d^74s$, $3d^75s$, $3d^74d$, $3d^75d$, $3d^64s^2$, $3d^64p^2$, $3d^64d^2$, $3d^64s5s$, and $3d^64s4d$ for the even parity, and $3d^74p$, $3d^75p$, $3d^74f$, $3d^75f$, $3d^64s4p$, $3d^64s5p$, $3d^64s4f$, and $3d^64p4d$ for the odd parity. The core-polarization parameters were the dipole polarizability of a Cu VI ionic core, as reported by Fraga et al. (1976), i.e., $\alpha_d = 0.67$ a.u., and the cut-off radius, $r_c = 0.80$ a.u., corresponding to the HFR mean value $\langle r \rangle$ of the outermost core orbital (3d). Using the experimental energy levels compiled at NIST (Kramida et al. 2019), some radial integrals (average energy, Slater, spin-orbit, and effective interaction parameters) of $3d^8$, $3d^74s$, $3d^75s$, $3d^74d$, $3d^64s^2$, and $3d^74p$ configurations were optimized by a well-established least-squares fitting procedure in which the mean deviations were found to be equal to 206 cm^{-1} for the even parity and 183 cm^{-1} for the odd parity. It is worth noting that when performing the fit we found that the experimental energy level at 306941.8 cm^{-1} was incorrectly classified as $J = 1$ in the NIST tables, while according to our calculations this level should be designated as $J = 2$.

For Cu V, the configurations included in the HFR model were $3d^7$, $3d^64s$, $3d^65s$, $3d^64d$, $3d^54s^2$, $3d^54p^2$, $3d^54d^2$, and $3d^54s4d$ for the even parity, and $3d^64p$, $3d^65p$, $3d^64f$, $3d^54s4p$, $3d^54s5p$, and $3d^54s4f$ for the odd parity. In this ion the semi-empirical process was carried out to optimize the radial integrals corresponding to $3d^7$, $3d^64s$, and $3d^64p$ configurations using the experimental levels reported in the NIST database (Kramida et al. 2019). The mean deviations between calculated and experimental energy levels were 325 cm^{-1} and 259 cm^{-1} for even and odd parities, respectively. Core-polarization effects were estimated using a dipole polarizability and a cut-off radius corresponding to a Cu VII ionic core, i.e., $\alpha_d = 0.47$ a.u. (Fraga et al. 1976), and $r_c = 0.75$ a.u.

In the case of Cu VI, the configuration interaction was considered among the following configurations: $3d^6$, $3d^54s$, $3d^55s$, $3d^54d$, $3d^55d$, $3d^44s^2$, $3d^44p^2$, $3d^44d^2$, $3d^44s4d$, $3d^44s5d$ (even parity) and $3d^54p$, $3d^55p$, $3d^54f$, $3d^44s4p$, $3d^44s5p$, $3d^44s4f$ (odd parity). The core-polarization parameters were those corresponding to a Cu VIII ionic core, i.e., $\alpha_d = 0.40$ a.u. (Fraga et al. 1976), and $r_c = 0.72$ a.u. The radial parameters of the $3d^6$, $3d^54s$, and $3d^54p$ configurations were optimized to minimize the differences between the computed Hamiltonian eigenvalues and the experimental energy levels listed at NIST (Kramida et al. 2019) giving rise to mean deviations of 442 cm^{-1} (even parity) and 429 cm^{-1} (odd parity).

Finally, for Cu VII, ten even- and eight odd-parity configurations were included in the HFR model to compute the radiative parameters, i.e., $3d^5$, $3d^44s$, $3d^45s$, $3d^44d$, $3d^45d$, $3d^34s^2$, $3d^34p^2$, $3d^34d^2$, $3d^34s5s$, $3d^34s4d$, and $3d^44p$, $3d^45p$, $3d^44f$, $3d^45f$, $3d^34s4p$, $3d^34s5p$, $3d^34s4f$, and $3d^34p4d$, respectively. An ionic core of the type Cu IX was considered to estimate the core-polarization effects with the parameters $\alpha_d = 0.34$ a.u. (Fraga et al. 1976) and $r_c = 0.70$ a.u. The semi-empirical optimization process was carried out to adjust the radial parameters in $3d^5$ and $3d^44p$ with the experimental energy levels taken from van het Hof et al. (1990) leading to average energy deviations of 78 cm^{-1} and 365 cm^{-1} for even and odd parities, respectively.

The parameters that we had adopted for our computations are given in Tables A.5 – A.8 and a comparison of calculated and experimental energies is shown in Tables A.9 – A.12 for Cu IV–VII, respectively. In Tables A.13 – A.16 (provided via the registered GAVO Tübingen Oscillator Strengths Service TOSS), we give the newly computed weighted oscillator strengths ($\log gf$) and transition probabilities (gA , in s^{-1}) together with the experimental values (in cm^{-1}) of the lower and upper energy levels and the corresponding Ritz wavelengths (in Å). In the final column of each table we also give the cancellation factor (CF), as defined by Cowan (1981).

Let us remind that very low values of the CF (typically < 0.05) indicate strong cancellation effects in the calculation of line strengths. In these cases, the corresponding $\log gf$ and gA values could be very inaccurate and therefore need to be considered with some care. As mentioned above, no radiative rates were previously published for the copper ions considered in our work except Cu VI, for which theoretical oscillator strengths were recently reported by Aggarwal et al. (2016), who used the quasi-relativistic approach (QR) with a very large configuration interaction expansion. When comparing these latter results with ours, we found an overall good agreement, in particular for the strongest lines with $\log gf > -1$, for which the mean deviation between the two sets of data was found to be about 20 %, with a general tendency such that our $\log gf$ values appear systematically slightly higher than those of Aggarwal et al. (2016).

4. Results and conclusions

We calculated oscillator strengths of Cu^{IV}-vii and compiled oscillator strengths of In^{IV} (Varshney & Tauheed 2013; Ryabtsev & Kononov 2016), In^V (Varshney & Tauheed 2016a,b; Ryabtsev 2018), and In^{VI} (Kononov et al. 2017; Ryabtsev et al. 2018) from the literature. These elements were included in our model-atmosphere calculations.

To unambiguously identify lines of one individual species, we calculated two spectra for each star (RE 0503–289 and G191–B2B), one with all opacities of that element included and one with its line opacities switched off artificially (cf. Figs. 3, 4, and 5). This enables us to identify Cu and In lines, even if they are blended with other lines (cf. Tables A.1, A.2, and A.3) or if they reduce the flux without exhibiting a complete line profile.

RE 0503–289. We identified 54 Cu lines (1 Cu^{IV}, 51 Cu^V, and 2 Cu^{VI}; Fig. 3, Table A.1) and 5 In^V lines (Fig. 4, Table A.2). From a detailed line-profile comparison of our model ($T_{\text{eff}} = 70\,000\,\text{K}$ and $\log g = 7.5$) with the UV observations, we found the best simultaneous agreement for all identified Cu and In lines at abundances of $9.3^{+3.0}_{-2.0} \times 10^{-5}$ (mass fraction, 132 times solar) and $3.0^{+0.5}_{-0.5} \times 10^{-6}$ (56 600 times solar), respectively. The T_{eff} and $\log g$ error propagation is evaluated from two models at the error limits with highest and lowest degree of ionization, i.e., $T_{\text{eff}} = 72\,000\,\text{K}$ and $\log g = 7.4$) and $T_{\text{eff}} = 68\,000\,\text{K}$ and $\log g = 7.6$), respectively. We found that this abundance error is smaller than 0.1 dex. Finally, we adopted the above Cu and In mass fractions with uncertainties of 0.2 dex.

G191–B2B. The four strongest Cu^V lines and/or blends in the synthetic spectrum are identified in the observation (Fig. 5, Table A.3). They are well reproduced by a model ($T_{\text{eff}} = 60\,000\,\text{K}$, $\log g = 7.6$) with a Cu mass fraction of $6.3^{+3.0}_{-2.0} \times 10^{-6}$ (nine times solar). The error estimation is performed analogously to that of RE 0503–289 (see above) and we found the same uncertainty of 0.2 dex.

No In line can be identified in the UV observation of G191–B2B. We used two of the strongest lines, namely In^V $\lambda\lambda 1334.123, 1339.599\,\text{\AA}$, to determine an upper abundance limit of 5.3×10^{-7} (mass fraction, 1000 times solar; Fig. 6).

To summarize, the determined Cu and In abundances closely match the already known TIE abundance patterns in G191–B2B and RE 0503–289 (Fig. 7), which is the result of effective radiative levitation (Rauch et al. 2016a). The TIE enrichment is much stronger in RE 0503–289 compared to that in G191–B2B due to the lower T_{eff} of the latter (Fig. 1, $T_{\text{eff}} = 60\,000 \pm 2000\,\text{K}$ and $\log g = 7.6 \pm 0.05$, Rauch et al. 2013). The relative TIE abundances in RE 0503–289, however, obviously resemble the relative solar abundance ratios (Fig. 7, cf. $29 \leq Z \leq 36$ and $49 \leq Z \leq 54$), i.e., higher abundances for species with even Z compared to those with odd Z (Oddo-Harkins rule, Oddo 1914; Harkins 1917).

Surface abundance patterns that are the result of diffusion (cf. Fig. 7) and exhibit strong TIE enrichment are also found recently in He-sdOs, e.g., LS IV–14°116 (Naslim et al. 2011), in Feige 46 (Latour et al. 2019), in HD 127493 and HZ 44, (Dorsch et al. 2019), and in the DAO-type star BD–22°3467 (Löbling et al. 2019). However, Hoyer et al. (2017) and Rauch et al. (2019) have already mentioned that strong radiative levitation of trans-iron TIEs wipes out all information about their AGB abundances, and thus previous stellar evolution. This is general for all species in all stars with a diffusion impact on their surface abundances.

Among the WDs, RE 0503–289 exhibits lines from an unrivaled number of TIEs: 18 species (<http://astro.uni-tuebingen.de/~TVIS/objects/RE0503-289>). Many more lines in the UV spectral region remain unidentified. Calculations of transition probabilities of other TIEs are necessary to make further progress.

Acknowledgements. The GAVO project had been supported by the Federal Ministry of Education and Research (BMBF) at Tübingen (05 AC 6 VTB, 05 AC 11 VTB) and is funded at Heidelberg (05 A 17 VH2). Financial support from the Belgian FRS-FNRS is also acknowledged. PQ is research director of this organization. Some of the data presented in this paper were obtained from the Mikulski Archive for Space Telescopes (MAST). STScI is operated by the Association of Universities for Research in Astronomy, Inc., under NASA contract NAS5-26555. Support for MAST for non-HST data is provided by the NASA Office of Space Science via grant NNX09AF08G and by other grants and contracts. The TIRO (<http://astro.uni-tuebingen.de/~TIRO>), TMAD (<http://astro.uni-tuebingen.de/~TMAD>), TOSS (<http://astro.uni-tuebingen.de/~TOSS>), and TVIS (<http://astro.uni-tuebingen.de/~TVIS>) tools and services were constructed as part of the Tübingen project (<https://uni-tuebingen.de/de/122430>) of the German Astrophysical Virtual Observatory (GAVO, <http://www.g-vo.org>). This research has made use of NASA's Astrophysics Data System and the SIMBAD database, operated at CDS, Strasbourg, France.

References

- Aggarwal, K. M., Bogdanovich, P., Keenan, F. P., & Kisielius, R. 2016, Atomic Data and Nuclear Data Tables, 111, 280
- Althaus, L. G., Panei, J. A., Miller Bertolami, M. M., et al. 2009, ApJ, 704, 1605
- Asplund, M., Grevesse, N., Sauval, A. J., & Scott, P. 2009, ARA&A, 47, 481
- Cowan, R. D. 1981, The theory of atomic structure and spectra (Berkeley, CA, University of California Press)
- Cowley, C. R. 1970, The theory of stellar spectra (Gordon & Breach, New York)
- Cowley, C. R. 1971, The Observatory, 91, 139
- Dorsch, M., Latour, M., & Heber, U. 2019, A&A, 630, A130
- Dreizler, S. & Werner, K. 1996, A&A, 314, 217
- Fraga, S., Karwowski, J., & Saxena, K. M. S. 1976, Handbook of Atomic Data (Elsevier, Amsterdam)
- Grevesse, N., Scott, P., Asplund, M., & Sauval, A. J. 2015, A&A, 573, A27
- Harkins, W. D. 1917, The Evolution of the Elements and the Stability of Complex Atoms. I. A New Periodic System Which Shows a Relation Between the Abundance of the Elements and the Structure of the Nuclei of Atoms.
- Hoyer, D., Rauch, T., Werner, K., Kruk, J. W., & Quinet, P. 2017, A&A, 598, A135
- Hubeny, I., Hummer, D. G., & Lanz, T. 1994, A&A, 282, 151
- Hügelmeyer, S. D., Dreizler, S., Homeier, D., et al. 2006, A&A, 454, 617
- Hummer, D. G. & Mihalas, D. 1988, ApJ, 331, 794
- Kepler, S. O., Pelisoli, I., Koester, D., et al. 2016, MNRAS, 455, 3413
- Kononov, E. Y., Kildiyarova, R. R., Ryabtsev, A. N., et al. 2017, in European Physical Journal Web of Conferences, Vol. 132, 03023
- Kramida, A., Ralchenko, Y., Reader, J., & NIST ASD Team. 2019, in NIST Atomic Spectra Database (version 5.7.1), [Online]. Available: <https://physics.nist.gov/asd> [Wed Mar 18 2020]. National Institute of Standards and Technology, Gaithersburg, MD. DOI: <https://doi.org/10.18434/T4W30F>, Vol. 2019
- Latour, M., Dorsch, M., & Heber, U. 2019, A&A, 629, A148
- Lemoine, M., Vidal-Madjar, A., Hébrard, G., et al. 2002, ApJS, 140, 67
- Löbling, L., Maney, M. A., Rauch, T., et al. 2019, MNRAS, 2831
- McCook, G. P. & Sion, E. M. 1999a, ApJS, 121, 1
- McCook, G. P. & Sion, E. M. 1999b, VizieR Online Data Catalog, 3210, 0
- Meinders, E. 1976, Physica B+C, 84, 117
- Meinders, E. & Uijlings, P. 1980, Physica B+C, 100, 389
- Miller Bertolami, M. M. 2016, A&A, 588, A25
- Müller-Ringat, E. 2013, Dissertation, University of Tübingen, Germany, <http://nbn-resolving.de/urn:nbn:de:bsz:21-opus-67747>
- Naslim, N., Jeffery, C. S., Behara, N. T., & Hibbert, A. 2011, MNRAS, 412, 363
- Oddo, G. 1914, Zeitschrift für anorganische Chemie, 87, 253
- Poppe, R., Van Kleef, T. A. M., & Raassen, A. J. J. 1974, Physica, 77, 165
- Quinet, P. 2017, Canadian Journal of Physics, 95, 790
- Quinet, P., Palmeri, P., Biémont, É., et al. 2002, J. Alloys Comp., 344, 255
- Quinet, P., Palmeri, P., Biémont, É., et al. 1999, MNRAS, 307, 934
- Raassen, A. J. J. & Van Kleef, T. A. M. 1981, Physica B+C, 103, 412
- Rauch, T. & Deetjen, J. L. 2003, in Astronomical Society of the Pacific Conference Series, Vol. 288, Stellar Atmosphere Modeling, ed. I. Hubeny, D. Mihalas, & K. Werner, 103

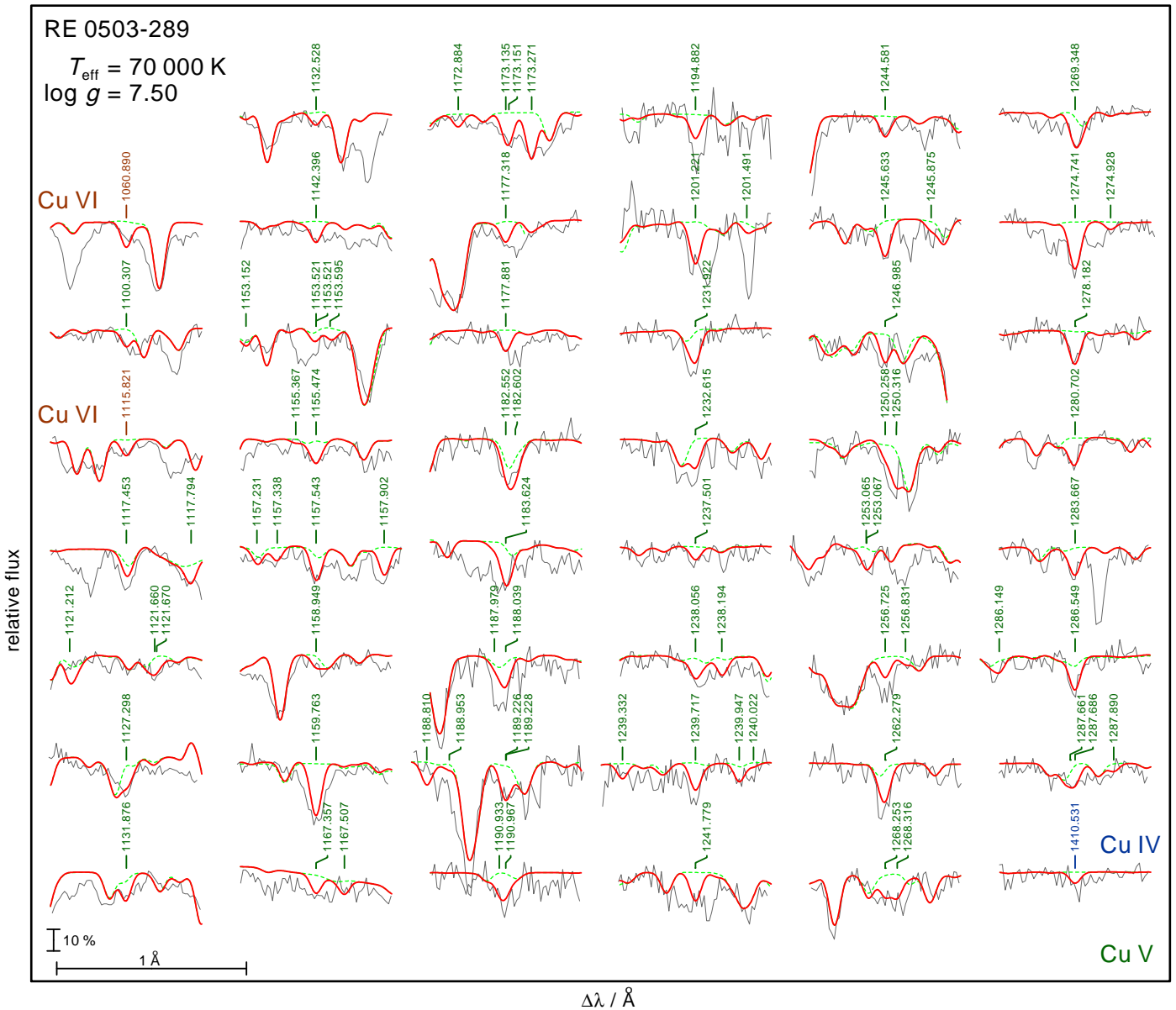


Fig. 3. Prominent Cu lines in the observation (gray line) of RE 0503–289, labeled with their wavelengths from Tables A.13, A.14, and A.15. Cu vi $\lambda\lambda 1060.890, 1100.307 \text{ \AA}$, and Cu iv $\lambda 1410.531 \text{ \AA}$ are indicated with an additional ion label, all other lines stem from Cu v. For the identification of other lines that are visible in the spectrum, please visit <http://astro.uni-tuebingen.de/~TVIS/objects/RE0503-289>, our Tübingen VISualization Tool (TVIS). The thick red spectrum is calculated from our best model with a Cu mass fraction of 9.3×10^{-5} . The dashed green line shows a synthetic spectrum calculated without Cu. The vertical bar indicates 10 % of the continuum flux.

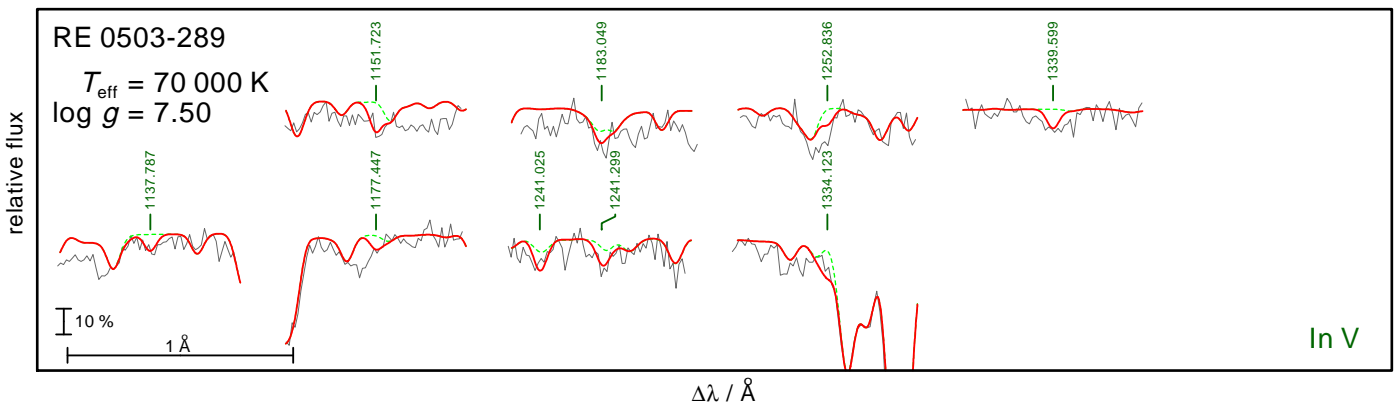


Fig. 4. Same as Fig. 3, but for In. Lines are labeled with their wavelengths from Table A.2. The synthetic spectrum is calculated with an In mass fraction of 3.0×10^{-6} .

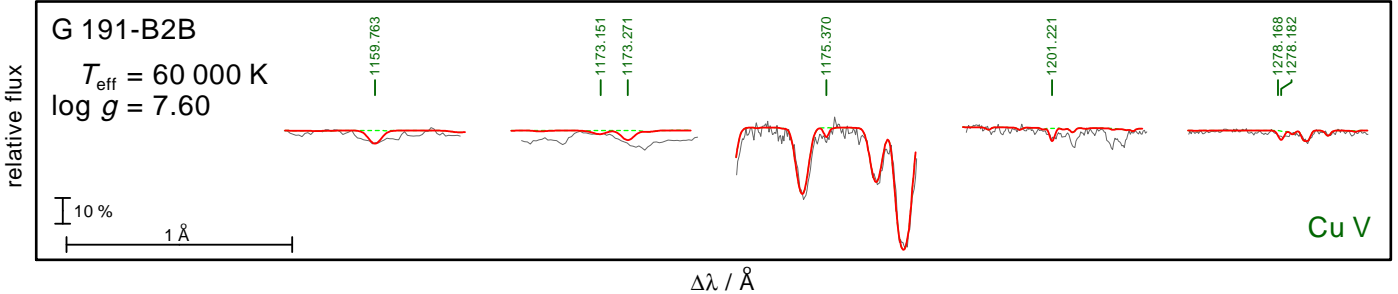


Fig. 5. Same as Fig. 3, but for G191–B2B.

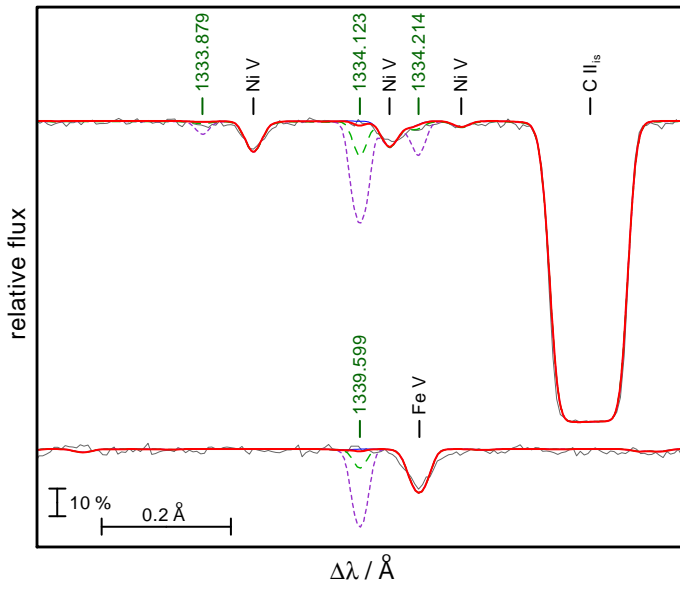


Fig. 6. STIS observation of G191–B2B (gray) compared with synthetic line profiles of In V λ 1334.123 Å and In VI λ 1339.599 Å calculated with four In abundances: without (thin blue line), with 1000 times (thick red), 10 000 times (short-dashed violet), and 100 000 times solar abundance (long-dashed green).

- Rauch, T., Gamrath, S., Quinet, P., et al. 2019, Astronomical Society of the Pacific Conference Series, Vol. 519, Heavy-metal Abundances in DO-type White Dwarfs (Astronomical Society of the Pacific), 175
 Rauch, T., Gamrath, S., Quinet, P., et al. 2017a, *A&A*, 599, A142
 Rauch, T., Hoyer, D., Quinet, P., Gallardo, M., & Raineri, M. 2015a, *A&A*, 577, A88
 Rauch, T., Quinet, P., Hoyer, D., et al. 2016a, *A&A*, 587, A39
 Rauch, T., Quinet, P., Hoyer, D., et al. 2016b, *A&A*, 590, A128
 Rauch, T., Quinet, P., Knörzer, M., et al. 2017b, *A&A*, 606, A105
 Rauch, T., Werner, K., Biémont, É., Quinet, P., & Kruk, J. W. 2012, *A&A*, 546, A55
 Rauch, T., Werner, K., Bohlin, R., & Kruk, J. W. 2013, *A&A*, 560, A106
 Rauch, T., Werner, K., Quinet, P., & Kruk, J. W. 2014a, *A&A*, 564, A41
 Rauch, T., Werner, K., Quinet, P., & Kruk, J. W. 2014b, *A&A*, 566, A10
 Rauch, T., Werner, K., Quinet, P., & Kruk, J. W. 2015b, *A&A*, 577, A6
 Reindl, N., Rauch, T., Werner, K., et al. 2014a, *A&A*, 572, A117
 Reindl, N., Rauch, T., Werner, K., Kruk, J. W., & Todt, H. 2014b, *A&A*, 566, A116
 Ryabtsev, A. N. 2018, *J. Quant. Spec. Radiat. Transf.*, 220, 106
 Ryabtsev, A. N. & Kononov, E. Y. 2016, *J. Quant. Spec. Radiat. Transf.*, 168, 89
 Ryabtsev, A. N., Tauheed, A., Swapnil, Kildiyarova, R. R., & Kononov, E. Y. 2018, *J. Quant. Spec. Radiat. Transf.*, 212, 50
 Schröder, J. F. & van Kleef, T. A. M. 1970, *Physica*, 49, 388
 Scott, P., Asplund, M., Grevesse, N., Bergemann, M., & Sauval, A. J. 2015a, *A&A*, 573, A26
 Scott, P., Grevesse, N., Asplund, M., et al. 2015b, *A&A*, 573, A25
 Seaton, M. J. 1962, in *Atomic and Molecular Processes*, ed. D. R. Bates (Academic Press, New York), 375
 Sugar, J. & Musgrove, A. 1990, *Journal of Physical and Chemical Reference Data*, 19, 527

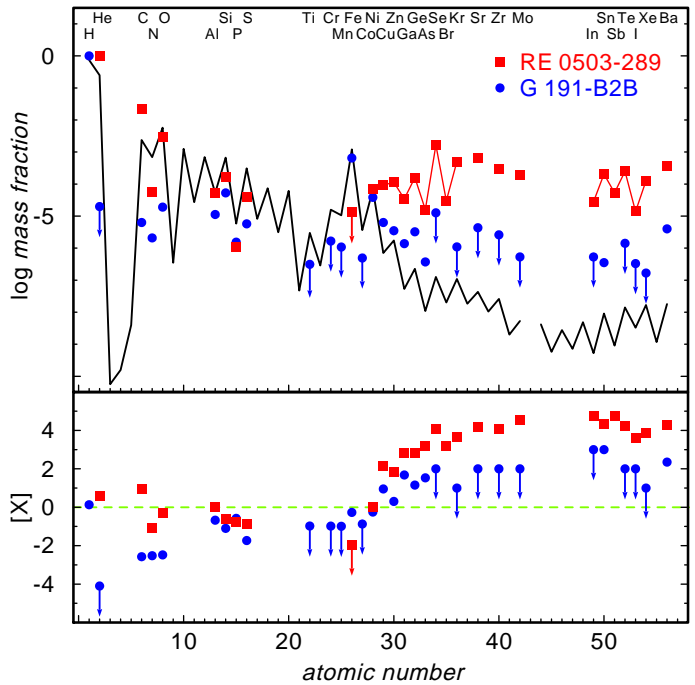


Fig. 7. Solar abundances (Asplund et al. 2009; Scott et al. 2015b,a; Grevesse et al. 2015, thick black line) compared with the determined photospheric abundances of G191–B2B (blue circles, Rauch et al. 2013, and this work) and RE 0503–289 (red squares, Dreizler & Werner 1996; Rauch et al. 2012, 2014a,b, 2015b, 2016a,b, 2017a,b, and this work). The uncertainties of the abundances are about 0.2 dex in general. Arrows indicate upper limits. Top panel: Abundances given as logarithmic mass fractions. Determined TIE abundances of subsequent species are combined with lines. Bottom panel: Abundance ratios to respective solar values, [X] denotes log (fraction / solar fraction) of species X. The dashed green line indicates solar abundances.

- Unglaub, K. & Bues, I. 2000, *A&A*, 359, 1042
 van het Hof, G. J., Raassen, A. J. J., Uylings, P. H. M., et al. 1990, *Physica Scripta*, 41, 240
 van Kleef, T. A. M., Joshi, Y. N., & Benschop, H. 1975, *Canadian Journal of Physics*, 53, 230
 van Kleef, T. A. M., Raasen, A. J. J., & Joshi, Y. N. 1976, *Physica B+C*, 84, 401
 van Regemorter, H. 1962, *ApJ*, 136, 906
 Varshney, S. & Tauheed, A. 2013, *J. Quant. Spec. Radiat. Transf.*, 129, 31
 Varshney, S. & Tauheed, A. 2016a, *J. Quant. Spec. Radiat. Transf.*, 168, 102
 Varshney, S. & Tauheed, A. 2016b, *J. Quant. Spec. Radiat. Transf.*, 168, 102
 Werner, K., Dreizler, S., & Rauch, T. 2012a, TMAP: Tübingen NLTE Model-Atmosphere Package, Astrophysics Source Code Library [record ascl:1212.015]
 Werner, K. & Herwig, F. 2006, *PASP*, 118, 183
 Werner, K., Rauch, T., Ringat, E., & Kruk, J. W. 2012b, *ApJ*, 753, L7

Appendix A: Additional tables

Table A.1. Identified Cu iv-vi lines in the UV spectrum of RE 0503–289.

Ion	Wavelength	$\log g_{\text{f},\text{fik}}$	Lower level			Upper level			Comment
			Energy cm ⁻¹	Parity	J	Energy cm ⁻¹	Parity	J	
Cu vi	1060.890	0.38	250877	e	3.0	345137	o	4.0	
Cu v	1100.307	-0.52	187779	e	4.5	278663	o	3.5	
Cu vi	1115.821	0.24	265639	e	2.0	355259	o	3.0	
Cu v	1117.453	-0.50	190100	e	1.5	279590	o	1.5	blend with Zn v λ 1117.466 Å
	1117.794	-0.28	188833	e	3.5	278295	o	2.5	
	1121.212	-0.39	190400	e	0.5	279590	o	1.5	too strong in model
	1121.660	-0.06	228048	e	4.5	317201	o	4.5	blend with Cu v λ 1121.670 Å
	1121.670	-0.22	265752	e	4.5	354905	o	3.5	blend with Cu v λ 1121.660 Å
	1127.298	-0.36	189587	e	2.5	278295	o	2.5	blend with strong unidentified line
	1131.876	0.21	227801	e	5.5	316149	o	5.5	
	1132.528	-0.25	221272	e	3.5	309570	o	2.5	
	1142.396	-0.41	188833	e	3.5	276368	o	3.5	
	1153.521	0.22	278380	e	3.5	365071	o	3.5	blend of two Cu v λ 1153.521 Å lines
	1153.521	0.14	272801	e	2.5	359492	o	2.5	blend of two Cu v λ 1153.521 Å lines
	1153.595	-0.30	236059	e	2.5	322744	o	3.5	
	1155.474	0.32	236331	e	3.5	322876	o	4.5	
	1157.231	-0.18	236331	e	3.5	322744	o	3.5	blend with Sr v λ 1157.230 Å, weak
	1157.338	0.03	236059	e	2.5	322464	o	3.5	
	1157.543	0.55	238234	e	6.5	324624	o	6.5	blend with Sr v λ 1157.580 Å
	1157.902	0.48	238305	e	5.5	324668	o	5.5	
	1158.949	-0.74	187779	e	4.5	274065	o	4.5	blend with Ni vi $\lambda\lambda$ 1158.998, 1159.000 Å and Ni v $\lambda\lambda$ 1159.023, 1159.035 Å, uncertain
	1159.763	0.52	187779	e	4.5	274004	o	5.5	
	1167.357	0.25	222401	e	4.5	308065	o	5.5	
	1167.507	0.32	234036	e	4.5	319689	o	4.5	
	1173.135	-0.11	221664	e	1.5	306906	o	2.5	blend with Cu v λ 1173.151 Å
	1173.151	-0.22	188833	e	3.5	274073	o	3.5	blend with Cu v λ 1173.135 Å
	1173.271	0.39	188833	e	3.5	274065	o	4.5	
	1177.318	0.08	222886	e	3.5	307825	o	4.5	blend with strong unidentified line
	1177.881	-0.19	200648	e	2.5	285546	o	1.5	blend with strong unidentified line
	1182.552	0.14	227543	e	4.5	312106	o	5.5	blend with O iii λ 1182.471 Å
	1182.602	-0.18	189587	e	2.5	274146	o	2.5	blend with O iii λ 1182.471 Å
	1183.624	0.15	189587	e	2.5	274073	o	3.5	blend with strong unidentified line
	1187.979	-0.45	236040	e	1.5	320216	o	0.5	blend with strong unidentified line, N iv λ 1188.005 Å, Cu v λ 1188.039 Å
	1188.039	0.27	226311	e	5.5	310483	o	5.5	blend with strong unidentified line, Cu v λ 1187.979 Å, N iv λ 1188.005 Å
	1189.226	0.21	227801	e	5.5	311889	o	6.5	blend with Cu v λ 1189.228 Å
	1189.228	-0.23	190100	e	1.5	274189	o	1.5	blend with Cu v λ 1189.226 Å
	1190.933	-0.01	228105	e	2.5	312073	o	3.5	blend with Cu v λ 1190.967 Å
	1190.967	0.25	239541	e	4.5	323506	o	5.5	blend with Cu v λ 1190.933 Å
	1194.882	0.24	227543	e	4.5	311233	o	4.5	blend with strong unidentified line
	1201.221	0.64	220208	e	6.5	303456	o	7.5	
	1231.922	0.63	238234	e	6.5	319408	o	7.5	blend with Sr iv λ 1231.878 Å
	1232.615	0.27	220208	e	6.5	301336	o	6.5	blend with Fe vi λ 1232.477 Å
	1237.501	-0.20	222401	e	4.5	303209	o	3.5	
	1238.056	-0.13	201850	e	0.5	282622	o	1.5	
	1238.194	-0.07	220623	e	5.5	301386	o	4.5	
	1239.332	0.02	230532	e	2.5	311220	o	3.5	
	1239.717	0.22	220623	e	5.5	301286	o	5.5	
	1239.947	-0.09	220938	e	4.5	301587	o	3.5	

Table A.1. continued.

Ion	Wavelength Å	$\log g_{\text{ijk}}$	Lower level			Upper level			Comment
			Energy cm^{-1}	Parity	J	Energy cm^{-1}	Parity	J	
	1241.779	0.08	201413	e	1.5	281942	o	2.5	blend with strong unidentified lines
	1244.581	0.05	220938	e	4.5	301286	o	5.5	
	1245.633	0.26	200648	e	2.5	280929	o	3.5	
	1246.985	0.32	220208	e	5.5	300401	o	6.5	
	1250.258	-0.15	221272	e	3.5	301255	o	3.5	blend with Cu v λ 1250.316 Å
	1250.316	0.39	199441	e	3.5	279421	o	4.5	blend with Cu v λ 1250.258 Å
	1253.065	0.18	239615	e	3.5	319419	o	4.5	blend with Cu v λ 1253.067 Å
	1253.067	-0.26	228105	e	2.5	307910	o	2.5	blend with Cu v λ 1253.065 Å
	1256.725	0.13	226311	e	5.5	305883	o	6.5	blend with strong unidentified line
	1256.831	-0.53	221272	e	3.5	300837	o	4.5	weak
	1262.279	0.19	199441	e	3.5	278663	o	3.5	blend with Zn v λ 1262.252 Å
	1268.253	-0.15	200648	e	2.5	279497	o	2.5	blend with Cu v λ 1268.316 Å
	1268.316	-0.15	200648	e	2.5	279497	o	2.5	blend with Cu v λ 1268.253 Å
	1269.348	-0.10	187779	e	4.5	266560	o	3.5	blend with N III λ 1269.412 Å
	1274.741	0.39	187779	e	4.5	266227	o	4.5	
	1274.928	-0.50	222401	e	4.5	300837	o	4.5	weak
	1278.182	-0.04	188833	e	3.5	267069	o	2.5	
	1280.702	0.24	227801	e	5.5	305883	o	6.5	
	1283.667	-0.12	189587	e	2.5	267489	o	1.5	
	1286.549	-0.01	188833	e	3.5	266560	o	3.5	blend with Sr v λ 1286.544 Å
	1287.661	-0.77	239541	e	4.5	317201	o	4.5	blend with Ga IV λ 1287.548 Å, Zn v λ 1287.644 Å
Cu IV	1287.686	-0.36	190100	e	1.5	267759	o	0.5	
	1410.531	0.47	119632	e	5.0	190528	o	5.0	weak

Table A.2. Same as Table A.1, but for In v.

Ion	Wavelength / Å	$\log g_i f_{ik}$	Lower level			Upper level			Comment
			Energy/cm ⁻¹	Parity	J	Energy/cm ⁻¹	Parity	J	
In v	1137.787	-0.09	163980	e	3.5	251868	o	4.5	
	1151.723	0.33	160428	e	4.5	247254	o	4.5	blend with Zn v λ 1151.787 Å
	1177.447	-0.01	167761	e	2.5	252691	o	2.5	weak
	1183.049	0.11	163980	e	3.5	248507	o	3.5	blend with Zn v $\lambda\lambda$ 1183.041, 1183.100 Å Ga v λ 1183.110 Å
	1241.025	0.39	171290	e	3.5	251868	o	4.5	blend with Ni v $\lambda\lambda$ 1241.015, 1241.047 Å
	1241.299	0.59	188396	e	4.5	268957	o	5.5	blend with O iii $\lambda\lambda$ 1241.125, 1241.176 Å
	1252.836	0.03	163980	e	3.5	243798	o	3.5	blend with Ni v λ 1252.765 Å
	1334.123	0.37	160428	e	4.5	235384	o	3.5	blend with interstellar C ii, weak
	1339.599	0.17	163980	e	3.5	238629	o	4.5	

Notes. The wavelengths, weighted oscillator strengths, and energies correspond to those in Varshney & Tauheed (2016a,b) and Ryabtsev (2018).

Table A.3. Same as Table A.1, but for G191–B2B.

Ion	Wavelength / Å	$\log g_i f_{ik}$	Lower level			Upper level			Comment
			Energy/cm ⁻¹	Parity	J	Energy/cm ⁻¹	Parity	J	
Cu v	1159.763	0.52	187779	e	4.5	274004	o	5.5	
	1173.151	-0.22	188833	e	3.5	274073	o	3.5	weak
	1173.271	0.39	188833	e	3.5	274065	o	4.5	blend with unidentified line
	1175.370	0.09	199441	e	3.5	284521	o	2.5	
	1201.221	0.64	220208	e	6.5	303456	o	7.5	
	1278.168	-0.49	229588	e	3.5	307825	o	4.5	blend with Cu v λ 1278.182 Å
	1278.182	-0.04	188833	e	3.5	267069	o	2.5	blend with Cu v λ 1278.168 Å

Table A.4. Ions with recently calculated oscillator strengths.

Cu	IV - VII	Rauch et al. this paper
Zn	IV - V	Rauch et al. (2014a)
Ga	IV - VI	Rauch et al. (2015b)
Ge	V - VI	Rauch et al. (2012)
Se	V	Rauch et al. (2017b)
Kr	IV - VII	Rauch et al. (2016b)
Sr	IV - VII	Rauch et al. (2017b)
Zr	IV - VII	Rauch et al. (2017a)
Mo	IV - VII	Rauch et al. (2016a)
Te	VI	Rauch et al. (2017b)
I	VI	Rauch et al. (2017b)
Xe	IV - V, VII	Rauch et al. (2015a, 2017a)
Ba	V - VII	Rauch et al. (2014b)

Table A.5. Radial parameters (in cm⁻¹) adopted for the calculations in Cu iv.

Configuration	Parameter	HFR	Fitted	Ratio	Note ^a
Even parity					
3d ⁸	E _{av}	17190	16729		
	F ² (3d,3d)	112092	98330	0.877	
	F ⁴ (3d,3d)	69989	60209	0.860	
	α	0	91		
	β	0	-237		
	ζ_{3d}	903	910	1.007	
3d ⁷ 4s	E _{av}	147324	152124		
	F ² (3d,3d)	118491	103197	0.871	
	F ⁴ (3d,3d)	74277	65197	0.878	
	α	0	99		
	β	0	-350		
	ζ_{3d}	978	979	1.001	
	G ² (3d,4s)	12035	10802	0.898	
3d ⁷ 5s	E _{av}	325664	330393		
	F ² (3d,3d)	119486	102897	0.861	
	F ⁴ (3d,3d)	74953	65472	0.874	
	α	0	100	F	
	β	0	-350	F	
	ζ_{3d}	986	986	1.000	F
	G ² (3d,4s)	2897	2608	0.900	F
3d ⁷ 4d	E _{av}	312783	320069		
	F ² (3d,3d)	119438	103540	0.867	
	F ⁴ (3d,3d)	74922	64201	0.857	
	α	0	73		
	β	0	361		
	ζ_{3d}	985	1021	1.037	
	ζ_{4d}	68	68	1.000	F
	F ² (3d,4d)	13224	12461	0.942	
	F ⁴ (3d,4d)	5529	5503	0.995	
	G ⁰ (3d,4d)	5169	3754	0.726	R
	G ² (3d,4d)	5040	3660	0.726	R
	G ⁴ (3d,4d)	3651	2651	0.726	R
3d ⁶ 4s ²	E _{av}	334825	345297		
	F ² (3d,3d)	124695	112225	0.900	F
	F ⁴ (3d,3d)	78447	70603	0.900	F
	α	0	0	F	
	β	0	0	F	
	ζ_{3d}	1056	1056	1.000	F
Odd parity					
3d ⁷ 4p	E _{av}	218061	224378		
	F ² (3d,3d)	118845	103882	0.874	
	F ⁴ (3d,3d)	74519	64989	0.872	
	α	0	101		
	β	0	-313		
	ζ_{3d}	980	1005	1.026	
	ζ_{4p}	1185	1383	1.168	
	F ² (3d,4p)	23861	22879	0.959	
	G ¹ (3d,4p)	8425	7395	0.878	
	G ³ (3d,4p)	7571	7132	0.942	

^a F: parameter fixed to its *ab initio* value; R: ratios of these parameters have been fixed in the fitting process

Table A.6. continued.

Configuration	Parameter	HFR	Fitted	Ratio	Note ^a
---------------	-----------	-----	--------	-------	-------------------

Table A.6. Radial parameters (in cm⁻¹) adopted for the calculations in Cu v.

Configuration	Parameter	HFR	Fitted	Ratio	Note ^a
Even parity					
3d ⁷	E _{av}	30899	30322		
	F ² (3d,3d)	119816	105551	0.881	
	F ⁴ (3d,3d)	75176	65503	0.871	
	α	0	109		
	β	0	-587		
	ζ_{3d}	989	1002	1.013	
3d ⁶ 4s	E _{av}	234957	237924		
	F ² (3d,3d)	125814	110315	0.877	
	F ⁴ (3d,3d)	79209	67072	0.847	
	α	0	117		
	β	0	-154		
	ζ_{3d}	1066	1154	1.082	
	G ² (3d,4s)	12797	11794	0.922	
Odd parity					
3d ⁶ 4p	E _{av}	316597	319750		
	F ² (3d,3d)	126094	109170	0.866	
	F ⁴ (3d,3d)	79402	66055	0.832	
	α	0	114		
	β	0	213		
	ζ_{3d}	1069	1180	1.104	
	ζ_{4p}	1596	1816	1.137	
	F ² (3d,4p)	28011	26960	0.962	
	G ¹ (3d,4p)	9612	9190	0.956	
	G ³ (3d,4p)	8916	7838	0.879	

Table A.7. Radial parameters (in cm⁻¹) adopted for the calculations in Cu vi.

Configuration	Parameter	HFR	Fitted	Ratio	Note ^a
Even parity					
3d ⁶	E _{av}	47058	46817		
	F ² (3d,3d)	127114	112843	0.888	
	F ⁴ (3d,3d)	80096	69557	0.868	
	α	0	103		
	β	0	-264		
	ζ_{3d}	1080	1142	1.057	
3d ⁵ 4s	E _{av}	332771	334360		
	F ² (3d,3d)	132805	116707	0.879	
	F ⁴ (3d,3d)	83932	74133	0.883	
	α	0	100	F	
	β	0	-250	F	
	ζ_{3d}	1161	1161	1.000	F
	G ² (3d,4s)	13493	12647	0.937	
Odd parity					
3d ⁵ 4p	E _{av}	424263	425870		
	F ² (3d,3d)	133032	116189	0.873	
	F ⁴ (3d,3d)	84088	72010	0.856	
	α	0	127		
	β	0	-286		
	ζ_{3d}	1163	1247	1.073	
	ζ_{4p}	2028	2320	1.144	

Table A.7. continued.

Configuration Parameter	HFR	Fitted	Ratio	Note ^a
$F^2(3d,4p)$	31832	30768	0.967	
$G^1(3d,4p)$	10697	10190	0.953	
$G^3(3d,4p)$	10151	9203	0.907	

^a F: parameter fixed to its *ab initio* value

Table A.8. Radial parameters (in cm⁻¹) adopted for the calculations in Cu vii.

Configuration Parameter	HFR	Fitted	Ratio	Note ^a
Even parity				
3d ⁵	E_{av}	78756	78522	
	$F^2(3d,3d)$	134086	119456	0.891
	$F^4(3d,3d)$	84807	74397	0.877
	α	0	118	
	β	0	-512	
	ζ_{3d}	1176	1202	1.022
Odd parity				
3d ⁴ 4p	E_{av}	553653	554223	
	$F^2(3d,3d)$	139722	123787	0.886
	$F^4(3d,3d)$	88617	78219	0.883
	α	0	123	
	β	0	-380	
	ζ_{3d}	1263	1121	0.888
	ζ_{4p}	2481	2647	1.067
	$F^2(3d,4p)$	35417	34983	0.988
	$G^1(3d,4p)$	11725	11199	0.955
	$G^3(3d,4p)$	11316	11458	1.013

Table A.9. Comparison between available experimental and calculated energy levels in Cu iv. Energies are given in cm⁻¹.

E_{exp}^a	E_{calc}^b	ΔE	J	Leading components (in %) in LS coupling ^c
Even parity				
0.0	8	-8	4 99	3d ⁸ ³ F
1861.4	1857	4	3 99	3d ⁸ ³ F
3077.6	3074	4	2 98	3d ⁸ ³ F
16248.0	16238	10	2 82	3d ⁸ ¹ D + 17 3d ⁸ ³ P
19696.6	19750	-53	2 82	3d ⁸ ³ P + 17 3d ⁸ ¹ D
20096.6	20072	25	1 99	3d ⁸ ³ P
20422.6	20405	18	0 99	3d ⁸ ³ P
26913.0	26912	1	4 99	3d ⁸ ¹ G
61456.4	61456	0	0 98	3d ⁸ ¹ S
119632.4	119747	-115	5 99	3d ⁷ (⁴ F)4s ⁵ F
120918.7	120980	-61	4 99	3d ⁷ (⁴ F)4s ⁵ F
121929.8	121955	-25	3 99	3d ⁷ (⁴ F)4s ⁵ F
122663.8	122666	-2	2 99	3d ⁷ (⁴ F)4s ⁵ F
123139.8	123128	12	1 99	3d ⁷ (⁴ F)4s ⁵ F
128343.3	128356	-13	4 98	3d ⁷ (⁴ F)4s ³ F
130060.3	130024	36	3 99	3d ⁷ (⁴ F)4s ³ F
131218.6	131157	62	2 99	3d ⁷ (⁴ F)4s ³ F
139695.3	139522	173	3 99	3d ⁷ (⁴ P)4s ⁵ P
140065.7	139952	114	2 96	3d ⁷ (⁴ P)4s ⁵ P
140715.0	140603	112	1 97	3d ⁷ (⁴ P)4s ⁵ P

Table A.9. continued.

E_{exp}^a	E_{calc}^b	ΔE	J	Leading components (in %) in LS coupling ^c
144065.9	143959	107	5	97 $3d^7(^2G)4s\ ^3G$
144749.0	144616	133	4	94 $3d^7(^2G)4s\ ^3G$
145579.9	145422	158	3	99 $3d^7(^2G)4s\ ^3G$
147736.6	147668	69	2	77 $3d^7(^4P)4s\ ^3P + 18\ 3d^7(^2P)4s\ ^3P$
147929.8	148006	-76	1	71 $3d^7(^4P)4s\ ^3P + 15\ 3d^7(^2P)4s\ ^3P + 11\ 3d^7(^2P)4s\ ^1P$
148233.8	148438	-204	0	67 $3d^7(^4P)4s\ ^3P + 33\ 3d^7(^2P)4s\ ^3P$
148860.7	148746	115	4	90 $3d^7(^2H)4s\ ^1G + 5\ 3d^7(^2H)4s\ ^3H$
148903.6	149198	-294	2	65 $3d^7(^2P)4s\ ^3P + 22\ 3d^7(^4P)4s\ ^3P + 7\ 3d^7(^2D)4s\ ^3D$
149667.2	149962	-295	1	67 $3d^7(^2P)4s\ ^3P + 21\ 3d^7(^4P)4s\ ^3P + 8\ 3d^7(^2D)4s\ ^3D$
151622.7	151769	-146	6	100 $3d^7(^2H)4s\ ^3H$
152231.7	152012	220	3	77 $3d^7(^2D)4s\ ^3D + 22\ 3d^7(^2D)4s\ ^3D$
152301.7	152407	-105	5	95 $3d^7(^2H)4s\ ^3H$
152400.2	152648	-248	1	38 $3d^7(^2D)4s\ ^3D + 35\ 3d^7(^2P)4s\ ^1P + 14\ 3d^7(^2P)4s\ ^3P$
153198.2	153260	-62	4	92 $3d^7(^2H)4s\ ^3H + 6\ 3d^7(^2G)4s\ ^1G$
153375.7	153186	190	2	65 $3d^7(^2D)4s\ ^3D + 17\ 3d^7(^2D)4s\ ^3D + 8\ 3d^7(^2P)4s\ ^3P$
155476.7	155645	-168	1	54 $3d^7(^2P)4s\ ^1P + 33\ 3d^7(^2D)4s\ ^3D + 7\ 3d^7(^2D)4s\ ^3D$
156458.7	156584	-125	5	96 $3d^7(^2H)4s\ ^1H$
157536.1	157257	279	2	71 $3d^7(^2D)4s\ ^1D + 18\ 3d^7(^2D)4s\ ^1D + 5\ 3d^7(^2D)4s\ ^3D$
170066.5	169989	78	2	99 $3d^7(^2F)4s\ ^3F$
170277.7	170245	33	3	98 $3d^7(^2F)4s\ ^3F$
170619.0	170661	-42	4	99 $3d^7(^2F)4s\ ^3F$
174831.3	174625	206	3	98 $3d^7(^2F)4s\ ^1F$
196853.5	196964	-111	1	80 $3d^7(^2D)4s\ ^3D + 19\ 3d^7(^2D)4s\ ^3D$
197138.5	197228	-90	2	78 $3d^7(^2D)4s\ ^3D + 20\ 3d^7(^2D)4s\ ^3D$
197659.5	197695	-36	3	77 $3d^7(^2D)4s\ ^3D + 22\ 3d^7(^2D)4s\ ^3D$
201771.0	201650	121	2	77 $3d^7(^2D)4s\ ^1D + 21\ 3d^7(^2D)4s\ ^1D$
287319.5	287391	-72	5	90 $3d^7(^4F)4d\ ^5F + 8\ 3d^7(^4F)4d\ ^5G$
287589.3	287966	-377	4	78 $3d^7(^4F)4d\ ^5F + 11\ 3d^7(^4F)4d\ ^5D + 7\ 3d^7(^4F)4d\ ^5G$
288566.4	288677	-111	3	70 $3d^7(^4F)4d\ ^5F + 14\ 3d^7(^4F)4d\ ^5D + 6\ 3d^7(^4F)4d\ ^5P$
288697.8	288687	11	6	94 $3d^7(^4F)4d\ ^5G + 6\ 3d^7(^4F)4d\ ^5H$
289370.2	289474	-104	2	82 $3d^7(^4F)4d\ ^5F + 9\ 3d^7(^4F)4d\ ^5D$
289529.7	289613	-83	3	74 $3d^7(^4F)4d\ ^5P + 12\ 3d^7(^4F)4d\ ^5F + 9\ 3d^7(^4F)4d\ ^5D$
289572.9	289542	31	5	66 $3d^7(^4F)4d\ ^5G + 20\ 3d^7(^4F)4d\ ^3G + 7\ 3d^7(^4F)4d\ ^5H$
289641.5	289963	-322	4	58 $3d^7(^4F)4d\ ^5D + 18\ 3d^64s^2\ ^5D + 16\ 3d^7(^4F)4d\ ^5G$
289688.2	289700	-12	7	99 $3d^7(^4F)4d\ ^5H$
289974.0	290076	-102	1	93 $3d^7(^4F)4d\ ^5F$
290445.4	290416	29	6	60 $3d^7(^4F)4d\ ^5H + 36\ 3d^7(^4F)4d\ ^3H$
290552.8	290575	-22	4	60 $3d^7(^4F)4d\ ^5G + 13\ 3d^7(^4F)4d\ ^5F + 10\ 3d^7(^4F)4d\ ^3G$
290773.5	290933	-160	2	54 $3d^7(^4F)4d\ ^5P + 29\ 3d^7(^4F)4d\ ^5D + 7\ 3d^7(^4F)4d\ ^5F$
290885.1	291074	-189	3	48 $3d^7(^4F)4d\ ^5G + 24\ 3d^7(^4F)4d\ ^5D + 9\ 3d^7(^4F)4d\ ^5P$
291147.3	291004	143	5	70 $3d^7(^4F)4d\ ^3G + 20\ 3d^7(^4F)4d\ ^5G + 6\ 3d^7(^4F)4d\ ^3H$
291298.7	291394	-95	3	37 $3d^7(^4F)4d\ ^5G + 21\ 3d^7(^4F)4d\ ^5D + 8\ 3d^64s^2\ ^5D$
291561.6	291570	-8	5	79 $3d^7(^4F)4d\ ^5H + 12\ 3d^7(^4F)4d\ ^3H + 5\ 3d^7(^4F)4d\ ^3G$
291570.8	291841	-270	1	55 $3d^7(^4F)4d\ ^5D + 27\ 3d^7(^4F)4d\ ^5P + 13\ 3d^64s^2\ ^5D$
291730.0	291745	-15	2	92 $3d^7(^4F)4d\ ^5G$
291865.0	291764	101	6	63 $3d^7(^4F)4d\ ^3H + 34\ 3d^7(^4F)4d\ ^5H$
291953.9	292147	-193	3	75 $3d^7(^4F)4d\ ^3D + 9\ 3d^7(^4F)4d\ ^5D + 6\ 3d^64s^2\ ^5D$
291997.1	292224	-227	2	39 $3d^7(^4F)4d\ ^5P + 36\ 3d^7(^4F)4d\ ^5D + 14\ 3d^64s^2\ ^5D$
292296.7	292187	110	4	65 $3d^7(^4F)4d\ ^3G + 16\ 3d^7(^4F)4d\ ^5G + 8\ 3d^7(^4F)4d\ ^5H$
292440.0	292414	26	4	79 $3d^7(^4F)4d\ ^5H + 16\ 3d^7(^4F)4d\ ^3G$
292639.1	292782	-143	1	71 $3d^7(^4F)4d\ ^5P + 19\ 3d^7(^4F)4d\ ^5D + 8\ 3d^64s^2\ ^5D$
292913.3	292946	-33	3	89 $3d^7(^4F)4d\ ^5H + 6\ 3d^7(^4F)4d\ ^5G$
293021.7	293176	-154	2	84 $3d^7(^4F)4d\ ^3D + 6\ 3d^7(^4F)4d\ ^3P$
293399.2	293267	132	5	80 $3d^7(^4F)4d\ ^3H + 14\ 3d^7(^4F)4d\ ^5H$
293513.5	293352	162	3	88 $3d^7(^4F)4d\ ^3G + 6\ 3d^7(^4F)4d\ ^5H$
294015.3	294184	-169	1	95 $3d^7(^4F)4d\ ^3D$

Table A.9. continued.

E_{exp}^a	E_{calc}^b	ΔE	J	Leading components (in %) in LS coupling ^c
294152.0	294269	-117	4	72 3d ⁶ 4s ² 5D + 21 3d ⁷ (⁴ F)4d 5D
294464.4	294316	148	4	89 3d ⁷ (⁴ F)4d 3H + 5 3d ⁷ (⁴ F)4d 5H
295307.8	295383	-75	3	72 3d ⁶ 4s ² 5D + 22 3d ⁷ (⁴ F)4d 5D
295910.4	295840	70	4	80 3d ⁷ (⁴ F)4d 3F + 7 3d ⁷ (² G)4d 3F
296040.3	296106	-66	2	71 3d ⁶ 4s ² 5D + 21 3d ⁷ (⁴ F)4d 5D
296494.2	296559	-65	1	73 3d ⁶ 4s ² 5D + 20 3d ⁷ (⁴ F)4d 5D
296573.4	296474	99	2	81 3d ⁷ (⁴ F)4d 3P + 5 3d ⁷ (⁴ F)4d 3D + 5 3d ⁷ (⁴ P)4d 3P
296912.3	296847	65	3	78 3d ⁷ (⁴ F)4d 3F + 7 3d ⁷ (² G)4d 3F
297554.4	297481	73	2	78 3d ⁷ (⁴ F)4d 3F + 8 3d ⁷ (² G)4d 3F
297931.0	297840	91	1	88 3d ⁷ (⁴ F)4d 3P + 6 3d ⁷ (⁴ P)4d 3P
301632.0	301720	-88	5	99 3d ⁷ (⁴ F)5s 5F
302682.3	302741	-59	4	82 3d ⁷ (⁴ F)5s 5F + 17 3d ⁷ (⁴ F)5s 3F
303798.4	303819	-21	3	91 3d ⁷ (⁴ F)5s 5F + 7 3d ⁷ (⁴ F)5s 3F
304244.9	304274	-29	4	82 3d ⁷ (⁴ F)5s 3F + 17 3d ⁷ (⁴ F)5s 5F
304599.7	304601	-1	2	96 3d ⁷ (⁴ F)5s 5F
305116.0	305106	10	1	98 3d ⁷ (⁴ F)5s 5F
305856.0	305842	14	3	91 3d ⁷ (⁴ F)5s 3F + 7 3d ⁷ (⁴ F)5s 5F
306941.8	306904	38	2	96 3d ⁷ (⁴ F)5s 3F
306982.5	306884	99	1	98 3d ⁷ (⁴ P)4d 5P
307167.0	307089	78	2	97 3d ⁷ (⁴ P)4d 5P
307517.3	307459	58	3	95 3d ⁷ (⁴ P)4d 5P
309413.9	309295	119	5	97 3d ⁷ (⁴ P)4d 5F
309490.4	309427	63	4	91 3d ⁷ (⁴ P)4d 5F
309653.1	309630	23	3	88 3d ⁷ (⁴ P)4d 5F
309864.7	309874	-9	2	88 3d ⁷ (⁴ P)4d 5F
310057.1	310095	-38	1	89 3d ⁷ (⁴ P)4d 5F + 5 3d ⁷ (² P)4d 3D
310800.2	310865	-65	3	80 3d ⁷ (² G)4d 3D + 5 3d ⁷ (⁴ P)4d 3F
311010.7	311031	-20	3	51 3d ⁷ (⁴ P)4d 3F + 23 3d ⁷ (² G)4d 1F + 5 3d ⁷ (² P)4d 1F
311177.0	311018	159	4	81 3d ⁷ (⁴ P)4d 3F + 9 3d ⁷ (² G)4d 3F
311274.0	311367	-93	2	44 3d ⁷ (² G)4d 3D + 30 3d ⁷ (⁴ P)4d 3F + 5 3d ⁷ (² P)4d 3D
311628.0	311504	124	7	95 3d ⁷ (² G)4d 3I
311726.7	311911	-184	1	37 3d ⁷ (⁴ P)4d 3P + 24 3d ⁷ (² G)4d 3D + 11 3d ⁷ (² P)4d 3P
311742.9	311630	113	6	67 3d ⁷ (² G)4d 3I + 24 3d ⁷ (² G)4d 1I
311998.3	312124	-126	5	61 3d ⁷ (² G)4d 3G + 20 3d ⁷ (² G)4d 3H + 11 3d ⁷ (² G)4d 3I
312061.4	312033	28	2	51 3d ⁷ (⁴ P)4d 3F + 30 3d ⁷ (² G)4d 3D + 5 3d ⁷ (⁴ P)4d 3P
312082.5	312061	22	3	56 3d ⁷ (² G)4d 1F + 22 3d ⁷ (⁴ P)4d 3F + 9 3d ⁷ (² G)4d 3D
312415.5	312373	43	5	37 3d ⁷ (² G)4d 3I + 31 3d ⁷ (² G)4d 3G + 16 3d ⁷ (² G)4d 1H
312466.7	312609	-142	4	65 3d ⁷ (² G)4d 3G + 18 3d ⁷ (⁴ P)4d 5D + 6 3d ⁷ (² G)4d 3H
312514.9	312454	61	6	75 3d ⁷ (² G)4d 3H + 20 3d ⁷ (² G)4d 1I
312601.5	312713	-112	2	34 3d ⁷ (⁴ P)4d 5D + 33 3d ⁷ (⁴ P)4d 3P + 9 3d ⁷ (² G)4d 3D
312629.9	312676	-46	4	74 3d ⁷ (⁴ P)4d 5D + 15 3d ⁷ (² G)4d 3G
312956.8	312990	-33	3	86 3d ⁷ (⁴ P)4d 5D
313253.3	313249	4	5	50 3d ⁷ (² G)4d 3I + 29 3d ⁷ (² G)4d 3H + 19 3d ⁷ (² G)4d 1H
313257.0	313454	-197	3	93 3d ⁷ (² G)4d 3G
313294.7	313245	50	2	56 3d ⁷ (⁴ P)4d 5D + 20 3d ⁷ (⁴ P)4d 3P + 7 3d ⁷ (⁴ P)4d 3D
313715.4	313602	113	6	53 3d ⁷ (² G)4d 1I + 28 3d ⁷ (² G)4d 3I + 18 3d ⁷ (² G)4d 3H
313871.5	313936	-65	4	89 3d ⁷ (² G)4d 3H + 9 3d ⁷ (² G)4d 3G
314262.2	314282	-20	5	59 3d ⁷ (² G)4d 1H + 36 3d ⁷ (² G)4d 3H
314987.8	315132	-144	4	50 3d ⁷ (² G)4d 3F + 14 3d ⁷ (² G)4d 1G + 8 3d ⁷ (² P)4d 3F
315450.0	314164	1286	3	84 3d ⁷ (⁴ P)4d 3D
315598.5	315602	-4	4	58 3d ⁷ (² G)4d 1G + 12 3d ⁷ (² H)4d 1G + 11 3d ⁷ (² G)4d 3F
315846.0	315136	710	2	47 3d ⁷ (² G)4d 1D + 11 3d ⁷ (² P)4d 1D + 8 3d ⁷ (² G)4d 3F
315912.2	315663	249	3	59 3d ⁷ (² G)4d 3F + 9 3d ⁷ (² P)4d 3F + 7 3d ⁷ (² H)4d 3F
316191.7	316424	-232	2	59 3d ⁷ (² G)4d 3F + 10 3d ⁷ (² H)4d 3F + 9 3d ⁷ (² P)4d 3F
316732.3	317512	-780	4	43 3d ⁷ (² P)4d 3F + 25 3d ⁷ (² H)4d 3F + 10 3d ⁷ (² D)4d 3F
317017.0	316886	131	3	68 3d ⁷ (² P)4d 3D + 7 3d ⁷ (² D)4d 3F + 5 3d ⁷ (² D)4d 3D

Table A.9. continued.

E_{exp}^a	E_{calc}^b	ΔE	J	Leading components (in %) in LS coupling ^c
317810.5	317611	200	3	26 3d ⁷ (² P)4d ¹ F + 22 3d ⁷ (² H)4d ³ F + 10 3d ⁷ (² P)4d ³ F
318452.4	318293	159	8	100 3d ⁷ (² H)4d ³ K
318510.0	318355	155	7	60 3d ⁷ (² H)4d ³ K + 39 3d ⁷ 4d (² H) ¹ K
318746.1	318838	-92	5	94 3d ⁷ (² H)4d ³ G
319268.4	318617	651	3	37 3d ⁷ (² H)4d ¹ F + 28 3d ⁷ 4d (² P) ³ F + 7 3d ⁷ (² H)4d ³ G
319586.7	319643	-56	4	43 3d ⁷ (² H)4d ³ G + 19 3d ⁷ 4d (² D) ³ F + 10 3d ⁷ (² H)4d ³ F
319703.7	319596	108	6	95 3d ⁷ (² H)4d ³ K
319896.1	320030	-134	4	41 3d ⁷ (² H)4d ³ G + 20 3d ⁷ 4d (² D) ³ F + 11 3d ⁷ (² P)4d ³ F
319992.7	319604	389	3	28 3d ⁷ (² D)4d ³ D + 26 3d ⁷ 4d (² H) ¹ F + 14 3d ⁷ (² P)4d ¹ F
320141.7	319962	180	7	59 3d ⁷ (² H)4d ¹ K + 37 3d ⁷ 4d (² H) ³ K
320601.1	320611	-10	6	58 3d ⁷ (² H)4d ³ H + 39 3d ⁶ 4s ² ³ H
320781.7	320746	36	5	73 3d ⁷ (² D)4d ³ G + 21 3d ⁷ 4d (² D) ³ G
320952.7	320917	36	4	38 3d ⁷ (² D)4d ¹ G + 30 3d ⁷ 4d (² D) ³ G + 11 3d ⁷ (² D)4d ¹ F
321064.0	321082	-18	5	50 3d ⁷ (² H)4d ³ H + 29 3d ⁶ 4s ² ³ H + 15 3d ⁷ (² H)4d ¹ H
321135.1	321194	-59	7	99 3d ⁷ (² H)4d ³ I
321542.1	321586	-44	6	82 3d ⁷ (² H)4d ³ I + 14 3d ⁷ 4d (² H) ¹ I
322051.3	322028	23	3	35 3d ⁷ (² D)4d ¹ F + 16 3d ⁷ 4d (² D) ³ F + 10 3d ⁷ (² D)4d ¹ F
322317.4	322358	-41	5	47 3d ⁷ (² H)4d ³ I + 33 3d ⁷ 4d (² H) ¹ H + 14 3d ⁶ 4s ² ³ H
322338.2	322156	182	3	95 3d ⁷ (⁴ P)5s ⁵ P
322524.0	322670	-146	5	46 3d ⁷ (² H)4d ³ I + 45 3d ⁷ 4d (² H) ¹ H
322608.1	322491	117	2	93 3d ⁷ (⁴ P)5s ⁵ P + 6 3d ⁷ 5s (² P) ³ P
323155.3	323377	-222	4	27 3d ⁷ (² D)4d ³ G + 24 3d ⁷ 4d (² D) ¹ G + 16 3d ⁷ (² P)4d ³ F
323249.0	323131	118	1	79 3d ⁷ (⁴ P)5s ⁵ P + 5 3d ⁷ 4d (² D) ³ D
323754.8	323586	169	6	44 3d ⁷ (² H)4d ¹ I + 32 3d ⁶ 4s ² ³ H + 18 3d ⁷ (² H)4d ³ H
324118.1	323759	359	6	38 3d ⁷ (² H)4d ¹ I + 22 3d ⁶ 4s ² ³ H + 22 3d ⁷ (² H)4d ³ H
324418.7	324414	5	2	75 3d ⁷ (⁴ P)5s ³ P + 9 3d ⁶ 4s ² ³ P + 6 3d ⁶ 4s ² ³ P
324619.3	324222	397	5	44 3d ⁶ 4s ² ³ H + 41 3d ⁷ 4d (² H) ³ H
324731.4	324455	276	4	45 3d ⁶ 4s ² ³ H + 42 3d ⁷ 4d (² H) ³ H
324759.9	324572	188	5	95 3d ⁷ (² G)5s ³ G
325225.9	325037	189	4	75 3d ⁷ (² G)5s ³ G + 17 3d ⁷ 5s (² G) ¹ G
326247.5	326050	198	3	99 3d ⁷ (² G)5s ³ G
326979.8	326764	216	4	69 3d ⁷ (² G)5s ¹ G + 21 3d ⁷ 5s (² G) ³ G
327356.7	327318	39	4	42 3d ⁷ (² H)4d ³ F + 13 3d ⁷ 4d (² D) ³ F + 9 3d ⁷ (² G)4d ³ F
328720.0	328760	-40	3	39 3d ⁷ (² H)4d ³ F + 12 3d ⁷ 4d (² D) ³ F + 11 3d ⁷ (² G)4d ³ F
329181.7	329441	-259	2	34 3d ⁷ (² H)4d ³ F + 12 3d ⁷ 4d (² G) ³ F + 11 3d ⁷ (² D)4d ³ F
329341.2	329712	-371	2	77 3d ⁷ (² P)5s ³ P + 8 3d ⁷ 5s (² D) ³ D + 5 3d ⁷ (⁴ P)5s ⁵ P
329632.8	330121	-488	1	51 3d ⁷ (² P)5s ³ P + 24 3d ⁷ 5s (² P) ¹ P + 14 3d ⁷ (² D)5s ³ D
331041.9	331669	-627	1	53 3d ⁷ (² P)5s ¹ P + 39 3d ⁷ 5s (² P) ³ P
332035.9	332203	-167	4	61 3d ⁷ (² H)4d ¹ G + 13 3d ⁷ 4d (² F) ¹ G + 11 3d ⁷ (² G)4d ¹ G
332436.4	332584	-148	6	99 3d ⁷ (² H)5s ³ H
332854.7	332986	-131	5	78 3d ⁷ (² H)5s ³ H + 20 3d ⁷ 5s (² H) ¹ H
333005.7	332799	207	3	77 3d ⁷ (² D)5s ³ D + 22 3d ⁷ 5s (² D) ³ D
333736.7	333127	610	2	27 3d ⁷ (² D)5s ³ D + 27 3d ⁷ 5s (² D) ¹ D + 8 3d ⁷ (² D)5s ¹ D
333868.7	333962	-93	4	95 3d ⁷ (² H)5s ³ H
334564.8	334649	-84	5	78 3d ⁷ (² H)5s ¹ H + 19 3d ⁷ (² H)5s ³ H
335885.5	335708	178	2	44 3d ⁷ (² D)5s ¹ D + 22 3d ⁷ (² D)5s ³ D + 11 3d ⁷ (² P)5s ³ P
338974.8	339070	-95	5	88 3d ⁷ (² F)4d ³ H + 8 3d ⁷ (² F)4d ¹ H
339378.8	339547	-168	6	96 3d ⁷ (² F)4d ³ H
339392.7	339687	-294	3	86 3d ⁷ (² F)4d ³ G + 6 3d ⁷ (² F)4d ¹ F
339763.8	340079	-315	4	89 3d ⁷ (² F)4d ³ G
339808.5	339916	-108	5	90 3d ⁷ (² F)4d ¹ H + 8 3d ⁷ (² F)4d ³ H
340161.9	340554	-392	5	94 3d ⁷ (² F)4d ³ G
347248.7	347352	-103	4	81 3d ⁷ (² F)4d ¹ G + 7 3d ⁷ (² H)4d ¹ G
351520.2	351425	95	3	93 3d ⁷ (² F)5s ³ F + 6 3d ⁷ (² F)5s ¹ F
351908.8	351901	8	4	99 3d ⁷ (² F)5s ³ F

Odd parity

Table A.9. continued.

E_{exp}^a	E_{calc}^b	ΔE	J	Leading components (in %) in LS coupling ^c
190527.7	190558	-30	5 91	$3d^7(^4F)4p\ ^5F + 7\ 3d^7(^4F)4p\ ^5G$
190553.6	190616	-62	4 54	$3d^7(^4F)4p\ ^5F + 38\ 3d^7(^4F)4p\ ^5D$
191761.8	191801	-39	3 70	$3d^7(^4F)4p\ ^5F + 23\ 3d^7(^4F)4p\ ^5D$
192741.0	192763	-22	2 83	$3d^7(^4F)4p\ ^5F + 12\ 3d^7(^4F)4p\ ^5D$
192752.8	192764	-11	4 51	$3d^7(^4F)4p\ ^5D + 34\ 3d^7(^4F)4p\ ^5F + 9\ 3d^7(^4F)4p\ ^5G$
193434.4	193443	-9	1 93	$3d^7(^4F)4p\ ^5F + 5\ 3d^7(^4F)4p\ ^5D$
193947.8	193923	25	6 99	$3d^7(^4F)4p\ ^5G$
194132.4	194149	-17	3 63	$3d^7(^4F)4p\ ^5D + 18\ 3d^7(^4F)4p\ ^5F + 11\ 3d^7(^4F)4p\ ^5G$
194339.1	194309	30	5 75	$3d^7(^4F)4p\ ^5G + 16\ 3d^7(^4F)4p\ ^3G + 9\ 3d^7(^4F)4p\ ^5F$
195054.9	195010	45	4 78	$3d^7(^4F)4p\ ^5G + 10\ 3d^7(^4F)4p\ ^5F + 7\ 3d^7(^4F)4p\ ^3G$
195085.9	195114	-28	2 71	$3d^7(^4F)4p\ ^5D + 11\ 3d^7(^4F)4p\ ^5G + 9\ 3d^7(^4F)4p\ ^5F$
195544.1	195496	48	3 80	$3d^7(^4F)4p\ ^5G + 10\ 3d^7(^4F)4p\ ^5F$
195684.3	195732	-48	1 84	$3d^7(^4F)4p\ ^5D + 10\ 3d^7(^4P)4p\ ^5D + 5\ 3d^7(^4F)4p\ ^5F$
195827.0	195780	47	2 84	$3d^7(^4F)4p\ ^5G + 6\ 3d^7(^4F)4p\ ^5F + 6\ 3d^7(^4F)4p\ ^5D$
195932.0	195990	-58	0 88	$3d^7(^4F)4p\ ^5D + 11\ 3d^7(^4P)4p\ ^5D$
197325.0	197340	-15	5 81	$3d^7(^4F)4p\ ^3G + 18\ 3d^7(^4F)4p\ ^5G$
198179.2	198209	-30	4 88	$3d^7(^4F)4p\ ^3F$
199202.3	199214	-12	4 86	$3d^7(^4F)4p\ ^3G + 10\ 3d^7(^4F)4p\ ^5G$
199598.8	199633	-34	3 84	$3d^7(^4F)4p\ ^3F + 5\ 3d^7(^4F)4p\ ^3D$
200482.6	200497	-14	3 92	$3d^7(^4F)4p\ ^3G$
200720.0	200734	-14	2 89	$3d^7(^4F)4p\ ^3F + 5\ 3d^7(^2G)4p\ ^3F$
201210.9	201378	-167	3 87	$3d^7(^4F)4p\ ^3D + 6\ 3d^7(^4F)4p\ ^3F$
202360.6	202528	-167	2 88	$3d^7(^4F)4p\ ^3D$
203139.5	203306	-167	1 90	$3d^7(^4F)4p\ ^3D$
203868.9	203936	-67	2 97	$3d^7(^4P)4p\ ^5S$
213360.4	213346	14	1 57	$3d^7(^4P)4p\ ^5D + 11\ 3d^7(^2P)4p\ ^3P + 10\ 3d^7(^4P)4p\ ^3S$
213534.5	213340	195	2 76	$3d^7(^4P)4p\ ^5D + 9\ 3d^7(^4F)4p\ ^5D$
213664.9	213412	253	3 78	$3d^7(^4P)4p\ ^5D + 8\ 3d^7(^4F)4p\ ^5D + 7\ 3d^7(^4P)4p\ ^3D$
213932.1	213784	148	0 82	$3d^7(^4P)4p\ ^5D + 11\ 3d^7(^4F)4p\ ^5D + 6\ 3d^7(^2P)4p\ ^3P$
214318.7	214025	294	4 89	$3d^7(^4P)4p\ ^5D + 6\ 3d^7(^4F)4p\ ^5D$
214413.4	214464	-51	1 42	$3d^7(^4P)4p\ ^3S + 25\ 3d^7(^4P)4p\ ^5D + 10\ 3d^7(^2P)4p\ ^3S$
214835.3	214638	197	5 67	$3d^7(^2G)4p\ ^3H + 17\ 3d^7(^2G)4p\ ^1H + 10\ 3d^7(^2G)4p\ ^3G$
215132.8	214971	162	4 55	$3d^7(^2G)4p\ ^3F + 12\ 3d^7(^2G)4p\ ^3G + 8\ 3d^7(^2G)4p\ ^3H$
215733.9	215533	201	4 82	$3d^7(^2G)4p\ ^3H + 8\ 3d^7(^2G)4p\ ^3F$
216071.3	215829	242	6 95	$3d^7(^2G)4p\ ^3H$
216428.9	216928	-499	0 67	$3d^7(^2P)4p\ ^3P + 16\ 3d^7(^2D)4p\ ^3P + 6\ 3d^7(^2D)4p\ ^3P$
216702.9	217017	-314	2 31	$3d^7(^2P)4p\ ^3P + 34\ 3d^7(^4P)4p\ ^5P + 16\ 3d^7(^4P)4p\ ^3D$
217079.2	216916	163	3 73	$3d^7(^2G)4p\ ^3F + 16\ 3d^7(^2G)4p\ ^3G$
217109.3	217546	-437	1 48	$3d^7(^2P)4p\ ^3P + 18\ 3d^7(^4P)4p\ ^5P + 9\ 3d^7(^2D)4p\ ^3P$
217444.6	217385	60	4 46	$3d^7(^2G)4p\ ^1G + 25\ 3d^7(^2G)4p\ ^3F + 16\ 3d^7(^2H)4p\ ^1G$
217621.1	217294	327	3 54	$3d^7(^4P)4p\ ^5P + 29\ 3d^7(^4P)4p\ ^3D + 8\ 3d^7(^4P)4p\ ^5D$
217649.6	217743	-93	2 48	$3d^7(^4P)4p\ ^5P + 26\ 3d^7(^4P)4p\ ^3D + 5\ 3d^7(^2D)4p\ ^3D$
217999.5	217971	29	5 79	$3d^7(^2G)4p\ ^3G + 15\ 3d^7(^2G)4p\ ^1H$
218027.5	217915	113	2 13	$3d^7(^2P)4p\ ^1D + 28\ 3d^7(^2P)4p\ ^3P + 16\ 3d^7(^4P)4p\ ^3D$
218137.6	217882	256	3 48	$3d^7(^4P)4p\ ^3D + 34\ 3d^7(^4P)4p\ ^5P$
218170.7	217871	300	1 63	$3d^7(^4P)4p\ ^5P + 24\ 3d^7(^4P)4p\ ^3S$
218628.0	218499	129	3 45	$3d^7(^2G)4p\ ^3G + 31\ 3d^7(^2G)4p\ ^1F + 9\ 3d^7(^2G)4p\ ^3F$
218631.1	218617	14	1 64	$3d^7(^4P)4p\ ^3D + 18\ 3d^7(^2P)4p\ ^3D$
218726.2	218501	225	2 92	$3d^7(^2G)4p\ ^3F + 5\ 3d^7(^4F)4p\ ^3F$
218814.5	218633	182	5 63	$3d^7(^2G)4p\ ^1H + 27\ 3d^7(^2G)4p\ ^3H + 8\ 3d^7(^2G)4p\ ^3G$
218944.8	218965	-20	4 72	$3d^7(^2G)4p\ ^3G + 11\ 3d^7(^2G)4p\ ^1G + 8\ 3d^7(^2G)4p\ ^3H$
219402.7	219383	20	3 36	$3d^7(^2G)4p\ ^1F + 34\ 3d^7(^2G)4p\ ^3G + 8\ 3d^7(^2G)4p\ ^3F$
219867.4	220519	-652	0 49	$3d^7(^4P)4p\ ^3P + 39\ 3d^7(^2P)4p\ ^1S + 9\ 3d^7(^2P)4p\ ^3P$
220315.6	220202	114	2 66	$3d^7(^4P)4p\ ^3P + 11\ 3d^7(^2D)4p\ ^3P + 6\ 3d^7(^4P)4p\ ^5P$
220917.0	220971	-54	5 92	$3d^7(^2H)4p\ ^3G + 5\ 3d^7(^2F)4p\ ^3G$
221271.6	221206	66	1 67	$3d^7(^4P)4p\ ^3P + 16\ 3d^7(^2P)4p\ ^3D$

Table A.9. continued.

E_{exp}^a	E_{calc}^b	ΔE	J	Leading components (in %) in LS coupling ^c
221601.6	221713	-111	6 69	$3d^7(^2H)4p\ ^3I + 28\ 3d^7(^2H)4p\ ^1I$
221650.0	222030	-380	3 61	$3d^7(^2P)4p\ ^3D + 14\ 3d^7(^2D)4p\ ^3D + 6\ 3d^7(^2D)4p\ ^3D$
221738.5	221783	-45	2 22	$3d^7(^4P)4p\ ^3D + 18\ 3d^7(^4P)4p\ ^3P + 15\ 3d^7(^2P)4p\ ^1D$
222335.9	222349	-13	1 29	$3d^7(^2P)4p\ ^3D + 24\ 3d^7(^2D)4p\ ^3D + 20\ 3d^7(^4P)4p\ ^3P$
222397.7	222405	-7	4 87	$3d^7(^2H)4p\ ^3G + 6\ 3d^7(^2F)4p\ ^3G$
222527.4	222622	-95	5 93	$3d^7(^2H)4p\ ^3I$
222602.5	222746	-144	2 29	$3d^7(^2D)4p\ ^3D + 24\ 3d^7(^2P)4p\ ^3D + 10\ 3d^7(^2P)4p\ ^1D$
222665.8	222751	-85	7 100	$3d^7(^2H)4p\ ^3I$
223000.0	222545	455	3 47	$3d^7(^2D)4p\ ^3D + 17\ 3d^7(^2D)4p\ ^3F + 12\ 3d^7(^2D)4p\ ^3D$
223623.0	223580	43	3 79	$3d^7(^2H)4p\ ^3G + 6\ 3d^7(^2F)4p\ ^3G$
223764.1	223734	30	1 29	$3d^7(^2D)4p\ ^3D + 27\ 3d^7(^2P)4p\ ^3D + 18\ 3d^7(^2P)4p\ ^1P$
223847.4	224457	-610	0 56	$3d^7(^2P)4p\ ^1S + 43\ 3d^7(^4P)4p\ ^3P$
224070.6	224131	-60	2 34	$3d^7(^2P)4p\ ^3D + 22\ 3d^7(^2D)4p\ ^3D + 16\ 3d^7(^2P)4p\ ^1D$
224959.1	225045	-86	6 69	$3d^7(^2H)4p\ ^1I + 27\ 3d^7(^2H)4p\ ^3I$
225386.9	225131	256	4 77	$3d^7(^2D)4p\ ^3F + 20\ 3d^7(^2D)4p\ ^3F$
225858.9	225659	200	3 48	$3d^7(^2D)4p\ ^3F + 13\ 3d^7(^2P)4p\ ^3D + 11\ 3d^7(^2D)4p\ ^3F$
226271.3	226057	214	2 51	$3d^7(^2D)4p\ ^3F + 11\ 3d^7(^2D)4p\ ^3D + 10\ 3d^7(^2D)4p\ ^3F$
226558.0	227127	-569	1 39	$3d^7(^2P)4p\ ^1P + 24\ 3d^7(^2P)4p\ ^3S + 11\ 3d^7(^2D)4p\ ^3P$
227159.6	227375	-215	1 53	$3d^7(^2P)4p\ ^3S + 20\ 3d^7(^2P)4p\ ^1P + 9\ 3d^7(^4P)4p\ ^3S$
227959.5	227765	195	2 28	$3d^7(^2D)4p\ ^1D + 23\ 3d^7(^2D)4p\ ^3P + 22\ 3d^7(^2P)4p\ ^1D$
227993.2	228180	-187	6 97	$3d^7(^2H)4p\ ^3H$
228479.7	228640	-160	5 93	$3d^7(^2H)4p\ ^3H$
229064.0	229213	-149	4 94	$3d^7(^2H)4p\ ^3H$
229694.2	229500	194	2 34	$3d^7(^2D)4p\ ^3P + 19\ 3d^7(^2D)4p\ ^1D + 13\ 3d^7(^2P)4p\ ^3P$
230235.9	230367	-131	4 67	$3d^7(^2H)4p\ ^1G + 29\ 3d^7(^2G)4p\ ^1G$
230331.1	230057	274	3 56	$3d^7(^2D)4p\ ^1F + 17\ 3d^7(^2G)4p\ ^1F + 13\ 3d^7(^2D)4p\ ^1F$
231216.3	231151	65	1 49	$3d^7(^2D)4p\ ^3P + 14\ 3d^7(^2P)4p\ ^1P + 11\ 3d^7(^2P)4p\ ^3P$
231825.2	231633	192	0 65	$3d^7(^2D)4p\ ^3P + 17\ 3d^7(^2P)4p\ ^3P + 12\ 3d^7(^2D)4p\ ^3P$
232441.8	232271	171	1 72	$3d^7(^2D)4p\ ^1P + 12\ 3d^7(^2D)4p\ ^1P + 5\ 3d^7(^2P)4p\ ^3S$
233298.6	233428	-129	5 94	$3d^7(^2H)4p\ ^1H$
241854.9	241819	36	2 57	$3d^7(^2F)4p\ ^1D + 32\ 3d^7(^2F)4p\ ^3F + 5\ 3d^7(^2F)4p\ ^3D$
242529.8	242488	42	3 74	$3d^7(^2F)4p\ ^3G + 15\ 3d^7(^2F)4p\ ^3F + 7\ 3d^7(^2H)4p\ ^3G$
243028.9	243071	-42	4 60	$3d^7(^2F)4p\ ^3G + 21\ 3d^7(^2F)4p\ ^3F + 11\ 3d^7(^2F)4p\ ^1G$
243725.3	243724	1	3 49	$3d^7(^2F)4p\ ^3D + 34\ 3d^7(^2F)4p\ ^3F + 7\ 3d^7(^2F)4p\ ^3G$
244071.6	244091	-19	2 62	$3d^7(^2F)4p\ ^3F + 28\ 3d^7(^2F)4p\ ^1D + 5\ 3d^7(^2F)4p\ ^3D$
244417.1	244379	38	3 46	$3d^7(^2F)4p\ ^3F + 38\ 3d^7(^2F)4p\ ^3D + 8\ 3d^7(^2F)4p\ ^3G$
244671.4	244680	-9	5 93	$3d^7(^2F)4p\ ^3G + 6\ 3d^7(^2H)4p\ ^3G$
244753.1	244733	20	4 40	$3d^7(^2F)4p\ ^3F + 31\ 3d^7(^2F)4p\ ^3G + 24\ 3d^7(^2F)4p\ ^1G$
244812.8	244714	99	2 80	$3d^7(^2F)4p\ ^3D + 10\ 3d^7(^2F)4p\ ^1D$
244943.0	244768	175	1 90	$3d^7(^2F)4p\ ^3D + 5\ 3d^7(^2D)4p\ ^3D$
245204.3	245250	-46	4 63	$3d^7(^2F)4p\ ^1G + 33\ 3d^7(^2F)4p\ ^3F$
250622.8	250488	135	3 95	$3d^7(^2F)4p\ ^1F$
266196.5	266194	3	2 77	$3d^7(^2D)4p\ ^3P + 20\ 3d^7(^2D)4p\ ^3P$
266460.9	266482	-21	1 78	$3d^7(^2D)4p\ ^3P + 18\ 3d^7(^2D)4p\ ^3P$
266775.0	266786	-11	0 81	$3d^7(^2D)4p\ ^3P + 17\ 3d^7(^2D)4p\ ^3P$
268006.0	268109	-103	2 76	$3d^7(^2D)4p\ ^3F + 18\ 3d^7(^2D)4p\ ^3F$
268956.3	269006	-50	3 74	$3d^7(^2D)4p\ ^3F + 19\ 3d^7(^2D)4p\ ^3F$
270239.5	270255	-16	4 75	$3d^7(^2D)4p\ ^3F + 21\ 3d^7(^2D)4p\ ^3F$
272352.4	272380	-28	1 79	$3d^7(^2D)4p\ ^1P + 12\ 3d^7(^2D)4p\ ^1P$
272943.7	272785	159	3 74	$3d^7(^2D)4p\ ^1F + 20\ 3d^7(^2D)4p\ ^1F$
275672.9	275697	-24	1 71	$3d^7(^2D)4p\ ^3D + 21\ 3d^7(^2D)4p\ ^3D$
275970.3	276048	-78	2 61	$3d^7(^2D)4p\ ^3D + 18\ 3d^7(^2D)4p\ ^3D + 13\ 3d^7(^2D)4p\ ^1D$
276545.9	276677	-131	2 58	$3d^7(^2D)4p\ ^1D + 20\ 3d^7(^2D)4p\ ^1D + 12\ 3d^7(^2D)4p\ ^3D$
277108.7	277111	-2	3 70	$3d^7(^2D)4p\ ^3D + 24\ 3d^7(^2D)4p\ ^3D$

^a From NIST compilation (Kramida et al. 2019).

^b This work.

^c Only the first three components higher than or equal to 5% are given.

Table A.10. Comparison between available experimental and calculated energy levels in Cu v. Energies are given in cm⁻¹.

E_{exp}^a	E_{calc}^b	ΔE	J	Leading components (in %) in LS coupling ^c
Even parity				
0.0	136	-136	4.5 99	3d ⁷ 4F
1615.9	1715	-99	3.5 100	3d ⁷ 4F
2759.3	2840	-81	2.5 99	3d ⁷ 4F
3528.1	3596	-68	1.5 99	3d ⁷ 4F
20826.8	20622	205	2.5 99	3d ⁷ 4P
21065.9	20952	114	1.5 91	3d ⁷ 4P + 8 3d ⁷ 2P
21935.1	21818	117	0.5 96	3d ⁷ 4P
22575.3	22345	230	4.5 96	3d ⁷ 2G
24099.8	23858	242	3.5 99	3d ⁷ 2G
27015.9	27397	-381	1.5 76	3d ⁷ 2P + 13 3d ⁷ 2D + 8 3d ⁷ 4P
28366.6	28954	-587	0.5 96	3d ⁷ 2P
30401.7	30561	-159	5.5 100	3d ⁷ 2H
30966.0	30512	454	2.5 77	3d ⁷ 2D + 22 3d ⁷ 2D
31823.4	31946	-123	4.5 97	3d ⁷ 2H
33292.4	32954	338	1.5 67	3d ⁷ 2D + 16 3d ⁷ 2D + 16 3d ⁷ 2P
49490.0	49377	113	2.5 99	3d ⁷ 2F
50071.9	50070	2	3.5 99	3d ⁷ 2F
76838.2	76962	-124	1.5 80	3d ⁷ 2D + 19 3d ⁷ 2D
77668.0	77725	-57	2.5 77	3d ⁷ 2D + 22 3d ⁷ 2D
187779.4	187825	-46	4.5 99	3d ⁶ (⁵ D)4s 6D
188832.7	188907	-74	3.5 99	3d ⁶ (⁵ D)4s 6D
189586.9	189682	-95	2.5 99	3d ⁶ (⁵ D)4s 6D
190100.3	190210	-110	1.5 99	3d ⁶ (⁵ D)4s 6D
190400.3	190520	-120	0.5 99	3d ⁶ (⁵ D)4s 6D
199441.3	199411	30	3.5 99	3d ⁶ (⁵ D)4s 4D
200648.2	200665	-17	2.5 99	3d ⁶ (⁵ D)4s 4D
201412.8	201459	-46	1.5 99	3d ⁶ (⁵ D)4s 4D
201849.7	201913	-63	0.5 99	3d ⁶ (⁵ D)4s 4D
219203.4	219228	-25	2.5 60	3d ⁶ (³ P)4s 4P + 39 3d ⁶ (³ P)4s 4P
220207.8	220486	-278	6.5 99	3d ⁶ (³ H)4s 4H
220622.8	220820	-197	5.5 96	3d ⁶ (³ H)4s 4H
220938.1	221022	-84	4.5 84	3d ⁶ (³ H)4s 4H + 6 3d ⁶ (³ F)4s 4F + 6 3d ⁶ (³ G)4s 4G
221271.9	221321	-49	3.5 89	3d ⁶ (³ H)4s 4H
221664.1	221818	-154	1.5 56	3d ⁶ (³ P)4s 4P + 35 3d ⁶ (³ P)4s 4P
222401.3	222321	80	4.5 64	3d ⁶ (³ P)4s 4F + 19 3d ⁶ (³ F)4s 4F + 12 3d ⁶ (³ H)4s 4H
222885.7	222810	76	3.5 69	3d ⁶ (³ P)4s 4F + 19 3d ⁶ (³ F)4s 4F + 7 3d ⁶ (³ H)4s 4H
223214.2	223136	78	2.5 76	3d ⁶ (³ P)4s 4F + 19 3d ⁶ (³ F)4s 4F
223375.5	223571	-196	0.5 60	3d ⁶ (³ P)4s 4P + 37 3d ⁶ (³ P)4s 4P
223476.5	223428	49	1.5 80	3d ⁶ (³ F)4s 4F + 19 3d ⁶ (³ F)4s 4F
226310.8	226324	-13	5.5 67	3d ⁶ (³ G)4s 4G + 30 3d ⁶ (³ H)4s 2H
226888.8	227030	-141	1.5 56	3d ⁶ (³ P)4s 2P + 35 3d ⁶ (³ P)4s 2P + 5 3d ⁶ (³ P)4s 4P
227542.6	227577	-34	4.5 66	3d ⁶ (³ G)4s 4G + 25 3d ⁶ (³ H)4s 2H + 5 3d ⁶ (³ F)4s 4F
227800.5	228027	-227	5.5 68	3d ⁶ (³ H)4s 2H + 29 3d ⁶ (³ G)4s 4G
228020.3	227952	68	3.5 76	3d ⁶ (³ G)4s 4G + 10 3d ⁶ (³ F)4s 2F + 5 3d ⁶ (³ F)4s 4F
228047.5	228150	-103	4.5 68	3d ⁶ (³ H)4s 2H + 24 3d ⁶ (³ G)4s 4G + 5 3d ⁶ (³ G)4s 2G
228105.3	227973	132	2.5 83	3d ⁶ (³ G)4s 4G + 10 3d ⁶ (³ F)4s 2F
229587.5	229420	168	3.5 60	3d ⁶ (³ F)4s 2F + 17 3d ⁶ (³ F)4s 2F + 15 3d ⁶ (³ G)4s 4G
229773.6	229975	-201	0.5 58	3d ⁶ (³ P)4s 2P + 36 3d ⁶ (³ P)4s 2P
230531.7	230526	6	2.5 70	3d ⁶ (³ F)4s 2F + 17 3d ⁶ (³ F)4s 2F + 13 3d ⁶ (³ G)4s 4G
234036.4	234037	-1	4.5 94	3d ⁶ (³ G)4s 2G
235052.5	235044	9	3.5 93	3d ⁶ (³ G)4s 2G + 5 3d ⁶ (³ F)4s 2F
236039.8	235553	487	1.5 98	3d ⁶ (³ D)4s 4D
236058.9	235609	450	2.5 98	3d ⁶ (³ D)4s 4D
236108.8	235599	510	0.5 98	3d ⁶ (³ D)4s 4D

Table A.10. continued.

E_{exp}^a	E_{calc}^b	ΔE	J	Leading components (in %) in LS coupling ^c
236331.2	235900	431	3.5	99 $3d^6(^3D)4s\ ^4D$
238233.6	238377	-143	6.5	99 $3d^6(^1I)4s\ ^2I$
238305.2	238426	-121	5.5	98 $3d^6(^1I)4s\ ^2I$
239540.9	238438	1103	4.5	63 $3d^6(^1G)4s\ ^2G + 32\ 3d^6(^1G)4s\ ^2G$
239614.5	238499	1116	3.5	63 $3d^6(^1G)4s\ ^2G + 32\ 3d^6(^1G)4s\ ^2G$
243140.4	242661	479	2.5	97 $3d^6(^3D)4s\ ^2D$
246476.5	247554	-1078	2.5	75 $3d^6(^1D)4s\ ^2D + 21\ 3d^6(^1D)4s\ ^2D$
246624.3	247631	-1007	1.5	74 $3d^6(^1D)4s\ ^2D + 20\ 3d^6(^1D)4s\ ^2D$
256272.5	256475	-203	3.5	96 $3d^6(^1F)4s\ ^2F$
256272.9	256496	-223	2.5	96 $3d^6(^1F)4s\ ^2F$
265691.5	265657	35	1.5	80 $3d^6(^3F)4s\ ^4F + 19\ 3d^6(^3F)4s\ ^4F$
265752.4	265730	22	4.5	77 $3d^6(^3F)4s\ ^4F + 22\ 3d^6(^3F)4s\ ^4F$
265886.0	265881	5	2.5	78 $3d^6(^3F)4s\ ^4F + 19\ 3d^6(^3F)4s\ ^4F$
265975.0	265980	-5	3.5	76 $3d^6(^3F)4s\ ^4F + 20\ 3d^6(^3F)4s\ ^4F$
272755.1	272606	149	3.5	76 $3d^6(^3F)4s\ ^2F + 21\ 3d^6(^3F)4s\ ^2F$
272800.8	272670	131	2.5	79 $3d^6(^3F)4s\ ^2F + 20\ 3d^6(^3F)4s\ ^2F$
278281.8	278581	-299	4.5	65 $3d^6(^1G)4s\ ^2G + 34\ 3d^6(^1G)4s\ ^2G$
278380.0	278641	-261	3.5	64 $3d^6(^1G)4s\ ^2G + 33\ 3d^6(^1G)4s\ ^2G$
Odd parity				
266226.7	266263	-36	4.5	97 $3d^6(^5D)4p\ ^6D$
266560.0	266652	-92	3.5	94 $3d^6(^5D)4p\ ^6D$
267068.8	267218	-149	2.5	96 $3d^6(^5D)4p\ ^6D$
267488.7	267680	-191	1.5	98 $3d^6(^5D)4p\ ^6D$
267759.0	267975	-216	0.5	99 $3d^6(^5D)4p\ ^6D$
274003.9	273786	218	5.5	99 $3d^6(^5D)4p\ ^6F$
274064.5	273895	170	4.5	92 $3d^6(^5D)4p\ ^6F + 5\ 3d^6(^5D)4p\ ^4F$
274073.2	273952	121	3.5	89 $3d^6(^5D)4p\ ^6F$
274146.2	274061	85	2.5	92 $3d^6(^5D)4p\ ^6F$
274188.5	274127	62	1.5	94 $3d^6(^5D)4p\ ^6F$
274209.7	274160	50	0.5	95 $3d^6(^5D)4p\ ^6F$
276368.0	276236	132	3.5	77 $3d^6(^5D)4p\ ^6P + 15\ 3d^6(^5D)4p\ ^4D$
278294.6	278210	85	2.5	79 $3d^6(^5D)4p\ ^6P + 16\ 3d^6(^5D)4p\ ^4D$
278663.1	278601	62	3.5	77 $3d^6(^5D)4p\ ^4D + 18\ 3d^6(^5D)4p\ ^6P$
279421.1	279246	175	4.5	92 $3d^6(^5D)4p\ ^4F + 6\ 3d^6(^5D)4p\ ^6F$
279496.8	279479	18	2.5	75 $3d^6(^5D)4p\ ^4D + 19\ 3d^6(^5D)4p\ ^6P$
279589.5	279530	60	1.5	84 $3d^6(^5D)4p\ ^6P + 13\ 3d^6(^5D)4p\ ^4D$
280065.7	280080	-14	1.5	78 $3d^6(^5D)4p\ ^4D + 14\ 3d^6(^5D)4p\ ^6P$
280373.3	280427	-54	0.5	91 $3d^6(^5D)4p\ ^4D$
280928.7	280810	119	3.5	93 $3d^6(^5D)4p\ ^4F + 5\ 3d^6(^5D)4p\ ^6F$
281942.4	281852	90	2.5	95 $3d^6(^5D)4p\ ^4F$
282621.5	282550	72	1.5	96 $3d^6(^5D)4p\ ^4F$
284520.9	284782	-261	2.5	96 $3d^6(^5D)4p\ ^4P$
285546.4	285841	-295	1.5	97 $3d^6(^5D)4p\ ^4P$
286068.7	286393	-324	0.5	97 $3d^6(^5D)4p\ ^4P$
300401.2	300616	-215	5.5	65 $3d^6(^3H)4p\ ^4G + 22\ 3d^6(^3F)4p\ ^4G + 8\ 3d^6(^3G)4p\ ^4G$
300837.1	300768	69	4.5	30 $3d^6(^3H)4p\ ^4G + 25\ 3d^6(^3F)4p\ ^4G + 10\ 3d^6(^3G)4p\ ^4G$
301080.5	301048	33	2.5	24 $3d^6(^3P)4p\ ^4P + 22\ 3d^6(^3P)4p\ ^4P + 10\ 3d^6(^3P)4p\ ^4D$
301255.4	301141	114	3.5	27 $3d^6(^3F)4p\ ^4G + 21\ 3d^6(^3H)4p\ ^4G + 11\ 3d^6(^3G)4p\ ^4G$
301286.4	301317	-31	5.5	50 $3d^6(^3H)4p\ ^4I + 32\ 3d^6(^3H)4p\ ^4H + 11\ 3d^6(^3G)4p\ ^4H$
301336.1	301490	-154	6.5	49 $3d^6(^3H)4p\ ^4I + 34\ 3d^6(^3H)4p\ ^4H + 10\ 3d^6(^3H)4p\ ^2I$
301385.6	301509	-123	4.5	35 $3d^6(^3H)4p\ ^4I + 29\ 3d^6(^3H)4p\ ^4H + 18\ 3d^6(^3H)4p\ ^4G$
301533.4	301520	13	2.5	43 $3d^6(^3F)4p\ ^4G + 34\ 3d^6(^3H)4p\ ^4G + 7\ 3d^6(^3G)4p\ ^4G$
301586.7	301667	-80	3.5	26 $3d^6(^3H)4p\ ^4H + 20\ 3d^6(^3H)4p\ ^4G + 17\ 3d^6(^3H)4p\ ^2G$
302961.2	303061	-100	0.5	44 $3d^6(^3P)4p\ ^4P + 42\ 3d^6(^3P)4p\ ^4P$
302980.4	302984	-4	4.5	43 $3d^6(^3H)4p\ ^4I + 16\ 3d^6(^3H)4p\ ^2G + 13\ 3d^6(^3H)4p\ ^4H$

Table A.10. continued.

E_{exp}^a	E_{calc}^b	ΔE	J	Leading components (in %) in LS coupling ^c
303209.3	303251	-42	3.5	20 3d ⁶ (³ H)4p ⁴ H + 17 3d ⁶ (³ F)4p ⁴ F
303241.7	303153	89	2.5	28 3d ⁶ (³ P)4p ² D + 19 3d ⁶ (³ P)4p ⁴ P + 19 3d ⁶ (³ P)4p ² D
303456.4	303417	39	7.5	99 3d ⁶ (³ H)4p ⁴ I
303479.1	303505	-26	2.5	47 3d ⁶ (³ F)4p ⁴ F + 16 3d ⁶ (³ F)4p ⁴ F + 8 3d ⁶ (³ D)4p ⁴ F
303679.5	303754	-75	1.5	60 3d ⁶ (³ F)4p ⁴ F + 20 3d ⁶ (³ F)4p ⁴ F + 11 3d ⁶ (³ D)4p ⁴ F
303734.1	303801	-67	1.5	23 3d ⁶ (³ P)4p ⁴ S + 21 3d ⁶ (³ P)4p ⁴ D + 7 3d ⁶ (³ P)4p ² D
303931.7	304054	-122	5.5	43 3d ⁶ (³ H)4p ⁴ H + 42 3d ⁶ (³ H)4p ⁴ I + 7 3d ⁶ (³ G)4p ⁴ H
304062.3	304286	-224	6.5	53 3d ⁶ (³ H)4p ⁴ H + 34 3d ⁶ (³ H)4p ⁴ I + 7 3d ⁶ (³ G)4p ⁴ H
304092.2	304129	-37	4.5	44 3d ⁶ (³ F)4p ⁴ F + 17 3d ⁶ (³ F)4p ⁴ F + 10 3d ⁶ (³ H)4p ⁴ G
304199.0	304174	25	3.5	46 3d ⁶ (³ P)4p ⁴ D + 27 3d ⁶ (³ P)4p ⁴ D + 7 3d ⁶ (³ H)4p ⁴ H
304456.1	304732	-276	4.5	38 3d ⁶ (³ H)4p ² G + 21 3d ⁶ (³ H)4p ⁴ H + 12 3d ⁶ (³ G)4p ² G
304655.0	304739	-84	3.5	20 3d ⁶ (³ H)4p ² G + 19 3d ⁶ (³ F)4p ⁴ F + 10 3d ⁶ (³ H)4p ⁴ G
305453.3	305657	-204	3.5	41 3d ⁶ (³ F)4p ⁴ D + 13 3d ⁶ (³ H)4p ² G + 9 3d ⁶ (³ F)4p ⁴ D
305844.4	306031	-187	1.5	16 3d ⁶ (³ P)4p ⁴ P + 16 3d ⁶ (³ P)4p ⁴ P + 14 3d ⁶ (³ P)4p ² D
305882.7	305838	45	6.5	79 3d ⁶ (³ H)4p ² I + 16 3d ⁶ (³ H)4p ⁴ I
306115.6	306249	-133	2.5	49 3d ⁶ (³ F)4p ⁴ D + 10 3d ⁶ (³ F)4p ⁴ D + 10 3d ⁶ (³ D)4p ⁴ D
306678.1	306886	-208	1.5	55 3d ⁶ (³ F)4p ⁴ D + 11 3d ⁶ (³ D)4p ⁴ D + 11 3d ⁶ (³ F)4p ⁴ D
306892.2	306715	177	5.5	74 3d ⁶ (³ H)4p ² I + 5 3d ⁶ (³ F)4p ⁴ G + 5 3d ⁶ (³ H)4p ⁴ I
306905.8	307159	-253	2.5	37 3d ⁶ (³ P)4p ⁴ D + 18 3d ⁶ (³ P)4p ⁴ D + 8 3d ⁶ (³ F)4p ⁴ D
306989.1	307210	-221	0.5	63 3d ⁶ (³ F)4p ⁴ D + 14 3d ⁶ (³ D)4p ⁴ D + 11 3d ⁶ (³ F)4p ⁴ D
307138.8	307406	-267	1.5	24 3d ⁶ (³ P)4p ⁴ D + 14 3d ⁶ (³ P)4p ² D + 10 3d ⁶ (³ P)4p ⁴ D
307824.5	307669	156	4.5	28 3d ⁶ (³ F)4p ⁴ G + 16 3d ⁶ (³ H)4p ⁴ G + 13 3d ⁶ (³ F)4p ² G
307909.5	307805	105	2.5	24 3d ⁶ (³ F)4p ² F + 14 3d ⁶ (³ G)4p ⁴ G + 14 3d ⁶ (³ H)4p ⁴ G
307990.7	307971	20	3.5	24 3d ⁶ (³ F)4p ⁴ G + 17 3d ⁶ (³ H)4p ⁴ G + 11 3d ⁶ (³ F)4p ² F
308064.9	308024	41	5.5	47 3d ⁶ (³ F)4p ⁴ G + 14 3d ⁶ (³ F)4p ⁴ G + 13 3d ⁶ (³ H)4p ² I
308817.8	308845	-27	4.5	53 3d ⁶ (³ G)4p ⁴ F + 23 3d ⁶ (³ G)4p ⁴ G + 7 3d ⁶ (³ D)4p ⁴ F
309269.1	309498	-229	5.5	31 3d ⁶ (³ G)4p ² H + 25 3d ⁶ (³ G)4p ⁴ G + 13 3d ⁶ (³ H)4p ⁴ H
309294.1	309129	165	3.5	22 3d ⁶ (³ F)4p ² F + 14 3d ⁶ (³ H)4p ⁴ G + 12 3d ⁶ (³ F)4p ² F
309569.9	309249	321	2.5	33 3d ⁶ (³ H)4p ⁴ G + 16 3d ⁶ (³ F)4p ⁴ G + 10 3d ⁶ (³ F)4p ⁴ G
309702.9	309831	-128	0.5	28 3d ⁶ (³ P)4p ² P + 25 3d ⁶ (³ P)4p ² P + 18 3d ⁶ (³ P)4p ² S
309772.0	309710	62	4.5	26 3d ⁶ (³ F)4p ² G + 22 3d ⁶ (³ G)4p ² H + 13 3d ⁶ (³ F)4p ⁴ G
309801.3	309738	63	3.5	40 3d ⁶ (³ G)4p ⁴ F + 36 3d ⁶ (³ G)4p ⁴ G + 5 3d ⁶ (³ F)4p ⁴ F
310450.4	310932	-482	1.5	42 3d ⁶ (³ P)4p ² P + 30 3d ⁶ (³ P)4p ² P + 5 3d ⁶ (³ G)4p ⁴ F
310483.1	310472	11	5.5	45 3d ⁶ (³ G)4p ⁴ G + 17 3d ⁶ (³ H)4p ² H + 14 3d ⁶ (³ H)4p ⁴ G
310753.8	310708	46	2.5	32 3d ⁶ (³ G)4p ⁴ F + 31 3d ⁶ (³ G)4p ⁴ G + 8 3d ⁶ (³ F)4p ² F
310874.9	310872	3	4.5	21 3d ⁶ (³ F)4p ² G + 13 3d ⁶ (³ H)4p ² H + 5 3d ⁶ (³ F)4p ² G
311220.3	310952	268	3.5	55 3d ⁶ (³ F)4p ² G + 13 3d ⁶ (³ F)4p ² G + 8 3d ⁶ (³ F)4p ⁴ G
311232.9	311297	-64	4.5	39 3d ⁶ (³ G)4p ⁴ G + 16 3d ⁶ (³ H)4p ² H + 10 3d ⁶ (³ H)4p ⁴ G
311582.4	311651	-69	3.5	39 3d ⁶ (³ G)4p ⁴ G + 24 3d ⁶ (³ G)4p ⁴ F + 9 3d ⁶ (³ D)4p ⁴ F
311706.3	311627	79	1.5	57 3d ⁶ (³ G)4p ⁴ F + 17 3d ⁶ (³ D)4p ⁴ F + 6 3d ⁶ (³ P)4p ² D
311837.8	311765	73	2.5	37 3d ⁶ (³ G)4p ⁴ G + 29 3d ⁶ (³ G)4p ⁴ F + 11 3d ⁶ (³ D)4p ⁴ F
311888.8	311877	12	6.5	82 3d ⁶ (³ G)4p ⁴ H + 13 3d ⁶ (³ H)4p ⁴ H
311982.0	312209	-227	0.5	49 3d ⁶ (³ P)4p ² S + 22 3d ⁶ (³ P)4p ² S + 9 3d ⁶ (³ P)4p ² P
312073.1	312087	-14	3.5	64 3d ⁶ (³ G)4p ⁴ H + 14 3d ⁶ (³ H)4p ⁴ H + 7 3d ⁶ (³ F)4p ² G
312105.5	312128	-23	5.5	66 3d ⁶ (³ G)4p ⁴ H + 14 3d ⁶ (³ H)4p ² H + 7 3d ⁶ (³ H)4p ⁴ H
312138.0	312122	16	4.5	65 3d ⁶ (³ G)4p ⁴ H + 10 3d ⁶ (³ H)4p ⁴ H + 8 3d ⁶ (³ H)4p ² H
314237.9	314264	-26	2.5	59 3d ⁶ (³ F)4p ² D + 10 3d ⁶ (³ P)4p ² D + 8 3d ⁶ (³ F)4p ² D
314988.0	315060	-72	1.5	61 3d ⁶ (³ F)4p ² D + 16 3d ⁶ (³ P)4p ² D + 6 3d ⁶ (³ P)4p ² D
316134.0	316427	-293	2.5	39 3d ⁶ (³ G)4p ² F + 22 3d ⁶ (³ D)4p ² F + 10 3d ⁶ (¹ D)4p ² F
316149.4	316217	-68	5.5	51 3d ⁶ (³ H)4p ² H + 37 3d ⁶ (³ G)4p ² H
316642.6	316833	-190	3.5	45 3d ⁶ (³ G)4p ² F + 21 3d ⁶ (³ D)4p ² F + 9 3d ⁶ (³ F)4p ² F
317201.1	317043	158	4.5	32 3d ⁶ (³ G)4p ² H + 31 3d ⁶ (³ H)4p ² H + 6 3d ⁶ (³ G)4p ² G
317240.4	317272	-32	6.5	96 3d ⁶ (¹ I)4p ² K
318923.1	318699	224	2.5	84 3d ⁶ (³ D)4p ⁴ P
319304.2	319143	161	3.5	61 3d ⁶ (³ G)4p ² G + 10 3d ⁶ (¹ G)4p ² F + 7 3d ⁶ (³ H)4p ² G
319404.1	319180	224	1.5	67 3d ⁶ (³ D)4p ⁴ P + 11 3d ⁶ (³ D)4p ² P + 8 3d ⁶ (³ D)4p ⁴ D

Table A.10. continued.

E_{exp}^a	E_{calc}^b	ΔE	J	Leading components (in %) in LS coupling ^c
319407.6	319379	29	7.5	99 $3d^6(^1I)4p\ ^2K$
319418.8	318815	604	4.5	42 $3d^6(^1G)4p\ ^2H + 19 3d^6(^1G)4p\ ^2H + 13 3d^6(^3G)4p\ ^2H$
319689.0	319707	-18	4.5	64 $3d^6(^3G)4p\ ^2G + 16 3d^6(^3H)4p\ ^2G + 10 3d^6(^3H)4p\ ^2H$
319951.5	319765	187	5.5	42 $3d^6(^1I)4p\ ^2H + 32 3d^6(^1G)4p\ ^2H + 9 3d^6(^1G)4p\ ^2H$
320216.4	320024	192	0.5	43 $3d^6(^3D)4p\ ^4P + 24 3d^6(^3D)4p\ ^4D + 17 3d^6(^3D)4p\ ^2P$
320935.3	320671	264	0.5	47 $3d^6(^3D)4p\ ^4P + 19 3d^6(^3D)4p\ ^4D + 16 3d^6(^3D)4p\ ^2P$
321074.0	320755	319	1.5	51 $3d^6(^3D)4p\ ^4F + 24 3d^6(^3G)4p\ ^4F + 7 3d^6(^3D)4p\ ^4D$
321364.9	321140	225	2.5	49 $3d^6(^3D)4p\ ^4F + 20 3d^6(^3G)4p\ ^4F + 13 3d^6(^3D)4p\ ^4D$
321433.0	320982	451	3.5	36 $3d^6(^1G)4p\ ^2G + 17 3d^6(^1G)4p\ ^2G + 11 3d^6(^3D)4p\ ^4F$
321443.1	321034	409	1.5	30 $3d^6(^3D)4p\ ^2P + 18 3d^6(^3D)4p\ ^4P + 18 3d^6(^3D)4p\ ^4D$
321795.8	321587	209	3.5	26 $3d^6(^3D)4p\ ^4D + 16 3d^6(^1G)4p\ ^2G + 11 3d^6(^3H)4p\ ^2G$
322192.1	321878	314	2.5	64 $3d^6(^3D)4p\ ^4D + 16 3d^6(^3D)4p\ ^4F + 7 3d^6(^3F)4p\ ^4D$
322375.9	321553	823	4.5	49 $3d^6(^1G)4p\ ^2G + 22 3d^6(^1G)4p\ ^2G + 8 3d^6(^1G)4p\ ^2H$
322464.1	321921	543	3.5	55 $3d^6(^3D)4p\ ^4F + 12 3d^6(^3G)4p\ ^4F + 11 3d^6(^1G)4p\ ^2F$
322470.0	322037	433	1.5	46 $3d^6(^3D)4p\ ^4D + 30 3d^6(^3D)4p\ ^2P + 7 3d^6(^1S)4p\ ^2P$
322569.0	322293	276	0.5	35 $3d^6(^3D)4p\ ^4D + 30 3d^6(^3D)4p\ ^2P + 12 3d^6(^1S)4p\ ^2P$
322744.4	322544	200	3.5	45 $3d^6(^3D)4p\ ^4D + 13 3d^6(^1G)4p\ ^2F + 7 3d^6(^3F)4p\ ^4D$
322875.8	322434	442	4.5	77 $3d^6(^3D)4p\ ^4F + 14 3d^6(^3G)4p\ ^4F$
323222.4	322958	264	2.5	34 $3d^6(^1G)4p\ ^2F + 16 3d^6(^3G)4p\ ^2F + 16 3d^6(^1G)4p\ ^2F$
323506.3	322768	738	5.5	29 $3d^6(^1G)4p\ ^2H + 28 3d^6(^1D)4p\ ^2H + 26 3d^6(^1G)4p\ ^2H$
323616.8	323762	-145	4.5	70 $3d^6(^1I)4p\ ^2H + 10 3d^6(^3G)4p\ ^2H + 9 3d^6(^1G)4p\ ^2H$
324623.5	324849	-226	6.5	97 $3d^6(^1I)4p\ ^2I$
324668.3	324824	-156	5.5	87 $3d^6(^1I)4p\ ^2I + 9 3d^6(^1I)4p\ ^2H$
324908.8	324866	43	1.5	70 $3d^6(^3D)4p\ ^2D + 8 3d^6(^1D)4p\ ^2P + 6 3d^6(^1F)4p\ ^2D$
325518.5	325443	76	2.5	84 $3d^6(^3D)4p\ ^2D$
325923.4	325688	235	1.5	32 $3d^6(^1S)4p\ ^2P + 20 3d^6(^1D)4p\ ^2P + 12 3d^6(^3D)4p\ ^2D$
326477.1	326236	241	3.5	64 $3d^6(^3D)4p\ ^2F + 11 3d^6(^1D)4p\ ^2F + 7 3d^6(^3G)4p\ ^2F$
327268.0	327269	-1	2.5	57 $3d^6(^3D)4p\ ^2F + 14 3d^6(^1D)4p\ ^2F + 7 3d^6(^1G)4p\ ^2F$
327379.7	326541	839	0.5	40 $3d^6(^1S)4p\ ^2P + 25 3d^6(^3D)4p\ ^2P + 12 3d^6(^1S)4p\ ^2P$
329339.6	329710	-370	2.5	25 $3d^6(^1D)4p\ ^2D + 24 3d^6(^1D)4p\ ^2F + 11 3d^6(^1F)4p\ ^2D$
329960.8	330412	-451	1.5	50 $3d^6(^1D)4p\ ^2D + 12 3d^6(^1F)4p\ ^2D + 10 3d^6(^1D)4p\ ^2D$
330765.1	331371	-606	2.5	30 $3d^6(^1D)4p\ ^2D + 23 3d^6(^1D)4p\ ^2F + 18 3d^6(^1F)4p\ ^2D$
331353.6	331611	-257	0.5	58 $3d^6(^1D)4p\ ^2P + 22 3d^6(^1D)4p\ ^2P + 9 3d^6(^1S)4p\ ^2P$
331435.0	332108	-673	3.5	54 $3d^6(^1D)4p\ ^2F + 14 3d^6(^1D)4p\ ^2F + 9 3d^6(^3G)4p\ ^2F$
332946.3	332577	369	1.5	32 $3d^6(^1D)4p\ ^2P + 17 3d^6(^1S)4p\ ^2P + 14 3d^6(^1D)4p\ ^2D$
335935.2	336160	-225	3.5	87 $3d^6(^1F)4p\ ^2G$
338015.8	338917	-901	2.5	48 $3d^6(^1F)4p\ ^2D + 20 3d^6(^1D)4p\ ^2D + 6 3d^6(^1D)4p\ ^2D$
338059.3	338289	-230	4.5	92 $3d^6(^1F)4p\ ^2G$
339377.8	339843	-465	1.5	28 $3d^6(^3F)4p\ ^4D + 22 3d^6(^3P)4p\ ^4D + 22 3d^6(^1F)4p\ ^2D$
339845.5	339817	29	0.5	38 $3d^6(^3P)4p\ ^4D + 35 3d^6(^3F)4p\ ^4D + 17 3d^6(^3P)4p\ ^4D$
340482.7	340952	-469	1.5	53 $3d^6(^1F)4p\ ^2D + 13 3d^6(^3P)4p\ ^4D + 10 3d^6(^3F)4p\ ^4D$
340722.8	340846	-123	2.5	39 $3d^6(^3F)4p\ ^4D + 28 3d^6(^3P)4p\ ^4D + 13 3d^6(^3P)4p\ ^4D$
340819.5	340897	-78	3.5	52 $3d^6(^3F)4p\ ^4D + 22 3d^6(^3P)4p\ ^4D + 11 3d^6(^3F)4p\ ^4D$
343301.1	343466	-165	2.5	80 $3d^6(^1F)4p\ ^2F + 5 3d^6(^1F)4p\ ^2D + 5 3d^6(^1G)4p\ ^2F$
343337.2	343465	-128	3.5	81 $3d^6(^1F)4p\ ^2F + 5 3d^6(^1G)4p\ ^2F$
347219.0	346993	226	2.5	76 $3d^6(^3F)4p\ ^4G + 17 3d^6(^3F)4p\ ^4G$
347793.1	347578	215	3.5	75 $3d^6(^3F)4p\ ^4G + 17 3d^6(^3F)4p\ ^4G$
348323.7	348098	226	4.5	71 $3d^6(^3F)4p\ ^4G + 17 3d^6(^3F)4p\ ^4G$
349167.6	348848	320	5.5	77 $3d^6(^3F)4p\ ^4G + 20 3d^6(^3F)4p\ ^4G$
349300.5	349038	263	1.5	72 $3d^6(^3P)4p\ ^4S + 25 3d^6(^3P)4p\ ^4S$
351430.8	351331	100	1.5	49 $3d^6(^3F)4p\ ^2D + 22 3d^6(^3P)4p\ ^2D + 9 3d^6(^3P)4p\ ^2D$
351671.9	351981	-309	0.5	46 $3d^6(^3P)4p\ ^4P + 39 3d^6(^3P)4p\ ^4P + 7 3d^6(^3P)4p\ ^2S$
352004.5	352402	-398	1.5	47 $3d^6(^3P)4p\ ^4P + 40 3d^6(^3P)4p\ ^4P$
352419.2	352501	-82	2.5	45 $3d^6(^3F)4p\ ^2D + 21 3d^6(^3P)4p\ ^2D + 11 3d^6(^3P)4p\ ^2D$
352582.3	352325	257	4.5	63 $3d^6(^3F)4p\ ^2G + 16 3d^6(^3F)4p\ ^2G$
353485.7	353743	-257	2.5	24 $3d^6(^3P)4p\ ^4P + 20 3d^6(^3P)4p\ ^4P + 12 3d^6(^3P)4p\ ^4D$

Table A.10. continued.

E_{exp}^a	E_{calc}^b	ΔE	J	Leading components (in %) in LS coupling ^c
353590.0	353445	145	0.5 45	$3d^6(^3F)4p\ ^4D + 22\ 3d^6(^3P)4p\ ^4D + 15\ 3d^6(^3P)4p\ ^4D$
353645.9	353464	182	3.5 65	$3d^6(^3F)4p\ ^2G + 15\ 3d^6(^3F)4p\ ^2G + 8\ 3d^6(^3F)4p\ ^4F$
354039.3	353996	43	1.5 29	$3d^6(^3F)4p\ ^4D + 19\ 3d^6(^3P)4p\ ^4D + 13\ 3d^6(^3P)4p\ ^4D$
354548.0	354714	-166	2.5 24	$3d^6(^3F)4p\ ^4F + 22\ 3d^6(^3P)4p\ ^4P + 19\ 3d^6(^3P)4p\ ^4P$
354796.7	354750	47	1.5 51	$3d^6(^3F)4p\ ^4F + 17\ 3d^6(^3F)4p\ ^4F + 9\ 3d^6(^3F)4p\ ^4D$
354905.2	354857	48	3.5 39	$3d^6(^3F)4p\ ^4F + 15\ 3d^6(^3F)4p\ ^4F + 15\ 3d^6(^3P)4p\ ^4D$
355606.0	355610	-4	2.5 34	$3d^6(^3F)4p\ ^4F + 20\ 3d^6(^3F)4p\ ^4D + 14\ 3d^6(^3P)4p\ ^4D$
355875.0	355799	76	4.5 64	$3d^6(^3F)4p\ ^4F + 25\ 3d^6(^3F)4p\ ^4F + 8\ 3d^6(^3F)4p\ ^2G$
356372.1	356428	-56	3.5 23	$3d^6(^3P)4p\ ^4D + 23\ 3d^6(^3F)4p\ ^4F + 20\ 3d^6(^3F)4p\ ^4D$
356661.9	356858	-196	1.5 26	$3d^6(^3F)4p\ ^2D + 21\ 3d^6(^3P)4p\ ^2D + 17\ 3d^6(^3P)4p\ ^2D$
357881.0	358177	-296	0.5 52	$3d^6(^3P)4p\ ^2P + 36\ 3d^6(^3P)4p\ ^2P$
357948.3	358385	-437	2.5 33	$3d^6(^3P)4p\ ^2D + 26\ 3d^6(^3P)4p\ ^2D + 24\ 3d^6(^3F)4p\ ^2D$
358724.8	359025	-300	3.5 51	$3d^6(^3F)4p\ ^2F + 22\ 3d^6(^3F)4p\ ^2F + 14\ 3d^6(^1G)4p\ ^2F$
359141.2	359648	-507	1.5 42	$3d^6(^3P)4p\ ^2P + 30\ 3d^6(^3P)4p\ ^2P + 8\ 3d^6(^3P)4p\ ^2D$
359491.9	359658	-166	2.5 66	$3d^6(^3F)4p\ ^2F + 25\ 3d^6(^3F)4p\ ^2F$
360058.2	360296	-238	4.5 57	$3d^6(^1G)4p\ ^2H + 34\ 3d^6(^1G)4p\ ^2H$
362142.8	362451	-308	3.5 26	$3d^6(^1G)4p\ ^2G + 25\ 3d^6(^1G)4p\ ^2F + 12\ 3d^6(^1G)4p\ ^2F$
362144.7	362340	-195	5.5 61	$3d^6(^1G)4p\ ^2H + 36\ 3d^6(^1G)4p\ ^2H$
363396.8	363765	-368	2.5 54	$3d^6(^1G)4p\ ^2F + 26\ 3d^6(^1G)4p\ ^2F + 8\ 3d^6(^1F)4p\ ^2F$
364606.6	364872	-265	4.5 63	$3d^6(^1G)4p\ ^2G + 27\ 3d^6(^1G)4p\ ^2G$
365071.1	365357	-286	3.5 40	$3d^6(^1G)4p\ ^2G + 17\ 3d^6(^1G)4p\ ^2G + 16\ 3d^6(^1G)4p\ ^2F$
386004.2	385757	247	1.5 78	$3d^6(^1D)4p\ ^2D + 17\ 3d^6(^1D)4p\ ^2D$
386705.0	386447	258	2.5 78	$3d^6(^1D)4p\ ^2D + 17\ 3d^6(^1D)4p\ ^2D$
392652.5	392333	320	2.5 69	$3d^6(^1D)4p\ ^2F + 22\ 3d^6(^1D)4p\ ^2F$
394248.5	393841	408	1.5 64	$3d^6(^1D)4p\ ^2P + 25\ 3d^6(^1D)4p\ ^2P + 7\ 3d^6(^1S)4p\ ^2P$
394391.0	394030	361	3.5 72	$3d^6(^1D)4p\ ^2F + 23\ 3d^6(^1D)4p\ ^2F$
394912.4	394512	400	0.5 65	$3d^6(^1D)4p\ ^2P + 25\ 3d^6(^1D)4p\ ^2P + 8\ 3d^6(^1S)4p\ ^2P$

^a From NIST compilation (Kramida et al. 2019).^b This work.^c Only the first three components greater than or equal to 5% are given.**Table A.11.** Comparison between available experimental and calculated energy levels in Cu vi. Energies are given in cm⁻¹.

E_{exp}^a	E_{calc}^b	ΔE	J	Leading components (in %) in LS coupling ^c
Even parity				
0.0	-84	84	4 99	$3d^6\ ^5D$
1195.8	1124	72	3 100	$3d^6\ ^5D$
1986.8	1925	62	2 99	$3d^6\ ^5D$
2489.4	2435	54	1 99	$3d^6\ ^5D$
2733.4	2683	50	0 99	$3d^6\ ^5D$
29285.0	29833	-548	2 60	$3d^6\ ^3P + 38\ 3d^6\ ^3P$
30417.6	30593	-175	6 99	$3d^6\ ^3H$
31009.2	31085	-76	5 95	$3d^6\ ^3H + 5\ 3d^6\ ^3G$
31287.6	31238	50	4 78	$3d^6\ ^3H + 9\ 3d^6\ ^3F + 7\ 3d^6\ ^3G$
32684.9	33379	-694	1 61	$3d^6\ ^3P + 37\ 3d^6\ ^3P$
32756.0	32863	-107	4 61	$3d^6\ ^3F + 18\ 3d^6\ ^3F + 17\ 3d^6\ ^3H$
33295.8	33384	-88	3 74	$3d^6\ ^3F + 20\ 3d^6\ ^3F + 6\ 3d^6\ ^3G$
33739.6	33871	-131	2 80	$3d^6\ ^3F + 19\ 3d^6\ ^3F$
33867.8	34556	-688	0 59	$3d^6\ ^3P + 36\ 3d^6\ ^3P$
37378.1	37313	65	5 95	$3d^6\ ^3G + 5\ 3d^6\ ^3H$
38468.9	38428	41	4 90	$3d^6\ ^3G + 6\ 3d^6\ ^3F$
38907.4	38799	108	3 93	$3d^6\ ^3G + 5\ 3d^6\ ^3F$
46405.8	46390	16	6 99	$3d^6\ ^1I$
46714.2	46253	461	2 97	$3d^6\ ^3D$
46848.3	46295	553	1 99	$3d^6\ ^3D$

Table A.11. continued.

E_{exp}^a	E_{calc}^b	ΔE	J	Leading components (in %) in LS coupling ^c
47119.1	46637	482	3 99	$3d^6 \ ^3D$
47611.6	46790	822	4 64	$3d^6 \ ^1G + 32 \ 3d^6 \ ^1G$
53786.6	51951	1836	0 75	$3d^6 \ ^1S + 21 \ 3d^6 \ ^1S$
54747.1	56277	-1530	2 76	$3d^6 \ ^1D + 21 \ 3d^6 \ ^1D$
64967.6	65300	-332	3 97	$3d^6 \ ^1F$
74712.0	74760	-48	0 63	$3d^6 \ ^3P + 37 \ 3d^6 \ ^3P$
75774.1	75865	-91	1 62	$3d^6 \ ^3P + 38 \ 3d^6 \ ^3P$
77145.0	77096	49	2 80	$3d^6 \ ^3F + 19 \ 3d^6 \ ^3F$
77223.8	77161	63	4 77	$3d^6 \ ^3F + 22 \ 3d^6 \ ^3F$
77467.9	77433	35	3 77	$3d^6 \ ^3F + 20 \ 3d^6 \ ^3F$
77908.8	78179	-270	2 60	$3d^6 \ ^3P + 39 \ 3d^6 \ ^3P$
87505.9	87861	-355	4 65	$3d^6 \ ^1G + 34 \ 3d^6 \ ^1G$
117084.3	116858	226	2 78	$3d^6 \ ^1D + 22 \ 3d^6 \ ^1D$
250876.6	250877	0	3 100	$3d^5(^6S)4s \ ^7S$
265639.1	265603	36	2 100	$3d^5(^6S)4s \ ^5S$
299143.0	299305	-162	6 100	$3d^5(^4G)4s \ ^5G$
299250.6	299155	96	2 99	$3d^5(^4G)4s \ ^5G$
299256.0	299330	-74	5 100	$3d^5(^4G)4s \ ^5G$
299282.1	299226	56	3 99	$3d^5(^4G)4s \ ^5G$
299292.9	299293	0	4 100	$3d^5(^4G)4s \ ^5G$
308997.5	309110	-113	5 99	$3d^5(^4G)4s \ ^3G$
309046.1	308936	110	3 49	$3d^5(^4G)4s \ ^3G + 43 \ 3d^5(^4D)4s \ ^5D + 7 \ 3d^5(^4P)4s \ ^5P$
309110.8	309120	-9	4 98	$3d^5(^4G)4s \ ^3G$
322791.9	322686	106	5 98	$3d^5(^2I)4s \ ^3I$
322804.7	322780	25	6 98	$3d^5(^2I)4s \ ^3I$
322877.3	322955	-78	7 100	$3d^5(^2I)4s \ ^3I$
Odd parity				
342225.2	342141	84	2 98	$3d^5(^6S)4p \ ^7P$
343276.6	343180	97	3 97	$3d^5(^6S)4p \ ^7P$
345137.1	345018	119	4 100	$3d^5(^6S)4p \ ^7P$
355259.2	355237	22	3 95	$3d^5(^6S)4p \ ^5P$
356137.2	356133	4	2 96	$3d^5(^6S)4p \ ^5P$
356674.0	356681	-7	1 97	$3d^5(^6S)4p \ ^5P$
388191.7	388311	-119	2 89	$3d^5(^4G)4p \ ^5G + 5 \ 3d^5(^4G)4p \ ^3F$
388236.1	388349	-113	3 77	$3d^5(^4G)4p \ ^5G + 16 \ 3d^5(^4G)4p \ ^5H$
388312.3	388472	-160	4 73	$3d^5(^4G)4p \ ^5G + 20 \ 3d^5(^4G)4p \ ^5H$
388442.1	388673	-231	5 73	$3d^5(^4G)4p \ ^5G + 20 \ 3d^5(^4G)4p \ ^5H$
388707.5	389019	-312	6 78	$3d^5(^4G)4p \ ^5G + 16 \ 3d^5(^4G)4p \ ^5H$
390618.2	390155	463	3 81	$3d^5(^4G)4p \ ^5H + 13 \ 3d^5(^4G)4p \ ^5G$
391198.1	390846	352	4 74	$3d^5(^4G)4p \ ^5H + 17 \ 3d^5(^4G)4p \ ^5G + 5 \ 3d^5(^4G)4p \ ^5F$
391691.7	391484	208	5 63	$3d^5(^4G)4p \ ^5H + 19 \ 3d^5(^4G)4p \ ^5F + 12 \ 3d^5(^4G)4p \ ^5G$
391986.5	391562	425	2 50	$3d^5(^4P)4p \ ^5D + 18 \ 3d^5(^4D)4p \ ^5D + 11 \ 3d^5(^4D)4p \ ^5F$
392255.1	391888	367	3 35	$3d^5(^4P)4p \ ^5D + 20 \ 3d^5(^4G)4p \ ^5F + 14 \ 3d^5(^4D)4p \ ^5F$
392516.7	392483	34	5 65	$3d^5(^4G)4p \ ^5F + 13 \ 3d^5(^4G)4p \ ^5H + 10 \ 3d^5(^4G)4p \ ^5G$
392593.6	392347	247	6 80	$3d^5(^4G)4p \ ^5H + 18 \ 3d^5(^4G)4p \ ^5G$
392712.6	392579	134	4 58	$3d^5(^4G)4p \ ^5F + 13 \ 3d^5(^4D)4p \ ^5F + 8 \ 3d^5(^4P)4p \ ^5D$
393090.2	392801	289	7 100	$3d^5(^4G)4p \ ^5H$
393425.4	393484	-59	2 63	$3d^5(^4P)4p \ ^5S + 10 \ 3d^5(^4P)4p \ ^3P + 8 \ 3d^5(^4G)4p \ ^5F$
394014.7	393843	172	1 66	$3d^5(^4G)4p \ ^5F + 18 \ 3d^5(^4D)4p \ ^5F + 7 \ 3d^5(^4F)4p \ ^5F$
394117.4	393985	132	3 53	$3d^5(^4G)4p \ ^5F + 16 \ 3d^5(^4P)4p \ ^5D + 12 \ 3d^5(^4P)4p \ ^5P$
394133.8	394018	116	2 55	$3d^5(^4G)4p \ ^5F + 16 \ 3d^5(^4P)4p \ ^5D + 10 \ 3d^5(^4P)4p \ ^5S$
395407.1	395136	271	4 58	$3d^5(^4P)4p \ ^5D + 19 \ 3d^5(^4G)4p \ ^5F + 17 \ 3d^5(^4D)4p \ ^5D$
395601.0	395515	86	3 38	$3d^5(^4P)4p \ ^5P + 32 \ 3d^5(^4D)4p \ ^5P + 15 \ 3d^5(^4P)4p \ ^5D$
396283.7	396337	-53	2 53	$3d^5(^4P)4p \ ^5P + 26 \ 3d^5(^4D)4p \ ^5P + 7 \ 3d^5(^4P)4p \ ^5S$
396454.5	396408	47	2 78	$3d^5(^4G)4p \ ^3F + 5 \ 3d^5(^4G)4p \ ^5G$

Table A.11. continued.

E_{exp}^a	E_{calc}^b	ΔE	J	Leading components (in %) in LS coupling ^c
396523.6	396301	223	1 68	$3d^5(^4P)4p\ ^5P + 12\ 3d^5(^4D)4p\ ^5P + 9\ 3d^5(^4P)4p\ ^3P$
396617.1	396817	-200	3 80	$3d^5(^4G)4p\ ^3F$
396929.1	397233	-304	4 86	$3d^5(^4G)4p\ ^3F + 5\ 3d^5(^4F)4p\ ^3F$
397404.4	397291	113	6 91	$3d^5(^4G)4p\ ^3H$
398022.8	397796	227	5 93	$3d^5(^4G)4p\ ^3H$
398273.1	398215	58	2 44	$3d^5(^4P)4p\ ^3P + 16\ 3d^5(^4D)4p\ ^3P + 14\ 3d^5(^4P)4p\ ^5S$
398376.6	398048	329	4 94	$3d^5(^4G)4p\ ^3H$
398722.7	398594	129	1 44	$3d^5(^4P)4p\ ^3P + 16\ 3d^5(^4D)4p\ ^3P + 9\ 3d^5(^4P)4p\ ^5P$
399112.8	399062	51	1 63	$3d^5(^4D)4p\ ^5F + 23\ 3d^5(^4G)4p\ ^5F + 7\ 3d^5(^4P)4p\ ^3P$
399329.0	399161	168	0 61	$3d^5(^4P)4p\ ^3P + 20\ 3d^5(^4D)4p\ ^3P + 12\ 3d^5(^4D)4p\ ^5D$
399434.6	399401	34	2 68	$3d^5(^4D)4p\ ^5F + 20\ 3d^5(^4G)4p\ ^5F$
399881.3	399835	46	3 69	$3d^5(^4D)4p\ ^5F + 13\ 3d^5(^4G)4p\ ^5F$
400562.7	400563	0	4 73	$3d^5(^4D)4p\ ^5F + 10\ 3d^5(^4G)4p\ ^5F + 9\ 3d^5(^4P)4p\ ^5D$
401264.1	401233	31	5 89	$3d^5(^4D)4p\ ^5F + 7\ 3d^5(^4G)4p\ ^5F$
402134.1	401793	341	3 48	$3d^5(^4D)4p\ ^5D + 17\ 3d^5(^4P)4p\ ^5D + 17\ 3d^5(^4P)4p\ ^3D$
402534.3	402164	370	4 67	$3d^5(^4D)4p\ ^5D + 20\ 3d^5(^4P)4p\ ^5D + 5\ 3d^5(^4F)4p\ ^5D$
402766.8	402492	275	2 51	$3d^5(^4D)4p\ ^5D + 16\ 3d^5(^4P)4p\ ^3D + 16\ 3d^5(^4P)4p\ ^5D$
402988.8	402994	-5	3 87	$3d^5(^4G)4p\ ^3G$
403086.6	403204	-117	4 89	$3d^5(^4G)4p\ ^3G$
403132.9	403356	-223	5 91	$3d^5(^4G)4p\ ^3G$
403358.0	403166	192	1 46	$3d^5(^4D)4p\ ^5D + 15\ 3d^5(^4P)4p\ ^5D + 13\ 3d^5(^4P)4p\ ^3D$
403366.0	403234	132	3 55	$3d^5(^4P)4p\ ^3D + 14\ 3d^5(^4D)4p\ ^5P + 8\ 3d^5(^4D)4p\ ^3F$
403961.1	403895	66	2 51	$3d^5(^4P)4p\ ^3D + 17\ 3d^5(^4D)4p\ ^5P + 6\ 3d^5(^4P)4p\ ^5P$
404096.2	404155	-59	1 38	$3d^5(^4P)4p\ ^3D + 34\ 3d^5(^4D)4p\ ^5P + 11\ 3d^5(^4D)4p\ ^3D$
404184.0	403885	299	0 60	$3d^5(^4D)4p\ ^5D + 21\ 3d^5(^4P)4p\ ^5D + 13\ 3d^5(^4P)4p\ ^3P$
404901.7	404853	49	1 37	$3d^5(^4D)4p\ ^5P + 18\ 3d^5(^4P)4p\ ^3D + 17\ 3d^5(^4D)4p\ ^5D$
405213.5	404932	282	3 47	$3d^5(^4D)4p\ ^3D + 14\ 3d^5(^4D)4p\ ^5D + 12\ 3d^5(^4P)4p\ ^5P$
405505.8	405583	-77	2 37	$3d^5(^4D)4p\ ^5P + 19\ 3d^5(^4P)4p\ ^5P + 14\ 3d^5(^4D)4p\ ^5D$
406659.4	406340	319	2 68	$3d^5(^4D)4p\ ^3D + 9\ 3d^5(^4D)4p\ ^5P + 8\ 3d^5(^4F)4p\ ^3D$
406752.6	406794	-41	3 35	$3d^5(^4D)4p\ ^5P + 29\ 3d^5(^4D)4p\ ^3D + 19\ 3d^5(^4P)4p\ ^5P$
407217.4	406829	388	1 58	$3d^5(^4D)4p\ ^3D + 22\ 3d^5(^4P)4p\ ^3D + 11\ 3d^5(^4F)4p\ ^3D$
407355.9	407418	-62	4 80	$3d^5(^4D)4p\ ^3F + 5\ 3d^5(^2G)4p\ ^3F$
408177.6	408244	-66	3 68	$3d^5(^4D)4p\ ^3F + 10\ 3d^5(^4P)4p\ ^3D + 5\ 3d^5(^2G)4p\ ^3F$
408281.7	408282	0	2 74	$3d^5(^4D)4p\ ^3F + 10\ 3d^5(^4P)4p\ ^3D + 5\ 3d^5(^2G)4p\ ^3F$
410288.7	410132	157	1 88	$3d^5(^4P)4p\ ^3S$
411872.1	411571	301	6 72	$3d^5(^2I)4p\ ^3K + 22\ 3d^5(^2I)4p\ ^3I$
412326.4	412417	-91	5 60	$3d^5(^2I)4p\ ^3I + 20\ 3d^5(^2I)4p\ ^1H + 8\ 3d^5(^2I)4p\ ^3H$
412439.9	412338	102	7 59	$3d^5(^2I)4p\ ^3K + 30\ 3d^5(^2I)4p\ ^3I + 9\ 3d^5(^2I)4p\ ^1K$
412469.3	412937	-468	0 73	$3d^5(^4D)4p\ ^3P + 21\ 3d^5(^4P)4p\ ^3P$
413072.5	413620	-548	1 64	$3d^5(^4D)4p\ ^3P + 20\ 3d^5(^4P)4p\ ^3P + 6\ 3d^5(^4P)4p\ ^3S$
413692.0	413746	-54	2 30	$3d^5(^2F)4p\ ^3F + 27\ 3d^5(^2D)4p\ ^3F + 9\ 3d^5(^2D)4p\ ^3F$
414203.7	414269	-65	6 52	$3d^5(^2I)4p\ ^3I + 22\ 3d^5(^2I)4p\ ^3H + 21\ 3d^5(^2I)4p\ ^3K$
414298.5	414354	-56	2 61	$3d^5(^4D)4p\ ^3P + 23\ 3d^5(^4P)4p\ ^3P + 6\ 3d^5(^2D)4p\ ^3P$
415258.3	414553	705	3 32	$3d^5(^2D)4p\ ^3F + 22\ 3d^5(^2F)4p\ ^3F + 14\ 3d^5(^2F)4p\ ^3G$
415520.0	415237	283	8 100	$3d^5(^2I)4p\ ^3K$
415694.4	415718	-24	7 65	$3d^5(^2I)4p\ ^3I + 35\ 3d^5(^2I)4p\ ^3K$
415851.8	415791	61	2 24	$3d^5(^2D)4p\ ^1D + 19\ 3d^5(^2D)4p\ ^3F + 16\ 3d^5(^2F)4p\ ^1D$
416024.9	416303	-278	5 46	$3d^5(^2I)4p\ ^1H + 31\ 3d^5(^2I)4p\ ^3I + 7\ 3d^5(^2I)4p\ ^3H$
416410.9	416685	-274	6 67	$3d^5(^2I)4p\ ^3H + 20\ 3d^5(^2I)4p\ ^3I$
417099.5	416822	278	4 34	$3d^5(^2D)4p\ ^3F + 26\ 3d^5(^2F)4p\ ^3F + 20\ 3d^5(^2F)4p\ ^3G$
417221.3	417595	-374	5 73	$3d^5(^2I)4p\ ^3H + 14\ 3d^5(^2I)4p\ ^1H$
417267.3	416949	318	7 89	$3d^5(^2I)4p\ ^1K + 5\ 3d^5(^2I)4p\ ^3K$
417511.5	417362	150	4 70	$3d^5(^2I)4p\ ^3H + 8\ 3d^5(^2G)4p\ ^3H$
419364.9	419479	-114	4 37	$3d^5(^2F)4p\ ^1G + 12\ 3d^5(^2I)4p\ ^3H + 10\ 3d^5(^2F)4p\ ^3G$
419365.2	419002	363	2 37	$3d^5(^2D)4p\ ^3P + 12\ 3d^5(^2D)4p\ ^3P + 11\ 3d^5(^2F)4p\ ^3D$
419605.8	419346	260	1 33	$3d^5(^2D)4p\ ^3P + 25\ 3d^5(^2D)4p\ ^3D + 10\ 3d^5(^2D)4p\ ^3P$

Table A.11. continued.

E_{exp}^a	E_{calc}^b	ΔE	J	Leading components (in %) in LS coupling ^c
419864.2	419166	698	3 36	$3d^5(^2F)4p\ ^3G + 25\ 3d^5(^2F)4p\ ^3F + 17\ 3d^5(^2D)4p\ ^1F$
420151.2	419979	172	2 73	$3d^5(^4F)4p\ ^5G + 7\ 3d^5(^2F)4p\ ^3F$
420201.1	420068	133	3 75	$3d^5(^4F)4p\ ^5G + 7\ 3d^5(^2F)4p\ ^3G$
420355.8	420300	56	3 34	$3d^5(^2F)4p\ ^3D + 30\ 3d^5(^2D)4p\ ^3D + 11\ 3d^5(^2D)4p\ ^3D$
420699.4	420569	130	4 64	$3d^5(^4F)4p\ ^5G + 5\ 3d^5(^2F)4p\ ^1G + 5\ 3d^5(^4F)4p\ ^5F$
420914.7	420771	144	5 53	$3d^5(^4F)4p\ ^5G + 9\ 3d^5(^4F)4p\ ^5F + 8\ 3d^5(^2G)4p\ ^3H$
421423.5	421052	372	0 64	$3d^5(^2D)4p\ ^3P + 20\ 3d^5(^2D)4p\ ^3P + 9\ 3d^5(^4F)4p\ ^5D$
421467.7	421427	41	2 44	$3d^5(^2D)4p\ ^3D + 15\ 3d^5(^2D)4p\ ^3D + 14\ 3d^5(^4F)4p\ ^5F$
421516.1	421296	220	1 28	$3d^5(^2D)4p\ ^3D + 24\ 3d^5(^2D)4p\ ^3P + 10\ 3d^5(^2D)4p\ ^3D$
421622.9	421647	-24	3 33	$3d^5(^2F)4p\ ^3D + 12\ 3d^5(^2D)4p\ ^3D + 11\ 3d^5(^2D)4p\ ^3F$
421924.7	421657	268	4 31	$3d^5(^2F)4p\ ^3F + 26\ 3d^5(^2F)4p\ ^3G + 12\ 3d^5(^4F)4p\ ^5F$
422221.2	422297	-76	3 55	$3d^5(^4F)4p\ ^5F + 23\ 3d^5(^4F)4p\ ^5D$
422269.8	422079	191	6 62	$3d^5(^4F)4p\ ^5G + 15\ 3d^5(^2I)4p\ ^1I + 12\ 3d^5(^2G)4p\ ^3H$
422425.6	422346	80	4 32	$3d^5(^4F)4p\ ^5F + 22\ 3d^5(^4F)4p\ ^5D + 16\ 3d^5(^2F)4p\ ^3F$
422613.1	422699	-86	2 49	$3d^5(^4F)4p\ ^5F + 25\ 3d^5(^4F)4p\ ^5D + 8\ 3d^5(^2D)4p\ ^3D$
422833.7	422345	489	5 53	$3d^5(^2F)4p\ ^3G + 23\ 3d^5(^4F)4p\ ^5G + 8\ 3d^5(^2H)4p\ ^3G$
422841.4	422565	276	4 33	$3d^5(^2G)4p\ ^3H + 31\ 3d^5(^2H)4p\ ^3H + 5\ 3d^5(^4F)4p\ ^5F$
422858.7	422845	14	6 63	$3d^5(^2I)4p\ ^1I + 26\ 3d^5(^4F)4p\ ^5G + 5\ 3d^5(^2H)4p\ ^3H$
423078.0	422925	153	1 33	$3d^5(^2F)4p\ ^3D + 25\ 3d^5(^2D)4p\ ^1P + 21\ 3d^5(^4F)4p\ ^5F$
423123.7	423192	-68	5 37	$3d^5(^4F)4p\ ^5F + 29\ 3d^5(^2F)4p\ ^3G + 9\ 3d^5(^4F)4p\ ^5G$
423304.7	423326	-21	1 50	$3d^5(^4F)4p\ ^5F + 15\ 3d^5(^4F)4p\ ^5D + 10\ 3d^5(^2D)4p\ ^3D$
423374.7	423293	82	2 29	$3d^5(^2F)4p\ ^3F + 19\ 3d^5(^2F)4p\ ^3D + 16\ 3d^5(^2D)4p\ ^3F$
423403.4	422923	480	3 17	$3d^5(^2F)4p\ ^3G + 15\ 3d^5(^2D)4p\ ^3F + 13\ 3d^5(^2F)4p\ ^3F$
423618.3	423551	67	5 29	$3d^5(^2G)4p\ ^3H + 28\ 3d^5(^4F)4p\ ^5F + 24\ 3d^5(^2H)4p\ ^3H$
424332.5	424006	327	4 16	$3d^5(^2D)4p\ ^3F + 15\ 3d^5(^2H)4p\ ^3G$
424482.8	424558	-75	3 17	$3d^5(^2D)4p\ ^1F + 16\ 3d^5(^2F)4p\ ^3G + 7\ 3d^5(^2F)4p\ ^3G$
424511.8	424603	-91	2 40	$3d^5(^2F)4p\ ^3D + 10\ 3d^5(^2D)4p\ ^3P + 9\ 3d^5(^4F)4p\ ^5F$
424590.4	424758	-168	5 43	$3d^5(^2H)4p\ ^3G + 13\ 3d^5(^2G)4p\ ^3G + 9\ 3d^5(^2F)4p\ ^3G$
424697.7	424804	-106	4 24	$3d^5(^2H)4p\ ^3G + 10\ 3d^5(^2G)4p\ ^3G + 7\ 3d^5(^2F)4p\ ^3G$
425101.8	425296	-194	4 41	$3d^5(^4F)4p\ ^5D + 25\ 3d^5(^4F)4p\ ^5F + 5\ 3d^5(^4F)4p\ ^5G$
425544.3	425465	79	6 30	$3d^5(^2H)4p\ ^3H + 29\ 3d^5(^2G)4p\ ^3H + 17\ 3d^5(^2I)4p\ ^1I$
425599.1	425439	160	3 25	$3d^5(^2H)4p\ ^3G + 14\ 3d^5(^2G)4p\ ^3G + 6\ 3d^5(^2D)4p\ ^1F$
425877.0	425993	-116	3 57	$3d^5(^4F)4p\ ^5D + 21\ 3d^5(^4F)4p\ ^5F + 5\ 3d^5(^4D)4p\ ^5D$
425954.6	426044	-89	0 87	$3d^5(^4F)4p\ ^5D + 7\ 3d^5(^2D)4p\ ^3P$
426008.4	426107	-99	1 73	$3d^5(^4F)4p\ ^5D + 10\ 3d^5(^4F)4p\ ^5F$
426112.6	426272	-159	2 59	$3d^5(^4F)4p\ ^5D + 15\ 3d^5(^4F)4p\ ^5F + 6\ 3d^5(^2F)4p\ ^3D$
427330.6	426943	388	5 80	$3d^5(^2H)4p\ ^3I + 9\ 3d^5(^2H)4p\ ^3H + 5\ 3d^5(^2G)4p\ ^3H$
427367.3	427382	-15	4 19	$3d^5(^2F)4p\ ^1G + 17\ 3d^5(^2G)4p\ ^1G + 16\ 3d^5(^2G)4p\ ^3G$
427940.9	427716	225	3 29	$3d^5(^2G)4p\ ^3G + 22\ 3d^5(^4F)4p\ ^3G + 9\ 3d^5(^2G)4p\ ^3F$
428048.7	427903	146	1 34	$3d^5(^2F)4p\ ^3D + 31\ 3d^5(^2D)4p\ ^1P + 8\ 3d^5(^2D)4p\ ^1P$
428386.0	428190	196	5 63	$3d^5(^4F)4p\ ^3G + 11\ 3d^5(^2G)4p\ ^3G + 11\ 3d^5(^4F)4p\ ^5F$
428430.6	428144	287	6 70	$3d^5(^2H)4p\ ^3I + 11\ 3d^5(^2H)4p\ ^1I + 8\ 3d^5(^2G)4p\ ^3H$
428503.5	428561	-58	2 47	$3d^5(^2F)4p\ ^1D + 22\ 3d^5(^2D)4p\ ^1D + 9\ 3d^5(^2G)4p\ ^3F$
428672.9	428362	311	4 55	$3d^5(^4F)4p\ ^3G + 13\ 3d^5(^2G)4p\ ^3G + 6\ 3d^5(^2F)4p\ ^1G$
429135.6	429119	17	3 30	$3d^5(^4F)4p\ ^3G + 26\ 3d^5(^2G)4p\ ^3F + 17\ 3d^5(^2F)4p\ ^1F$
429577.5	429705	-128	4 46	$3d^5(^2G)4p\ ^3F + 15\ 3d^5(^2G)4p\ ^1G + 9\ 3d^5(^2F)4p\ ^1G$
429657.4	429915	-258	2 51	$3d^5(^2G)4p\ ^3F + 10\ 3d^5(^4F)4p\ ^3F + 7\ 3d^5(^4D)4p\ ^3F$
429749.9	429487	263	7 94	$3d^5(^2H)4p\ ^3I$
429873.4	429616	257	3 40	$3d^5(^2F)4p\ ^1F + 28\ 3d^5(^2G)4p\ ^3F + 6\ 3d^5(^4F)4p\ ^3D$
431218.3	430922	296	6 72	$3d^5(^2H)4p\ ^1I + 11\ 3d^5(^2H)4p\ ^3H + 10\ 3d^5(^2H)4p\ ^3I$
431231.7	431470	-238	2 46	$3d^5(^4F)4p\ ^3D + 14\ 3d^5(^2F)4p\ ^1D + 10\ 3d^5(^2F)4p\ ^3F$
431530.7	431645	-114	3 39	$3d^5(^4F)4p\ ^3D + 12\ 3d^5(^2F)4p\ ^3D + 12\ 3d^5(^2F)4p\ ^3F$
431766.6	432093	-326	4 56	$3d^5(^4F)4p\ ^3F + 25\ 3d^5(^2F)4p\ ^3F$
432272.4	432478	-206	1 76	$3d^5(^4F)4p\ ^3D + 7\ 3d^5(^4D)4p\ ^3D + 6\ 3d^5(^2F)4p\ ^3D$
432839.7	433122	-282	3 57	$3d^5(^4F)4p\ ^3F + 17\ 3d^5(^4F)4p\ ^3D + 11\ 3d^5(^2F)4p\ ^3F$
432840.8	432637	204	5 31	$3d^5(^2G)4p\ ^3H + 25\ 3d^5(^2G)4p\ ^3G + 21\ 3d^5(^2H)4p\ ^3H$

Table A.11. continued.

E_{exp}^a	E_{calc}^b	ΔE	J	Leading components (in %) in LS coupling ^c
432939.3	432771	168	4 38	$3d^5(^2H)4p\ ^3H + 28\ 3d^5(^2G)4p\ ^3H + 7\ 3d^5(^2H)4p\ ^1G$
433257.9	433681	-423	2 56	$3d^5(^4F)4p\ ^3F + 14\ 3d^5(^4F)4p\ ^3D + 14\ 3d^5(^2F)4p\ ^3F$
434063.7	433893	171	5 24	$3d^5(^2F)4p\ ^3G + 21\ 3d^5(^2H)4p\ ^3H + 18\ 3d^5(^2G)4p\ ^3G$
434264.0	434216	48	3 29	$3d^5(^2F)4p\ ^3G + 25\ 3d^5(^4F)4p\ ^3G + 25\ 3d^5(^2G)4p\ ^3G$
434286.4	434177	109	4 25	$3d^5(^2F)4p\ ^3G + 15\ 3d^5(^4F)4p\ ^3G + 12\ 3d^5(^2H)4p\ ^3H$
434722.8	434735	-12	6 44	$3d^5(^2G)4p\ ^3H + 36\ 3d^5(^2H)4p\ ^3H + 15\ 3d^5(^2H)4p\ ^1I$
434812.2	434270	542	4 32	$3d^5(^2F)4p\ ^1G + 19\ 3d^5(^2G)4p\ ^3G + 12\ 3d^5(^2G)4p\ ^1G$
435369.7	435912	-542	3 33	$3d^5(^2G)4p\ ^1F + 27\ 3d^5(^2F)4p\ ^3F + 7\ 3d^5(^4F)4p\ ^3F$
435379.2	435701	-322	2 35	$3d^5(^2F)4p\ ^1D + 19\ 3d^5(^4F)4p\ ^3F + 14\ 3d^5(^4F)4p\ ^3D$
435676.7	435632	45	5 51	$3d^5(^2G)4p\ ^1H + 24\ 3d^5(^2H)4p\ ^1H + 13\ 3d^5(^2I)4p\ ^1H$
436243.7	436572	-328	3 31	$3d^5(^2G)4p\ ^1F + 21\ 3d^5(^2F)4p\ ^3F + 11\ 3d^5(^2G)4p\ ^3F$
436475.9	436626	-150	2 41	$3d^5(^2F)4p\ ^3F + 32\ 3d^5(^2F)4p\ ^1D + 12\ 3d^5(^2G)4p\ ^3F$
436506.5	436937	-431	4 48	$3d^5(^2F)4p\ ^3F + 18\ 3d^5(^4F)4p\ ^3F + 7\ 3d^5(^2F)4p\ ^1G$
437233.9	437113	121	5 63	$3d^5(^2H)4p\ ^1H + 27\ 3d^5(^2G)4p\ ^1H$
438607.7	438028	580	1 54	$3d^5(^2F)4p\ ^3D + 25\ 3d^5(^2S)4p\ ^3P + 5\ 3d^5(^2D)4p\ ^3P$
439180.1	438670	510	3 56	$3d^5(^2F)4p\ ^3D + 17\ 3d^5(^4F)4p\ ^3D + 9\ 3d^5(^2F)4p\ ^3D$
439327.1	438564	763	2 70	$3d^5(^2F)4p\ ^3D + 8\ 3d^5(^2F)4p\ ^3D + 6\ 3d^5(^4F)4p\ ^3D$
439706.8	439557	150	3 45	$3d^5(^2H)4p\ ^3G + 31\ 3d^5(^2F)4p\ ^3G + 11\ 3d^5(^2G)4p\ ^3G$
439775.0	439309	466	1 54	$3d^5(^2S)4p\ ^3P + 27\ 3d^5(^2F)4p\ ^3D + 8\ 3d^5(^2D)4p\ ^3P$
440372.2	440206	166	4 40	$3d^5(^2H)4p\ ^3G + 41\ 3d^5(^2F)4p\ ^3G + 9\ 3d^5(^2G)4p\ ^3G$
440896.3	440593	303	5 53	$3d^5(^2F)4p\ ^3G + 34\ 3d^5(^2H)4p\ ^3G + 8\ 3d^5(^2G)4p\ ^3G$
441375.8	441168	208	2 72	$3d^5(^2S)4p\ ^3P + 16\ 3d^5(^2D)4p\ ^3P$
443432.9	443588	-155	4 42	$3d^5(^2H)4p\ ^1G + 32\ 3d^5(^2F)4p\ ^1G + 22\ 3d^5(^2G)4p\ ^1G$
444432.7	444820	-387	1 68	$3d^5(^2S)4p\ ^1P + 18\ 3d^5(^2D)4p\ ^1P + 7\ 3d^5(^2D)4p\ ^1P$
445290.5	445891	-601	3 82	$3d^5(^2F)4p\ ^1F + 8\ 3d^5(^2F)4p\ ^1F$
453663.5	453452	212	2 55	$3d^5(^2D)4p\ ^3F + 31\ 3d^5(^2D)4p\ ^3D + 5\ 3d^5(^2G)4p\ ^3F$
454176.3	454028	148	3 42	$3d^5(^2D)4p\ ^3F + 33\ 3d^5(^2D)4p\ ^3D + 11\ 3d^5(^2D)4p\ ^1F$
454317.5	453641	677	1 89	$3d^5(^2D)4p\ ^3D$
454921.2	454443	478	2 54	$3d^5(^2D)4p\ ^3D + 30\ 3d^5(^2D)4p\ ^3F$
456264.2	455816	448	3 54	$3d^5(^2D)4p\ ^3D + 38\ 3d^5(^2D)4p\ ^3F$
456545.2	456543	2	4 90	$3d^5(^2D)4p\ ^3F + 6\ 3d^5(^2G)4p\ ^3F$
457544.9	457456	89	3 69	$3d^5(^2D)4p\ ^1F + 12\ 3d^5(^2G)4p\ ^1F + 10\ 3d^5(^2D)4p\ ^3F$
458688.9	459139	-450	0 84	$3d^5(^2D)4p\ ^3P + 14\ 3d^5(^2S)4p\ ^3P$
458731.8	459104	-372	2 66	$3d^5(^2D)4p\ ^3P + 16\ 3d^5(^2S)4p\ ^3P + 7\ 3d^5(^2D)4p\ ^3D$
458778.9	459173	-394	1 72	$3d^5(^2D)4p\ ^3P + 15\ 3d^5(^2S)4p\ ^3P + 5\ 3d^5(^2D)4p\ ^3D$
460536.5	460634	-98	1 70	$3d^5(^2D)4p\ ^1P + 16\ 3d^5(^2S)4p\ ^1P + 7\ 3d^5(^2D)4p\ ^3P$
461609.3	461150	459	2 82	$3d^5(^2D)4p\ ^1D + 7\ 3d^5(^2D)4p\ ^3P + 5\ 3d^5(^2F)4p\ ^1D$
464741.7	464767	-25	4 53	$3d^5(^2G)4p\ ^3H + 24\ 3d^5(^2G)4p\ ^3F + 17\ 3d^5(^2G)4p\ ^3G$
465130.4	465125	5	4 54	$3d^5(^2G)4p\ ^3F + 33\ 3d^5(^2G)4p\ ^3H + 5\ 3d^5(^2G)4p\ ^1G$
465460.0	465330	130	5 73	$3d^5(^2G)4p\ ^3H + 16\ 3d^5(^2G)4p\ ^3G + 8\ 3d^5(^2G)4p\ ^1H$
465803.6	465969	-165	3 50	$3d^5(^2G)4p\ ^3F + 40\ 3d^5(^2G)4p\ ^3G$
467531.5	467729	-198	2 89	$3d^5(^2G)4p\ ^3F + 7\ 3d^5(^2D)4p\ ^3F$
467599.8	467392	208	6 97	$3d^5(^2G)4p\ ^3H$
467819.2	467954	-135	3 54	$3d^5(^2G)4p\ ^3G + 39\ 3d^5(^2G)4p\ ^3F$
468335.2	468448	-113	4 79	$3d^5(^2G)4p\ ^3G + 9\ 3d^5(^2G)4p\ ^3F + 8\ 3d^5(^2G)4p\ ^3H$
468738.6	468841	-102	5 75	$3d^5(^2G)4p\ ^3G + 20\ 3d^5(^2G)4p\ ^3H$
471595.2	471450	145	5 88	$3d^5(^2G)4p\ ^1H + 5\ 3d^5(^2G)4p\ ^3G$
471769.3	471973	-204	4 91	$3d^5(^2G)4p\ ^1G$
473212.1	473441	-229	3 76	$3d^5(^2G)4p\ ^1F + 10\ 3d^5(^2D)4p\ ^1F + 5\ 3d^5(^2D)4p\ ^1F$
481411.7	481292	120	0 74	$3d^5(^2P)4p\ ^3P + 21\ 3d^5(^2D)4p\ ^3P$
481793.2	481612	181	1 72	$3d^5(^2P)4p\ ^3P + 22\ 3d^5(^2D)4p\ ^3P$
483006.9	482815	192	2 70	$3d^5(^2P)4p\ ^3P + 24\ 3d^5(^2D)4p\ ^3P$
488810.3	488641	169	2 55	$3d^5(^2P)4p\ ^3D + 28\ 3d^5(^2P)4p\ ^1D + 6\ 3d^5(^2D)4p\ ^1D$
488869.4	488819	50	1 88	$3d^5(^2P)4p\ ^3D + 6\ 3d^5(^2D)4p\ ^3D$
491155.1	491019	136	3 87	$3d^5(^2P)4p\ ^3D + 8\ 3d^5(^2D)4p\ ^3D$
491878.9	491764	115	2 46	$3d^5(^2P)4p\ ^1D + 34\ 3d^5(^2P)4p\ ^3D + 12\ 3d^5(^2D)4p\ ^1D$

Table A.11. continued.

E_{exp}^a	E_{calc}^b	ΔE	J	Leading components (in %) in LS coupling ^c
493316.5	493517	-201	1 80	$3d^5(^2P)4p\ ^3S + 14\ 3d^5(^2P)4p\ ^1P$
495292.7	494929	364	1 59	$3d^5(^2P)4p\ ^1P + 17\ 3d^5(^2P)4p\ ^3S + 16\ 3d^5(^2D)4p\ ^1P$
502689.0	502588	101	2 61	$3d^5(^2D)4p\ ^3F + 19\ 3d^5(^2D)4p\ ^3F + 8\ 3d^5(^2D)4p\ ^3D$
503114.1	502969	145	3 58	$3d^5(^2D)4p\ ^3F + 18\ 3d^5(^2D)4p\ ^3F + 9\ 3d^5(^2D)4p\ ^3D$
504630.2	504513	117	1 70	$3d^5(^2D)4p\ ^3D + 21\ 3d^5(^2D)4p\ ^3D + 7\ 3d^5(^2P)4p\ ^3D$
505107.8	504938	170	4 71	$3d^5(^2D)4p\ ^3F + 23\ 3d^5(^2D)4p\ ^3F + 6\ 3d^5(^2G)4p\ ^3F$
507108.1	507066	42	3 58	$3d^5(^2D)4p\ ^3D + 18\ 3d^5(^2D)4p\ ^3D + 10\ 3d^5(^2D)4p\ ^3F$
507132.9	507310	-177	2 41	$3d^5(^2D)4p\ ^1D + 17\ 3d^5(^2P)4p\ ^1D + 14\ 3d^5(^2D)4p\ ^1D$
509325.1	509521	-196	2 41	$3d^5(^2D)4p\ ^3P + 21\ 3d^5(^2P)4p\ ^3P + 15\ 3d^5(^2D)4p\ ^3P$
509967.2	509818	149	3 68	$3d^5(^2D)4p\ ^1F + 21\ 3d^5(^2D)4p\ ^1F + 6\ 3d^5(^2G)4p\ ^1F$
510178.2	510388	-210	1 54	$3d^5(^2D)4p\ ^3P + 25\ 3d^5(^2P)4p\ ^3P + 19\ 3d^5(^2D)4p\ ^3P$
510942.6	511192	-249	0 55	$3d^5(^2D)4p\ ^3P + 24\ 3d^5(^2P)4p\ ^3P + 19\ 3d^5(^2D)4p\ ^3P$

^a From NIST compilation (Kramida et al. 2019).^b This work.^c Only the first three components greater than or equal to 5% are given.**Table A.12.** Comparison between available experimental and calculated energy levels in Cu vii. Energies are given in cm⁻¹.

E_{exp}^a	E_{calc}^b	ΔE	J	Leading components (in %) in LS coupling ^c
Even parity				
0.0	-13	13	2.5 100	$3d^5\ ^6S$
46442.7	46565	-122	5.5 100	$3d^5\ ^4G$
46515.3	46383	132	2.5 99	$3d^5\ ^4G$
46575.0	46604	-29	4.5 100	$3d^5\ ^4G$
46578.2	46520	58	3.5 99	$3d^5\ ^4G$
50731.7	50742	-10	2.5 86	$3d^5\ ^4P + 12\ 3d^5\ ^4D$
51066.6	51059	8	1.5 89	$3d^5\ ^4P + 10\ 3d^5\ ^4D$
51406.6	51420	-13	0.5 96	$3d^5\ ^4P$
55742.2	55792	-50	3.5 99	$3d^5\ ^4D$
56209.9	56168	42	0.5 96	$3d^5\ ^4D$
56427.2	56473	-46	2.5 87	$3d^5\ ^4D + 12\ 3d^5\ ^4P$
56428.5	56434	-6	1.5 89	$3d^5\ ^4D + 10\ 3d^5\ ^4P$
67757.3	67660	97	5.5 98	$3d^5\ ^2I$
67917.9	67993	-75	6.5 100	$3d^5\ ^2I$
70875.6	70762	114	2.5 49	$3d^5\ ^2D + 32\ 3d^5\ ^2F + 15\ 3d^5\ ^2D$
72226.8	72213	14	1.5 68	$3d^5\ ^2D + 21\ 3d^5\ ^2D + 11\ 3d^5\ ^4F$
74407.6	74668	-260	3.5 92	$3d^5\ ^2F + 5\ 3d^5\ ^4F$
75930.5	75980	-50	4.5 93	$3d^5\ ^4F + 6\ 3d^5\ ^2G$
76019.0	76095	-76	2.5 73	$3d^5\ ^4F + 22\ 3d^5\ ^2F$
76349.1	76277	72	3.5 91	$3d^5\ ^4F + 6\ 3d^5\ ^2F$
76886.0	76876	10	1.5 89	$3d^5\ ^4F + 9\ 3d^5\ ^2D$
77529.3	77389	140	2.5 44	$3d^5\ ^2F + 24\ 3d^5\ ^2D + 23\ 3d^5\ ^4F$
80717.0	80653	64	4.5 71	$3d^5\ ^2H + 25\ 3d^5\ ^2G$
81954.4	81992	-38	5.5 97	$3d^5\ ^2H$
82745.5	82790	-45	3.5 97	$3d^5\ ^2G$
83910.4	83935	-25	4.5 68	$3d^5\ ^2G + 28\ 3d^5\ ^2H$
87979.2	88025	-46	2.5 97	$3d^5\ ^2F$
88279.7	88128	152	3.5 97	$3d^5\ ^2F$
95875.4	95932	-57	0.5 100	$3d^5\ ^2S$
106957.0	106878	79	1.5 100	$3d^5\ ^2D$
107130.6	107135	-4	2.5 99	$3d^5\ ^2D$
119534.0	119545	-11	4.5 100	$3d^5\ ^2G$
119605.4	119648	-43	3.5 99	$3d^5\ ^2G$
143933.7	143910	24	1.5 99	$3d^5\ ^2P$
144077.2	144131	-54	0.5 100	$3d^5\ ^2P$

Table A.12. continued.

E_{exp}^a	E_{calc}^b	ΔE	J	Leading components (in %) in LS coupling ^c
156224.4	156181	43	2.5	77 3d ⁵ 2D + 23 3d ⁵ 2D
156373.6	156377	-3	1.5	76 3d ⁵ 2D + 23 3d ⁵ 2D
Odd parity				
497624.0	497489	135	1.5	90 3d ⁴ (⁵ D)4p 6P + 7 3d ⁴ (⁵ D)4p 4P
497863.0	497657	206	2.5	93 3d ⁴ (⁵ D)4p 6P
498317.0	498057	260	3.5	98 3d ⁴ (⁵ D)4p 6P
498775.0	499069	-294	0.5	65 3d ⁴ (⁵ D)4p 4P + 32 3d ⁴ (⁵ D)4p 6D
500706.0	500802	-96	1.5	51 3d ⁴ (⁵ D)4p 4P + 36 3d ⁴ (⁵ D)4p 6D + 10 3d ⁴ (⁵ D)4p 6P
502909.0	502882	27	2.5	58 3d ⁴ (⁵ D)4p 6D + 34 3d ⁴ (⁵ D)4p 4P + 6 3d ⁴ (⁵ D)4p 6P
504338.0	504276	62	0.5	68 3d ⁴ (⁵ D)4p 6D + 31 3d ⁴ (⁵ D)4p 4P
504729.0	504631	98	1.5	60 3d ⁴ (⁵ D)4p 6D + 38 3d ⁴ (⁵ D)4p 4P
505447.0	505280	167	2.5	59 3d ⁴ (⁵ D)4p 4P + 38 3d ⁴ (⁵ D)4p 6D
508524.0	508408	116	1.5	94 3d ⁴ (⁵ D)4p 4F
508877.0	508703	174	2.5	92 3d ⁴ (⁵ D)4p 4F
509418.0	509167	251	3.5	89 3d ⁴ (⁵ D)4p 4F + 5 3d ⁴ (⁵ D)4p 6D
510250.0	509928	322	4.5	81 3d ⁴ (⁵ D)4p 4F + 14 3d ⁴ (⁵ D)4p 6D
517847.0	518055	-208	0.5	96 3d ⁴ (⁵ D)4p 4D
518282.0	518443	-161	1.5	96 3d ⁴ (⁵ D)4p 4D
518863.0	518976	-113	2.5	96 3d ⁴ (⁵ D)4p 4D
519415.0	519509	-94	3.5	96 3d ⁴ (⁵ D)4p 4D
528494.0	528566	-72	3.5	74 3d ⁴ (³ H)4p 4H + 21 3d ⁴ (³ G)4p 4H
529027.0	529068	-41	4.5	69 3d ⁴ (³ H)4p 4H + 19 3d ⁴ (³ G)4p 4H + 8 3d ⁴ (³ H)4p 4I
529891.0	529884	7	5.5	70 3d ⁴ (³ H)4p 4H + 17 3d ⁴ (³ G)4p 4H + 11 3d ⁴ (³ H)4p 4I
531047.0	531008	39	6.5	76 3d ⁴ (³ H)4p 4H + 13 3d ⁴ (³ G)4p 4H + 9 3d ⁴ (³ H)4p 4I
532460.0	532075	385	2.5	40 3d ⁴ (³ P)4p 4D + 26 3d ⁴ (³ P)4p 4D + 17 3d ⁴ (³ F)4p 4D
533066.0	533079	-13	3.5	27 3d ⁴ (³ F)4p 4G + 17 3d ⁴ (³ G)4p 4G + 14 3d ⁴ (³ F)4p 4G
533103.0	532965	138	4.5	58 3d ⁴ (³ H)4p 4I + 8 3d ⁴ (³ H)4p 4H + 7 3d ⁴ (³ H)4p 2G
533685.0	533587	98	0.5	41 3d ⁴ (³ P)4p 4P + 22 3d ⁴ (³ P)4p 4P + 15 3d ⁴ (³ P)4p 2S
534128.0	533733	395	4.5	29 3d ⁴ (³ H)4p 4I + 14 3d ⁴ (³ F)4p 4G + 13 3d ⁴ (³ H)4p 4G
534204.0	533796	408	3.5	31 3d ⁴ (³ F)4p 4D + 25 3d ⁴ (³ P)4p 4D + 16 3d ⁴ (³ P)4p 4D
534912.0	534654	258	5.5	67 3d ⁴ (³ H)4p 4I + 11 3d ⁴ (³ H)4p 4G + 11 3d ⁴ (³ H)4p 4H
535632.0	535162	470	5.5	38 3d ⁴ (³ H)4p 4G + 25 3d ⁴ (³ G)4p 4G + 19 3d ⁴ (³ H)4p 4I
536229.0	536291	-62	1.5	55 3d ⁴ (³ P)4p 4P + 29 3d ⁴ (³ P)4p 4P
536650.0	536534	116	4.5	31 3d ⁴ (³ H)4p 2G + 20 3d ⁴ (³ F)4p 2G + 14 3d ⁴ (³ G)4p 4G
537169.0	537180	-11	2.5	33 3d ⁴ (³ H)4p 4G + 27 3d ⁴ (³ F)4p 4G + 14 3d ⁴ (³ G)4p 4G
537802.0	537633	169	3.5	46 3d ⁴ (³ H)4p 4G + 32 3d ⁴ (³ F)4p 4G + 14 3d ⁴ (³ G)4p 4G
537874.0	537807	67	2.5	44 3d ⁴ (³ F)4p 4F + 11 3d ⁴ (³ F)4p 2D + 9 3d ⁴ (³ H)4p 4G
538144.0	537939	205	4.5	42 3d ⁴ (³ F)4p 4G + 36 3d ⁴ (³ H)4p 4G + 7 3d ⁴ (³ F)4p 4G
538624.0	538331	293	2.5	54 3d ⁴ (³ P)4p 4P + 28 3d ⁴ (³ P)4p 4P + 5 3d ⁴ (³ P)4p 2D
538749.0	538777	-28	3.5	60 3d ⁴ (³ F)4p 4F + 11 3d ⁴ (³ F)4p 4F + 10 3d ⁴ (³ G)4p 4F
539041.0	538800	241	5.5	60 3d ⁴ (³ F)4p 4G + 18 3d ⁴ (³ H)4p 4G + 13 3d ⁴ (³ F)4p 4G
539146.0	539272	-126	4.5	54 3d ⁴ (³ F)4p 4F + 15 3d ⁴ (³ G)4p 4F + 10 3d ⁴ (³ F)4p 4F
539640.0	539940	-300	2.5	14 3d ⁴ (³ F)4p 2D + 14 3d ⁴ (³ G)4p 4F + 12 3d ⁴ (³ G)4p 2F
540086.0	540131	-45	1.5	21 3d ⁴ (³ F)4p 2D + 21 3d ⁴ (³ F)4p 4F + 9 3d ⁴ (³ D)4p 2D
540915.0	540877	38	1.5	37 3d ⁴ (³ F)4p 4D + 13 3d ⁴ (³ F)4p 4D + 10 3d ⁴ (³ G)4p 4F
540925.0	540904	21	3.5	22 3d ⁴ (³ G)4p 4F + 22 3d ⁴ (³ P)4p 4D + 14 3d ⁴ (³ P)4p 4D
541444.0	541807	-363	2.5	27 3d ⁴ (³ G)4p 2F + 14 3d ⁴ (³ D)4p 2F + 12 3d ⁴ (³ F)4p 4D
541457.0	541680	-223	4.5	31 3d ⁴ (³ H)4p 2H + 26 3d ⁴ (³ G)4p 4H + 12 3d ⁴ (³ G)4p 2H
541509.0	540981	528	6.5	82 3d ⁴ (³ H)4p 2I + 11 3d ⁴ (³ G)4p 4H
541884.0	541745	139	3.5	69 3d ⁴ (³ G)4p 4H + 21 3d ⁴ (³ H)4p 4H
542239.0	542259	-20	4.5	49 3d ⁴ (³ G)4p 4F + 18 3d ⁴ (³ F)4p 4F + 9 3d ⁴ (³ D)4p 4F
542362.0	542676	-314	3.5	16 3d ⁴ (³ G)4p 2F + 16 3d ⁴ (³ D)4p 2F + 16 3d ⁴ (³ G)4p 4F
542394.0	542133	261	1.5	21 3d ⁴ (³ G)4p 4F + 14 3d ⁴ (³ F)4p 4F
542776.0	542901	-125	2.5	37 3d ⁴ (³ G)4p 4F + 15 3d ⁴ (³ F)4p 4F + 15 3d ⁴ (³ F)4p 4D
543188.0	543060	128	5.5	36 3d ⁴ (³ G)4p 4H + 26 3d ⁴ (³ H)4p 2H + 16 3d ⁴ (³ G)4p 2H
543217.0	543139	78	3.5	24 3d ⁴ (³ F)4p 4D + 19 3d ⁴ (³ G)4p 4F + 10 3d ⁴ (³ F)4P

Table A.12. continued.

E_{exp}^a	E_{calc}^b	ΔE	J	Leading components (in %) in LS coupling ^c
543244.0	543002	242	1.5 22	$3d^4(^3G)4p^4F + 19 3d^4(^3P)4p^2P + 14 3d^4(^3F)4p^4D$
543574.0	543293	281	4.5 48	$3d^4(^3G)4p^4H + 23 3d^4(^3H)4p^2H + 11 3d^4(^3H)4p^4H$
544873.0	544242	631	1.5 36	$3d^4(^3P)4p^2D + 23 3d^4(^3P)4p^2D + 9 3d^4(^3G)4p^4F$
546268.0	545746	522	2.5 41	$3d^4(^3P)4p^2D + 26 3d^4(^3P)4p^2D + 5 3d^4(^3P)4p^4P$
546771.0	546378	393	2.5 55	$3d^4(^3F)4p^2F + 20 3d^4(^3G)4p^2F + 5 3d^4(^3P)4p^2D$
546881.0	546990	-109	3.5 26	$3d^4(^3F)4p^2G + 15 3d^4(^3F)4p^2G + 14 3d^4(^3H)4p^2G$
547090.0	547235	-145	5.5 38	$3d^4(^3G)4p^2H + 18 3d^4(^3H)4p^2H + 16 3d^4(^3G)4p^4G$
547381.0	547495	-114	4.5 23	$3d^4(^3F)4p^2G + 12 3d^4(^3F)4p^2G + 12 3d^4(^3G)4p^2G$
547565.0	547500	65	3.5 50	$3d^4(^3F)4p^2F + 30 3d^4(^3G)4p^2F$
548001.0	547913	88	2.5 52	$3d^4(^3G)4p^4G + 32 3d^4(^3H)4p^4G + 5 3d^4(^3F)4p^2F$
548491.0	548364	127	3.5 49	$3d^4(^3G)4p^4G + 24 3d^4(^3H)4p^4G + 6 3d^4(^3F)4p^2G$
549249.0	549135	114	4.5 40	$3d^4(^3G)4p^4G + 18 3d^4(^3H)4p^4G + 13 3d^4(^3G)4p^2H$
550007.0	549870	137	5.5 46	$3d^4(^3G)4p^4G + 21 3d^4(^3G)4p^2H + 18 3d^4(^3H)4p^4G$
550053.0	550667	-614	2.5 61	$3d^4(^3D)4p^4P + 26 3d^4(^3D)4p^4D + 5 3d^4(^3P)4p^4P$
551508.0	552407	-899	3.5 75	$3d^4(^3D)4p^4D + 7 3d^4(^3D)4p^4F + 5 3d^4(^3G)4p^4F$
551743.0	552463	-720	2.5 48	$3d^4(^3D)4p^4D + 26 3d^4(^3D)4p^4P + 8 3d^4(^3D)4p^4F$
551903.0	551648	255	6.5 60	$3d^4(^1I)4p^2I + 34 3d^4(^1I)4p^2K + 6 3d^4(^3H)4p^2I$
552334.0	553189	-855	3.5 46	$3d^4(^1G)4p^2F + 20 3d^4(^1G)4p^2F + 18 3d^4(^3G)4p^2G$
552359.0	552167	192	5.5 88	$3d^4(^1I)4p^2I$
553130.0	553419	-289	1.5 69	$3d^4(^3D)4p^4P + 11 3d^4(^3D)4p^4D + 7 3d^4(^3D)4p^4F$
553490.0	553853	-363	4.5 51	$3d^4(^3G)4p^2G + 21 3d^4(^3H)4p^2G + 11 3d^4(^1G)4p^2G$
553703.0	553770	-67	3.5 49	$3d^4(^3G)4p^2G + 17 3d^4(^3H)4p^2G + 9 3d^4(^1G)4p^2F$
553950.0	554244	-294	0.5 87	$3d^4(^3D)4p^4P + 7 3d^4(^3P)4p^4P$
554123.0	554268	-145	4.5 47	$3d^4(^1G)4p^2H + 21 3d^4(^1G)4p^2H + 10 3d^4(^3G)4p^2H$
554201.0	555068	-867	0.5 39	$3d^4(^3D)4p^2P + 35 3d^4(^1S)4p^2P + 9 3d^4(^3D)4p^4D$
555069.0	555490	-421	5.5 54	$3d^4(^1G)4p^2H + 18 3d^4(^1G)4p^2H + 11 3d^4(^1I)4p^2H$
555137.0	556274	-1137	1.5 62	$3d^4(^3D)4p^2P + 19 3d^4(^1S)4p^2P + 6 3d^4(^3D)4p^4D$
555295.0	554827	468	6.5 64	$3d^4(^1I)4p^2K + 35 3d^4(^1I)4p^2I$
555314.0	555863	-549	2.5 49	$3d^4(^1G)4p^2F + 23 3d^4(^1G)4p^2F + 6 3d^4(^3G)4p^2F$
555395.0	555919	-524	3.5 63	$3d^4(^3D)4p^4F + 19 3d^4(^3G)4p^4F + 12 3d^4(^3D)4p^4D$
555800.0	556340	-540	4.5 76	$3d^4(^3D)4p^4F + 19 3d^4(^3G)4p^4F$
558348.0	559260	-912	3.5 45	$3d^4(^1G)4p^2G + 30 3d^4(^1G)4p^2G + 9 3d^4(^3G)4p^2G$
559339.0	560050	-711	4.5 42	$3d^4(^1G)4p^2G + 32 3d^4(^1G)4p^2G + 18 3d^4(^3G)4p^2G$
560328.0	560307	21	1.5 34	$3d^4(^1D)4p^2D + 18 3d^4(^1S)4p^2P$
560658.0	560942	-284	5.5 65	$3d^4(^1I)4p^2H + 13 3d^4(^1G)4p^2H + 9 3d^4(^3G)4p^2H$
561271.0	561860	-589	0.5 40	$3d^4(^3D)4p^2P + 29 3d^4(^1S)4p^2P + 12 3d^4(^1D)4p^2P$
561677.0	561998	-321	4.5 80	$3d^4(^1I)4p^2H + 10 3d^4(^3G)4p^2H + 8 3d^4(^1G)4p^2H$
561985.0	561596	389	2.5 47	$3d^4(^1D)4p^2D + 19 3d^4(^3D)4p^2D + 17 3d^4(^1D)4p^2D$
562178.0	562598	-420	3.5 62	$3d^4(^3D)4p^2F + 10 3d^4(^3G)4p^2F + 7 3d^4(^1F)4p^2F$
562816.0	563160	-344	2.5 49	$3d^4(^3D)4p^2F + 19 3d^4(^1F)4p^2F + 16 3d^4(^3G)4p^2F$
563705.0	564030	-325	1.5 25	$3d^4(^1D)4p^2D + 24 3d^4(^1S)4p^2P + 12 3d^4(^3D)4p^2P$
565170.0	565169	1	1.5 70	$3d^4(^3D)4p^2D + 15 3d^4(^3F)4p^2D + 5 3d^4(^1D)4p^2D$
565670.0	565238	432	2.5 35	$3d^4(^1D)4p^2F + 20 3d^4(^3D)4p^2D + 16 3d^4(^3D)4p^2F$
567069.0	566385	684	2.5 35	$3d^4(^3D)4p^2D + 18 3d^4(^1D)4p^2F + 16 3d^4(^1D)4p^2D$
567778.0	566943	835	3.5 49	$3d^4(^1D)4p^2F + 28 3d^4(^1F)4p^2F + 12 3d^4(^1D)4p^2F$
572310.0	571556	754	2.5 61	$3d^4(^1F)4p^2F + 12 3d^4(^1G)4p^2F + 11 3d^4(^1D)4p^2F$
573402.0	573064	338	0.5 68	$3d^4(^1D)4p^2P + 14 3d^4(^1D)4p^2P + 9 3d^4(^1S)4p^2P$
573463.0	572399	1064	3.5 46	$3d^4(^1F)4p^2F + 23 3d^4(^1D)4p^2F + 10 3d^4(^1G)4p^2F$
574043.0	573284	759	1.5 56	$3d^4(^1D)4p^2P + 16 3d^4(^1S)4p^2P + 12 3d^4(^1G)4p^2P$
575709.0	575410	299	3.5 84	$3d^4(^1F)4p^2G + 6 3d^4(^1F)4p^2F$
578193.0	577847	346	4.5 90	$3d^4(^1F)4p^2G$
582101.0	582247	-146	2.5 59	$3d^4(^3F)4p^4F + 11 3d^4(^3P)4p^4D + 8 3d^4(^3F)4p^4F$
582434.0	582473	-39	3.5 65	$3d^4(^3F)4p^4F + 8 3d^4(^3F)4p^4D + 8 3d^4(^3F)4p^4F$
582632.0	582763	-131	1.5 37	$3d^4(^3F)4p^4F + 13 3d^4(^1F)4p^2D + 11 3d^4(^3P)4p^4D$
583223.0	583285	-62	4.5 82	$3d^4(^3F)4p^4F + 9 3d^4(^3F)4p^4F$
583496.0	583891	-395	1.5 20	$3d^4(^3P)4p^4P + 16 3d^4(^3P)4p^4D + 16 3d^4(^3F)4p^4F$
583853.0	583914	-61	2.5 23	$3d^4(^3P)4p^4D + 21 3d^4(^3F)4p^4F + 12 3d^4(^3P)4p^4D$

Table A.12. continued.

E_{exp}^a	E_{calc}^b	ΔE	J	Leading components (in %) in LS coupling ^c
584627.0	584697	-70	3.5 32	3d ⁴ (³ P)4p ⁴ D + 19 3d ⁴ (³ F)4p ⁴ D + 16 3d ⁴ (³ F)4p ⁴ F
586361.0	586509	-148	2.5 29	3d ⁴ (³ F)4p ⁴ G + 17 3d ⁴ (³ P)4p ⁴ P + 13 3d ⁴ (³ F)4p ² F
587400.0	587450	-50	3.5 37	3d ⁴ (³ F)4p ⁴ G + 28 3d ⁴ (³ F)4p ² F + 12 3d ⁴ (³ F)4p ⁴ G
588525.0	588525	0	2.5 26	3d ⁴ (¹ F)4p ² D + 19 3d ⁴ (³ P)4p ² D + 13 3d ⁴ (³ P)4p ² D
589098.0	589136	-38	3.5 39	3d ⁴ (³ F)4p ² F + 31 3d ⁴ (³ F)4p ⁴ G + 10 3d ⁴ (³ F)4p ⁴ G
589132.0	589220	-88	1.5 33	3d ⁴ (¹ F)4p ² D + 21 3d ⁴ (³ P)4p ² D + 17 3d ⁴ (³ F)4p ² D
596473.0	596393	80	4.5 70	3d ⁴ (³ F)4p ² G + 20 3d ⁴ (³ F)4p ² G
596790.0	597023	-233	1.5 61	3d ⁴ (³ P)4p ² P + 25 3d ⁴ (³ P)4p ² P + 7 3d ⁴ (³ D)4p ² P
597774.0	597560	214	3.5 72	3d ⁴ (³ F)4p ² G + 22 3d ⁴ (³ F)4p ² G
599993.0	599594	399	4.5 40	3d ⁴ (¹ G)4p ² H + 22 3d ⁴ (¹ G)4p ² G + 19 3d ⁴ (¹ G)4p ² H
600555.0	600479	76	3.5 51	3d ⁴ (¹ G)4p ² G + 31 3d ⁴ (¹ G)4p ² G + 7 3d ⁴ (¹ G)4p ² F
601692.0	601391	301	0.5 54	3d ⁴ (³ P)4p ² S + 41 3d ⁴ (³ P)4p ² S
603569.0	603112	457	4.5 37	3d ⁴ (¹ G)4p ² G + 23 3d ⁴ (¹ G)4p ² H + 22 3d ⁴ (¹ G)4p ² G
604021.0	603515	506	5.5 65	3d ⁴ (¹ G)4p ² H + 31 3d ⁴ (¹ G)4p ² H
604655.0	604594	61	3.5 53	3d ⁴ (¹ G)4p ² F + 16 3d ⁴ (¹ G)4p ² F + 8 3d ⁴ (¹ G)4p ² G
605306.0	605304	2	2.5 58	3d ⁴ (¹ G)4p ² F + 18 3d ⁴ (¹ G)4p ² F + 9 3d ⁴ (¹ D)4p ² F
608598.0	608701	-103	2.5 49	3d ⁴ (³ F)4p ² D + 18 3d ⁴ (³ F)4p ² D + 16 3d ⁴ (³ P)4p ² D
609072.0	609176	-104	1.5 44	3d ⁴ (³ F)4p ² D + 21 3d ⁴ (³ P)4p ² D + 18 3d ⁴ (³ F)4p ² D
634888.0	634813	75	3.5 72	3d ⁴ (¹ D)4p ² F + 19 3d ⁴ (¹ D)4p ² F + 5 3d ⁴ (¹ G)4p ² F

^a From van het Hof et al. (1990).^b This work.^c Only the first three components higher than or equal to 5% are given.**Table A.13.** Calculated HFR oscillator strengths ($\log g_i f_{ik}$) and transition probabilities ($g_k A_{ki}$) in Cu iv. CF is the absolute value of the cancellation factor as defined by Cowan (1981). In Cols. 3 and 6, e represents even and o odd. This table is only available via the GAVO service TOSS (<http://dc.g-vo.org/TOSS>).

Wavelength ^a / Å	Lower level			Upper level			CF
	Energy ^b / cm ⁻¹	Parity	J	Energy ^b / cm ⁻¹	Parity	J	
Notes. ^(a) All wavelengths (given in vacuum for $\lambda < 2000 \text{ Å}$, air for $2000 \text{ Å} \leq \lambda \leq 20000 \text{ Å}$, vacuum for $20000 \text{ Å} < \lambda$) are deduced from experimental energy levels. ^(b) Experimental energy levels taken from Kramida et al. (2019)							

Table A.14. Calculated HFR oscillator strengths ($\log g_i f_{ik}$) and transition probabilities ($g_k A_{ki}$) in Cu v. CF is the absolute value of the cancellation factor as defined by Cowan (1981). In Cols. 3 and 6, e represents even and o odd. This table is only available via the GAVO service TOSS (<http://dc.g-vo.org/TOSS>).

Wavelength ^a / Å	Lower level			Upper level			CF
	Energy ^b / cm ⁻¹	Parity	J	Energy ^b / cm ⁻¹	Parity	J	
Notes. ^(a) All wavelengths (given in vacuum for $\lambda < 2000 \text{ Å}$, air for $2000 \text{ Å} \leq \lambda \leq 20000 \text{ Å}$, vacuum for $20000 \text{ Å} < \lambda$) are deduced from experimental energy levels. ^(b) Experimental energy levels taken from Kramida et al. (2019)							

Table A.15. Calculated HFR oscillator strengths ($\log g_i f_{ik}$) and transition probabilities ($g_k A_{ki}$) in Cu vi. CF is the absolute value of the cancellation factor as defined by Cowan (1981). In Cols. 3 and 6, e represents even and o odd. This table is only available via the GAVO service TOSS (<http://dc.g-vo.org/TOSS>).

Wavelength ^a / Å	Lower level			Upper level			$\log g_i f_{ik}$	$g_k A_{ki}$ / s ⁻¹	CF		
	Energy ^b / cm ⁻¹	Parity J	Energy ^b / cm ⁻¹	Parity J							
Notes. ^(a) All wavelengths (given in vacuum for $\lambda < 2000$ Å, air for $2000 \text{ Å} \leq \lambda \leq 20000$ Å, vacuum for $20000 \text{ Å} < \lambda$) are deduced from experimental energy levels. ^(b) Experimental energy levels taken from Kramida et al. (2019)											

Table A.16. Calculated HFR oscillator strengths ($\log g_i f_{ik}$) and transition probabilities ($g_k A_{ki}$) in Cu vii. CF is the absolute value of the cancellation factor as defined by Cowan (1981). In Cols. 3 and 6, e represents even and o odd. This table is only available via the GAVO service TOSS (<http://dc.g-vo.org/TOSS>).

Wavelength ^a / Å	Lower level			Upper level			$\log g_i f_{ik}$	$g_k A_{ki}$ / s ⁻¹	CF		
	Energy ^b / cm ⁻¹	Parity J	Energy ^b / cm ⁻¹	Parity J							
Notes. ^(a) All wavelengths (given in vacuum for $\lambda < 2000$ Å, air for $2000 \text{ Å} \leq \lambda \leq 20000$ Å, vacuum for $20000 \text{ Å} < \lambda$) are deduced from experimental energy levels. ^(b) Experimental energy levels taken from van het Hof et al. (1990)											